Over expression of insulin receptor substrate 2 in oligodendrocytes

I n a u g u r a l - D i s s e r t a t i o n
zur
Erlangung des Doktorgrades
der Mathematisch-Naturwissenschaftlichen Fakultät
der Universität zu Köln

vorgelegt von
Jessica Rosina Brigitte Drake

aus Krefeld-Uerdingen
Köln 2013

Berichterstatter:

Prof. Dr. Jens C. Brüning

Prof. Dr. Wilhelm Krone

Tag der letzten mündlichen Prüfung: 22.1.13

Every adventure requires a first step. Trite, but true, even here.

— Lewis Carroll, Alice in Wonderland

Figure Index

Table Index

List of Abbreviations

α2M	alpha 2 macroglobulin
aa	amino acids
AKT	PKB synonym
ALS	Amyotrophic lateral sclerosis
APS	Ammonium-persulfate
APC	*adenomatous polyposis coli* gene product
ATP	Adenosintriphosphate
BACE-1	Beta-site APP Cleaving Enzyme-1
BAD	Bcl-2/Bcl-X-associated death promoter
BBB	Blood brain barrier
BME	Basal medium eagle
BSA	Bovine serum albumin
CC	Heterozygous CNP deficient mouse
CC -/-	Homozygous CNP deficient mouse
Cat	Catenin
CDK	Cyclin-depentent kinase
CK1	casein kinase 1
CNS	Central Nervous System
CNP	2',3'-Cyclic nucleotide-3'-phosphatase
CRAF	c-raf leukemia viral oncogene
CREB	cAMP response element binding
ddH2O	Double-disalled water
DMSO	Dimethyl sulfoxide
DM20	PLP isoform
Dvl	Dishevelled
EAE	experimental allergic (autoimmune) encephalomyelitis
4E-BP	4E binding protein
eEFs	elongation factors
eEF2	eukaryotic elongation factor 2
eIF4E	eukaryotic initiation factor 4E
ELISA	Enzyme Linked Immunosorbent Assays
ER	Endoplasmic reaculum
ERK	Extracellular signal-regulated kinase
FAK	focal adhesion kinase
FCS	Fetal calf serum
FKHR	forkhead domain

FOS	FBJ osteosarcoma oncogene
FoxO	Forkhead box-O transcription factor
FRE	FoxO-recognized element
Fz	Frizzled
GalC	Galactosylceramides
GDP	Guanosine-diphosphate
GH	Growth hormone
GHR	Growth hormone receptor
GHRH	Growth hormone releasing hormone
GHRHR	Growth hormone releasing hormone receptor
GlcC	glucocerebroside
GM4	sialosylgalactosylceramide
GRB2	Growth factor receptor binding protein 2
GS	glycogen synthase kinase
GSLs	glycosphingolipids
GSK-3α/β	Glycogen synthase kinase 3α/β
GTP	Guanosine-triphosphate
GTPase RHEB	RAS homolg enriched in brain
IDE	Insulin degrading enzyme
IGF	Insulin-like growth factor
IGFBP	Insulin-like growth factor binding protein
IGF1R ^{Olig} -/-	Homozygous IGF1R knockout in Olig1 expressing cells
IGF1R ^{PLP} -/-	Homozygous IGF1R knockout in PLP expressing cells
IGF1R	Insulin-like growth factor receptor 1
IGF2R	Insulin-like growth factor receptor 2
IHC	Immunohistochemistry
IKKβ	inhibitory-κB kinase β
InR	Insulin Receptor
InRa	Insulin receptor isoform a
InRb	Insulin receptor isoform b
IR	Heterozygous IRS-2 over expressing transgenice mouse
IRCC	Heterozygous IRS-2 over expressing CC mouse
IRR	insulin receptor-related
IRS-1	Insulin receptor substrate 1
IRS-1 -/-	Homozygous IRS-1 knockout
IRS-2	Insulin receptor substrate 2
IRS-2 -/-	Homozygous IRS-2 knockout

IRSs	Insulin receptor substrates
JNK	C-June-N-terminal kinase
kDA	kilo Dalton
LacC	lactosylceramide
LRP	lipoprotein receptor related protein
mA	milli Ampere
MAPK	Mitogen-activated protein kinase
MAPKKK	MAPK kinase kinase
MAG	myelin-associated glycoprotein
MBP	Myelin basic protein
MEK	Mitogen-acavated protein kinase kinase
MMP	Matrix metalloproteinases
MnSOD	Manganese dependent superoxide dismutase
MOBP	myelin-associated oligodendrocyte basic protein
MOG	myelin oligodendrocyte glycoprotein
MS	Multiple sclerosis
mTOR	target of rapamycin
NAD	nicotinamide adenine dinucleotide
NFTs	Neurofibrillary tangles
NSCs	Neural stem cells
NPCs	Neural precursor cells
OPCs	oligodendrocytes precursors
$p90^{RSK}$	RSK; ribosomal protein S6 kinase
P/S	Penicillin-Streptomycin; Pen Strep
PAGE	Polyacrylamide gel electrophoresis
PAK	p21-activated kinase
PBS	Phosphate buffered saline
PCAF	p300-associated factor
PDK1	Phosphoinosiade-dependent protein kinase 1
PDVF	Polyvinylidene difluoride
PH	Pleckstrin homology
PI	Phosphatidylinositide
PI3K	Phosphadylinositol-tri-phosphat kinase
$PI_{3,4}P$	Phosphadylinositol-di-phosphat
$PI_{3,4,5}P$	Phosphadylinositol-tri-phosphat
PKB	Protein kinase B
PLP	Proteolipid protein

PNS	peripheral nervous system
PP2A	Protein phosphatase 2A
PRMT1	Protein arginine N-terminal methyltransferase
PTB	Phosphotyrosin-binding
PTEN	Phosphatase and tensin homolog
PTPs	protein tyrosine phosphatases
rpm	Rotations per minute
S6K	p70S6 kinase
SCF^{Skip}	Skp1/culcin 1/F-box protein
SDS	Sodium dodecyl sulfate
SDS-PAGE	Sodium dodecyl sulfate-polyacrylamide gel electrophoresis
Ser	Serine
SGK	Glucocorticoid-inducible kinases
SH	Src homology
sIFs	specific translation initiation
SIRT1	silent information regulator 1
SOS	Son of sevenless
TBS	Tris buffered saline
TBS-T	Tris buffered saline 2% TWEEN 20®
TCF/ LEF	T cell factor lymphoid enhancer factor
TEMED	N,N,N',N'-tetramethylethylenediamine
Thr	Threonine
TNFα	Tumor necrosis factor α
TSC-2	tuberin 2
TWEEN 20®	Polyoxyethylene (20) sorbitan monolaurate (Polysorbate 20)
Tyr	Tyrosine
WT	Wildtype

1. Introduction

1.1. Insulin-like growth factor and insulin receptor signaling

The insulin-like growth factor (IGF) signaling (Fig.1) is known to have an essential role in the normal growth and development of the central nervous system (CNS). IGF signaling possesses pleiotropic effects on all major neural cell types, as well as neural stem cells (NSCs), post-mitotic neurons, oligodendrocytes and astrocytes. IGF-I and IGF-II are able, by interacting with the type 1 IGF receptor (IGF1R) to promote proliferation, maturation, survival as well as growth of neural cells. Furthermore there is evidence that IGF signaling is able to influence specific biological processes by modulating neural signals. This can facilitate primary instructive signals to steer NSC in the direction of a specific cell lineage during early development [O'Kusky and Ye, 2012; Broughton and Partridge, 2009].

The IGF system consists of IGF-I, IGF-II, the IGF1R, the type 2 IGF receptor (IGF2R), and the IGF binding proteins (IGFBPs). Growth promoting actions of the IGFs are for the most part mediated by the IGF1R. Receptor binding and biological activities are regulated by IGFBPs. Here at least 10 IGFBPs, where six are high-affinity and four low-affinity IGFBPs, are known. Both IGFs are able to bind at high concentrations to the insulin receptor (InR). Especially the InR is competent to mediate IGF-II actions [Louvi et al., 1997; Morrione et al., 1997].
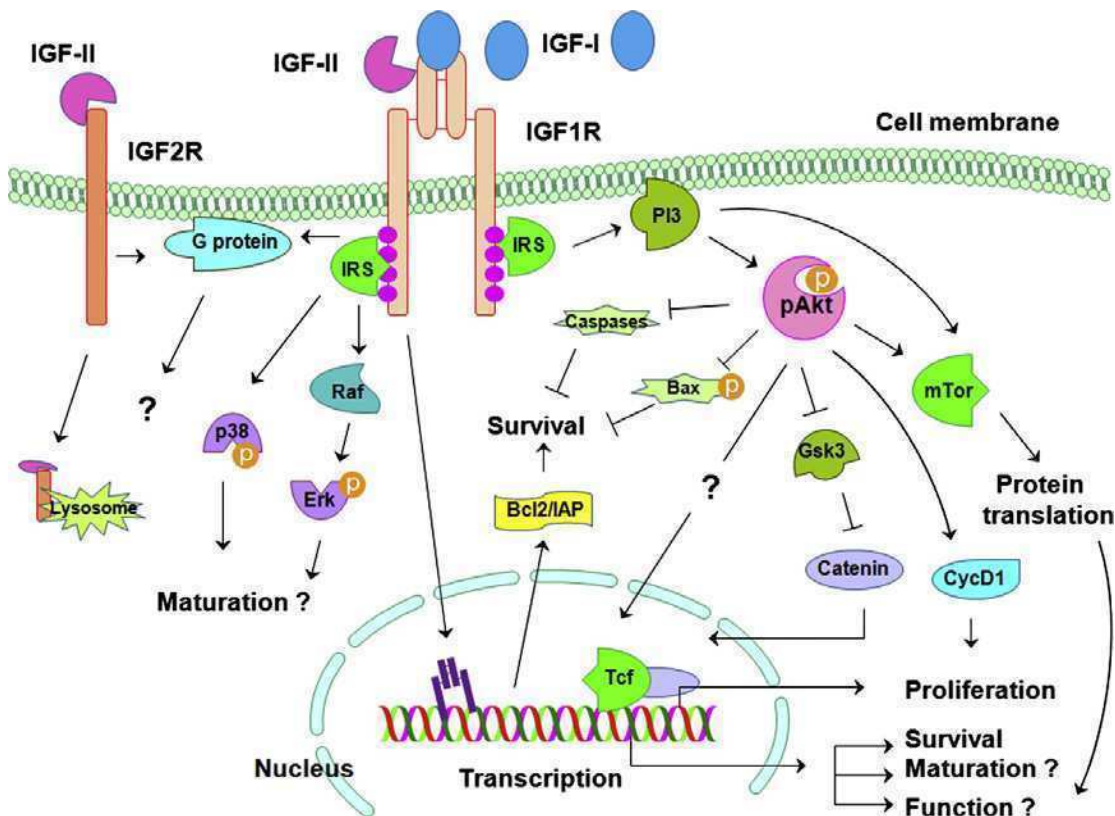
Figure 1: IGF signaling in the brain
IGF signaling pathways in the CNS are schematically pictured. Signaling molecules and pathways in non-neuronal cells are not shown. ⊥ = inhibitory modification, and ↓ = stimulatory modification [O'Kusky and Ye, 2012]

1.1.1. The insulin receptor

The InR, with more than 150 kilobases in length containing 22 exons and 21 introns and is located on the short arm of the human chromosom 19 [Seino and Bell, 1990]. It consists of two α-subunits which are both linked to a β-subunit and to each other via disulfide bonds (Fig.2) [Seino and Bell, 1990]. There are two different isoforms present due to alternative splicing of exon 11 which encodes for 12 amino acids (aa). The first isoform A lacks those 12 aa while isoform B contains those. In contrast the IGF1R gene possesses no equivalent to exon 11, therefore no alternative splicing has been described, yet. Both isoforms of the InR are able to bind with the same affinity to insulin [McClain, 1991]. Alongside isoform A reveals a higher affinity to IGFs than isoform B [Yamaguchi et al., 1991; Frasca et al., 1999]. Isoform A is mainly expressed in fetal tissue, hematopoietic cells and in the adult nervous system, isoform B predominatly is found in adipose tissue, muscle and liver [Seino and Bell 1989; Moller et al., 1989; Goldstein and Kahn, 1989; Mosthaf et al., 1990].
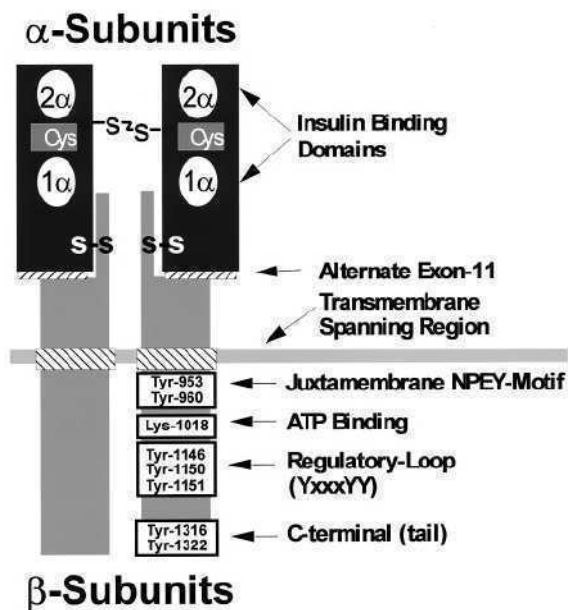
Figure 2: Schematic diagram of the insulin receptor tretramer
The cell membrane is pictured as a horizontal line. The insulin binding sites are presented in the α-subunit, and the autophosphorylation sites are numerated in the β-subunuits. [White, 1997]

As the α-subunits are entirely located outside of the cell and comprise the side for insulin binding. The β-subunits include an extracellular, a transmembrane and an intracellular domain containing the insulin-regulated tyrosine protein kinase. There are two other structurally related molecules, which belong to the insulin receptor family, the IGF1R and the insulin receptor-related (IRR) receptor, which is an orphan receptor for which, no ligand has yet been indentified [Shier and Watt, 1989].

1.1.2. The IGF1R and IGF2R

The IGF1R was discovered later than the InR (1974), which tyrosine activity was found in 1982 [Megyesi et al., 1974; Kasuga et al., 1982; Kasuga et al. 1982], and then as well classified as a receptor tyrosine kinase [Megyesi et al., 1974; Jacobs et al., 1983; Rubin et al., 1983]. Also the IGF1R is ubiquitously expressed in all neural cell types (also neural stem cells and neural precursor cells) [Popken, Dechert-Zeger, Ye and D'Ercole, 2005]. The abundance of the IGF1R is corellated to cell proliferation and growth [O'Kusky and Ye, 2012; Zhang, Moats-Staats, Ye and D'Ercole, 2007].

As the InR, the IGF1R is a heterotetrameric glycoprotein which, is linked by disulfide bounds α- and β-subunits. The 135kDa α-subunits are located outside the cell and are able to bind IGFs [Van Obberghen et al., 1981; Ullrich et al., 1986]. The β-subunits with a size of 95kDa consist of a long intracytoplasmic domain which contains intrinsic tyrosine kinase activity as well as critical tyrosine and serine residues. As the IGF1R has a 46% homology with the InR, both receptors can form hybrid receptors. To form those they use the α- or β- subunits of each other. IGF1R/InR hybrids remain capable to transduce both IGF and/ or insulin signaling, even though the exact functional significance is still unkown. Dependent on the assembly of InR or IGF1R, different affinities of binding to insulin or IGF-I occur [Pandini et al., 2002]. Whereas IGF-II and insulin are bound to the hybrid of IGF1R and the isoform A of the InR with similar affinity, the hybrid of IGF1R and isoform B is only capable to bind IGFs [Louvi, Accili, and Efstratiadis, 1997].

Binding of IGF-I to the α-subunit of the IGF1R triggers a conformation change leading to autophosphorylation of the β-subunit at Tyr1131, 1135 and 1136. This stimulates signaling cascades which result in phosphorylation of a variety of intracellular substrate proteins [LeRoith et al. 1995] for instance insulin receptor substrate (IRS) -1 and 2. The same happens to the InR, here are the autophosphorylation sides Tyr 1146, 1150 and 1151 [Kahn et al., 1978; Kasuga et al., 1982; Chou et al., 1987; White, 1998].

The IGF2R is in contrast a single chain transmembrane protein. It's construction is identical to the cation-independent mannose-6-phosphate receptor and works to translocate proteins which contain mannose-6-phosphate motives and IGF-II to lysosomes for their degradation. Intrinsic enzymatic activity for the intracellular domain of the IGF2R has not been observed. Besides that there is evidence, that it interacts with IGF-I and that it might mediate partially IGF growth promoting activity in the brain [O'Kusky and Ye, 2012]. Additionally IGF-II has a growth- promoting function during mouse embryogenesis, which is partly mediated by signaling through the InR [Efstratiadis et al., 1997].
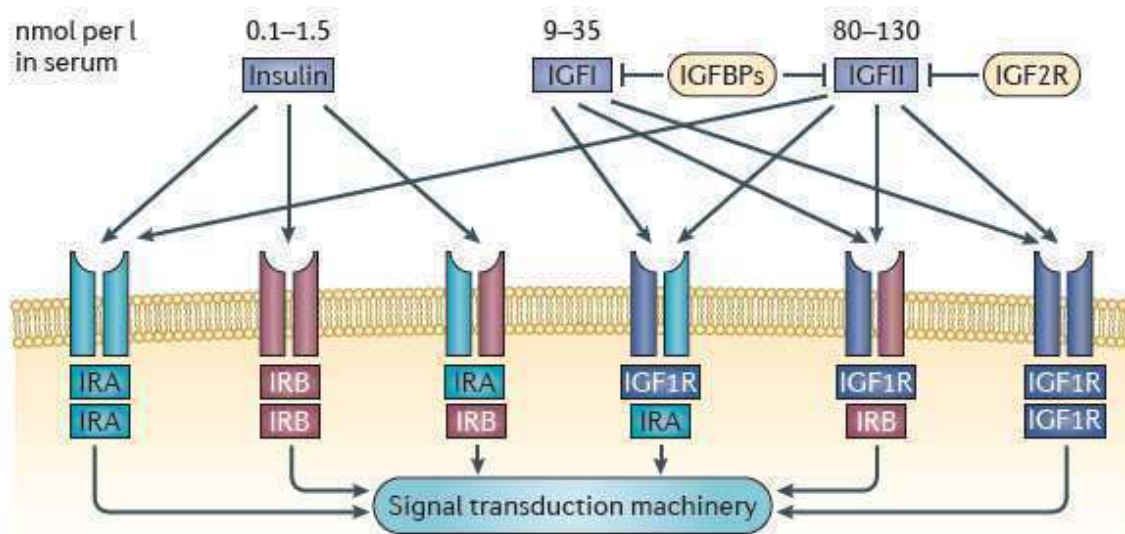
Figure 3: The InR and IGF1R family
Shown are the two splice variant isoforms of InR (InRa and InRb) and the IGF1R. Those can dimerize to form six receptor species, which vary in their ligand affinitiy. Insulin circulates in lower concentrations than IGFs, but has direct access to target tissues. Whereas IGFs can be bound by IGFBPs and therefore cannot reach the receptor. Or as IGFII through IGF2R, which targets the ligand for degradation without signal transduction. [Pollak, 2012]

1.1.3. IGF binding proteins

At least 10 IGFBPs, where six are high-affinity and four are low-affinity IGFBPs, are known. IGF-I and IGF-II which are circulating and found in the extracellular space of most tissues are almost completely bound by the IGFBPs. The high affinity IGFBPs are represented by IGFBP-1 to IGFBP-6. These share their structural homology and bind specifically to IGF-I and IGF-II [Jones and Clemmons, 1995]. Through this interaction they are either able to attenuate (mostly IGFBP-4 and -6) or increase (mainly IGFBP-3 and -5) binding of IGF-I to its receptor [Rajaram, Baylink and Mohan, 1997; Mohan et al., 1995; Qin et al., 1998; Jones and Clemmons, 1995; Firth and Baxter, 2002; Rechler and Clemmons, 1998].Their affinity to bind IGFs is equally or even higher than that of the IGF1R [Duan and Xu, 2005]. Within the brain IGFBP-2 to -5 are the most abundant. The IGFBPs are expressed within the CNS in a specific temporal-spatial pattern, but their exact function needs further investigation.

There are differencing proposals on how they might act: (1) transport proteins in the plasma, (2) prolongation of the half live of IGFs during circulation, (3) determination of the tissue- and cell-specific localization of IGFs and, (4) control the biological actions of IGFs via modulation of the interaction with their receptor [Jones and Clemmons, 1995; O'Kusky and Ye, 2012].

Additionally to this some IGFBPs may act independent to the IGFs. IGFBP-1 is for instance able to activate integrin-mediated intracellular signaling in trophoblast and enhances oligodendrocytes migration [Gleeson et al., 2001, Chesik et al., 2010]. Furthermore IGFBPs reduce the beneficial effect of IGF-I as a neurotrophic and survival factor for postnatal neurons [Vaught et al., 1993]. IGF-I has an important potential for treatment of amyotrophic

lateral sclerosis (ALS). It has been shown that IGF-I in combination with glial cell line-derived neurotrophic factor was able to rescue completely rat motor neurons from chronic glutamate-mediated toxicity and showed a additive neuroprotection [Bilak, Corse and Kuncl, 2001].

As the IGFBPs modulate the action of the IGFs, they are themselves regulates through IGFBP proteases [Mohan et al., 2002].

1.1.4. Insulin receptor substrates

Upon insulin or IGFs binding to the InR or the IGF1R a conformational change is triggered, leading to the autophosporylation of the β-subunits. Afterwards the IRS are recruited to the receptor, which leads to phosphorylation of the IRS proteins. There are at least 4 IRS proteins known, IRS-1 to IRS-4 [Sun et al., 1991; Lavan et al., 1997; Lavan, Lane, and Lienhard, 1997]. In 1985 the first IRS was found and called pp185 (as it is 185kDa in size). It was cloned in 1991 and later named IRS-1 [White, Maron, and Kahn, 1985; Sun et al., 1991]. Furthermore, IRS-2 (160kDa) was discovered 1995 and IRS-3 (60kDa) likewise IRS-4 (160kDa) in 1997 [Sun et. al., 1995; Lavan et al., 1997; Lavan, Lane, and Lienhard, 1997].

The IRS proteins are widely expressed in the CNS, IRS-1, -2, -4 and Gab-1 in an tempo-spatial specific pattern [Fantin et al., 1999; Folli, 1994; Holgado-Madruga, 1996; Numan and Russell, 1999; Sciacchitano and Taylor, 1997; Ye, Li, Lund and D'Ercole, 2002] and only a small amount of IRS-3 proteins are dectected in the adult brain [Sciacchitano and Taylor, 1997]. All of the IRS have a similar structure. They consists of a N-terminal pleckstrin homology (PH), a phosphotyrosine-binding (PTB) domain and C-terminus, which contains multiple tyrosine phosphorylation sides. Those phosphortyrosine motifs are binding sides for Src homology (SH) 2 domain containing proteins [Yenush and White, 1997; White, 1997]. The PTB domain is able to bind to the phosphorylated NPXP motif at the juxtamembrane domain of the receptor, after IGFs or Insulin has bound, linking the IRS proteins to the particular receptor [Cheatham and Kahn, 1995; White, 2002]. The PH domain couples to lipids and with a high affintiy to phosphoinosides [Fruman, Rameh and Cantley, 1999; Moll, Zemva and Schubert, 2011].

There are 21 putative tyrosine phosphorylation sides within IRS-1 and in different tyrosine kinase specifity motives [Songyang, 1995; Sun et al., 1991]. Compared to IRS-1, 14 of this tyrosine phosphorylation sides are conserved, four sides contain alternate surrounding sequences, three are not found and four sides are exclusively present in IRS-2 (Fig. 4) [Sun et al., 1995; White, 1997]. In contrats to IRS-1, IRS-2 includes a domain that can bind to the phosphorylated kinase regulatory loop of the β-subunit of the InR. It is called KLRB domain [Sawka-Verhelle et al., 1997; Sawka-Verhelle et al., 1996] and its physiological function remains unclear [Moll, Zemva and Schubert, 2011].

Insulin binding induces tyrosine and serine phoyphorylation in IRS-1 [Gual, Le Marchand-Brustel and Tanti., 2005]. This serine phosphorylation is a tool to regulate IRS-1 action, positives and negatives [Weigert et al., 2005; Weigert et al., 2008]. Responsible for the different effects are not ony the location of the Ser phosphorylation sites within the IRS-1 protein but also the timing of the phosphorylation.The sides with positive effect are thought to be phosphorylated first, so that IRS-1 is protected from negative actions, due to phosphorylation at inhibitory residues [Weigert et al., 2005; Weigert et al., 2008; Gual, Le Marchand-Brustel and Tanti., 2005; Luo et al., 2007] and therefore preventing the association with tyrosine phosphatases [Luo et al., 2005]. Negative effects are caused by phosphorylation of serine sides near the PTB domain, this disrupts the association between IRS-1 and the particular receptor leading to degradation of IRS-1. If serine residues in the C-terminus are phosphorylated, the interaction between IRS-1 and the phosphatidylinositide (PI)3-kinase might be disturbed [Gual, Le Marchand-Brustel and Tanti., 2005; Boura-Halfon and Zick, 2009]. Those serin sides are phosphorylated via serine kinases like mammalian traget of rapamycin (mTOR), PKCzeta and p70S6 (S6K) kinase [Boura-Halfon and Zick, 2009, Herschkovitz et al., 2007; Gual et al., 2003; Moll, Zemva and Schubert, 2011]. Further Ser phosphorylation of IRS-1 might case insulin/ IGF-I resitance. Here c-Jun N-terminal kinase (JNK), mTor/S6K, inhibitory-κB kinase β (IKK β), SIK-2 and extracelluar signal regulated kinase (ERK) seem to be included [Moll, Zemva and Schubert, 2011; Boura-Halfon and Zick, 2009; Herschkovitz et al., 2007]. Furthermore it has been shown, that TNFα is able to induce serine phosphorylation of IRS-1 in cultured adipocytes and Fao cells, which inhibits insulin signaling [Hotamisligi,l 1996; Kanety, 1995; Shier, 1989].

The role of serine phosphorylation sides in IRS-2 are still under inverstigation. However it has been shown, that a disruption between IRS-2 and its receptor can be caused, via the phosphorylation of JNK at Thr 348 [Solinas et al., 2006].

Even tough the IRS proteins contain the same functional domains, they regulate different processes due to their distinct cellular distribution and their individual abundance in specific cells. For both proteins it is known, that they play a role during insulin-stimulated glucose transport [Hara et al., 1994; Okada et al., 1994; Quon et al., 1994; White, 1997].

IRS-1 is able to mediate some neural actions, but it seems that it is not essential for neural IGF-I signaling [Pete, 1999; Schubert, 2003; Ye, Li, Lund and D'Ercole, 2002]. Deletion of IRS-1 expression does not inhibit IGF-I stimulated brain growth and myelin-specific expression [Ye, Li, Lund and D'Ercole, 2002]. Those mice showed a significant higher level of IRS-2 and -4, so that it is reasonable to assume that the different IRS proteins compensate for each other [O'Kusky ,2012].

In contrast deleting IRS-2 globally (IRS-2 ($^{-/-}$)) [Schubert, 2003] or specific within nestin-expressing cells [Taguchi, 2007], decreased brain weight by 30-38 %. It seems that IRS-2 plays a more significant role in mediating IGF-I/ insulin signaling in the CNS. IRS-2 ($^{-/-}$) mice exhibit at E14-E16 less proliferating neural cells, but no changes in apoptosis [Schubert, 2003]. Thus IRS-2 appears to be able to transduce proliferation signaling at this stage, on the other hand it is not crucial for pro-survival signaling. However IRS-2 is competent of mediating pro-survival signaling in certain cells. Which was shown via an increased number of apoptotic photoreceptors (50%) in the retina of 2 weeks old IRS-2 ($^{-/-}$) mice [O'Kusky, 2012; Yi et al., 2005]. Furthermore, a decreased amount of multiple myelin-specific proteins appeared during the first two weeks of postnatal life [Freude et al., 2008], which is compensated during ageing in IRS-2 ($^{-/-}$) mice [Freude et al., 2008, O'Kusky, 2012].
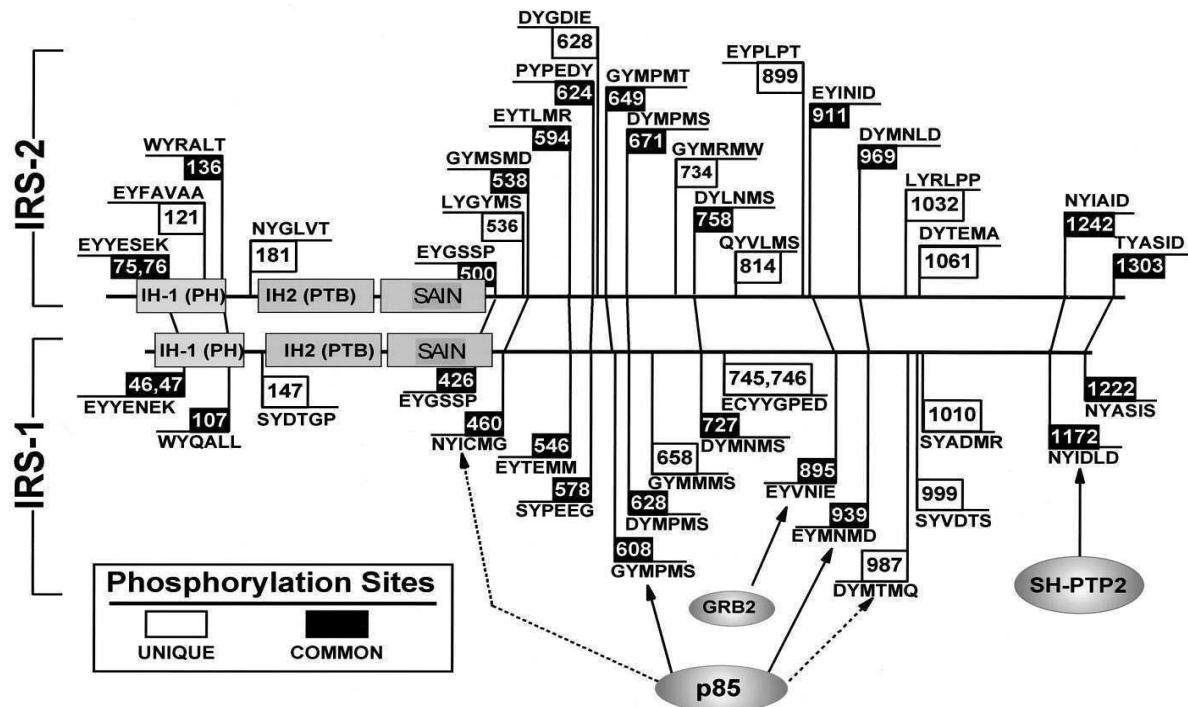
Figure 4: IRS-1 and IRS-2 and their phosphorylation sites
At the NH$_2$-terminus is schematic shown the two or rather three conserved modules (IH1^{PH}, IH2^{PTB} and SAIN), which are believed to interfere with receptors or other interaction partners. Putative tyrosine phosphorylation sides are pictured in the COOH-terminal region. In open boxes entirely unique sides and conserved (but not absolutely) motifs are displayed in black boxes. Visible is that IRS-2 is about 100 residues longer than IRS-1. [White, 1997]

1.1.5. Phosphatidylinositide(PI)3 kinase signaling

There are three classes of PI3K (class I-III) and class I is further subdivided into Ia and Ib [Vanhaesebroeck et al., 2005]. These kinases are heterodimeric containing a 110kDa catalytic subunit (p110) and a regulatory subunit (p85). The catalytic subunit is non-covalently connected to the regulatory [Moll, Zemva and Schubert, 2011]. Class Ia is the best characterized and multiple Ia isoforms for the regulatory subunit (p85α, p85β, p55α, p50α and p55γ) and the catalytic subunit (p110α, p110β and p110δ) are known [Wymann and Pirola, 1998; Acebes and Morales, 2012]. This Class of PI3K is involved in the IGF1 and insulin signaling pathway [Fruman, Meyers and Cantley, 1998]. After activation of the InR and IRS binding, the PI3K is recruited to the membrane via the p85 regulatory subunit. Furthermore other factors, such as growth factor receptor binding protein (GRB)-2 and the SH2 Phosphatase (SHP)2 are recruited to the IRS proteins. The catalytic subunit phosphorylates phosphatidylinositide-diphosphate ($PI_{4,5}P$) to generate phosphatidylinositide-triphosphate ($PI_{3,4,5}P$) [Vanhaesebroeck et al., 2001; Wu et al., 2007]. The opposing phosphatase of this reaction in PTEN (the phosphatase and tensin homolog deleted on chromosome ten), which can induce a reverse [Maehama and Dixon, 1998]. After the generation of $PI_{3,4,5}P$ further downstream targets are activated, like phosphoinositide-dependent protein kinase(PDK)-1/-2, protein kinase B (PKB, also known as AKT), and inhibition of glycogen synthase kinase-3 (GSK-3) is induced. PKB is found in two isoforms PDK-1 and PDK-2. PDK-1 can partly activate the serine/ threonine kinase AKT (57kDa) by phosphorylation at Thr308, but for full activation the phosphorylation of Ser473 is required [Alessi et al., 1996; Lawor and Alessi, 2001; Stokoe et al., 1997; Freude, 2010]. The three isoforms of AKT contain a conserved kinase domain, a PH-domain at the N-terminus next to a regulatory subunit at the C-terminus [Hresko, Murata and Mueckler, 2003]. Furthermore $PI_{3,4,5}P$ activates AKT, which leads to phosphorylation of tuberin 2 (TSC-2). A heterodimer of TSC-1 and TSC-2 with GTPase activity is formed, which then can inhibit the GTPase RHEB (RAS homolg enriched in brain) [Astrinidis and Henske, 2005; Hay and Sonnenberg, 2004]. PDK-1 and mTOR activate via phosphorylation S6K. mTor itself is negatively regulated through GSK-3 and human tuberin [Ruggero and Sonenberg, 2005; Manning and Cantley, 2007; Acebes and Morales, 2012] . The regulation of protein synthesis via IGF-I starts due to the control of the intrinsic activity and/or binding properties of specific translation initiation (sIFs) and elongation factors (eEFs). Phosphorylation of 4E-BP (4E binding protein) via mTOR leads to the release of eIF4E (eukaryotic initiation factor 4E). eIF4E is now able to form an active complex. This complex formation boosts the start of translation and the activation of S6K [Nojima et al., 2003; Oshiro et al., 2004; Freude, 2010; Moll, Zemva and Schubert, 2011].

Furthermore GSK-3β, a major tau kinase and BAD (Bcl-2 Bcl-X-associated death promoter), a proapoptotic factor are inactivated [Song, Ouyang and Bao, 2005] via the InR and IGF1R signaling cascade. BAD interacts with Bcl-2, a apoptosis suppressor, but more intensely with Bcl-X$_L$ via its BH3 homology domain [Yang et al., 1997; Zha et al., 1997]. This is regulated via the phosphorylation state of BAD by the InR/ IGF1R signaling cascade.

Taken together the IGF1R signaling pathway is potent in inhibiting neural apoptosis [Schubert et al., 2003; Moll, Zemva and Schubert, 2011].

1.1.6. Glycogen synthase kinase-3

GSK3 is a constitutive active kinase, which regulates cell metabolism by phosphorylation of glycogen synthase (GS) and other substrates. Inhibition of GS through GSK3 leads to a reduction of glycogen synthesis and inhibition of GSK3 to increased glycogen synthesis [Henriksen and Dokken, 2006; Lee and Kim, 2007]. Upon stimulation of the InR/ IGF1R signaling cascade phosphorylation of GSK3α/β at the regulatory of Ser21(α) or 9(β) leading to inhibition of the kinase [Gao, Hölscher, Liu and Li, 2012]. Alternatively GSK3 is activated via protein kinase C (PKC). It has been shown, that inhibition of PI3K and PKC results in over activation of GSK3 [Liu et al., 2008]. Additionally GSK3 is able to regulate protein synthesis via controlling inhibition factor 2B (IF2B) activity [Welsh and Proud, 1993; Van Wauwe and Haefner, 2003].

Moreover GSK3 is also involved in Wnt signaling. Thus GSK3 is a connection between the InR/ IGFR- and the Wnt-signaling pathway. The essence of Wnt is the phosphorylation/ degaradation of cytosolic β-catenin (Figure 5). Is Wnt absent, cytoplasmic β-catenin is permanent degraded by the axin complex. This axin complex consists of the scaffolding protein axin, the tumor suppressor *adenomatous polyposis coli* gene product (APC), casein kinase 1 (CK1), and GSK3. Axin uses different domains to interact with GSK3, CK1 and β-catenin. It thereby coordinates sequential phosphorylation of β-catenin at Ser45 by CK1α, followed by phosphorylation of Thr41, Ser37 and Ser33 by GSK [Kimelman and Xu, 2006; He et al.,2004]. If β-catenin is phosphorylated at Ser33 and Ser 37, a binding site for E3 ubiquitin ligase β-Trcp is created, which leads to ubiquitination and degradation by the proteasome [He et al 2004]. Due to β-catenin degradation, Wnt target genes are repressed by the DNA-bound T cell factor lymphoid enhancer factor (TCF/ LEF) family of proteins (Fig 5 A: Wnt off state).

Activation of the Wnt pathway occurs via Wnt ligand binding to a seven-pass transmembrane Frizzled (Fz) receptor and its co-receptor, low-density lipoprotein receptor related protein 6 (LRP6) or its close relative LRP5. The Wnt-Fz-LRP6 complex is formed and recruitment of the scaffolding protein Dishevelled (Dvl) results in LRP6 phosphorylation and activation. In

additional the axin complex is guided to the receptors. This results in the inhibtion of axin-mediated β-catenin phosphorylation and hence stabilization of β-catenin takes place, which can now reach the nucleus to form a complex with TCF/LEF and activates Wnt target gene expression (Fig 5 B: Wnt on state) [MacDonald, Tamai and He, 2009].
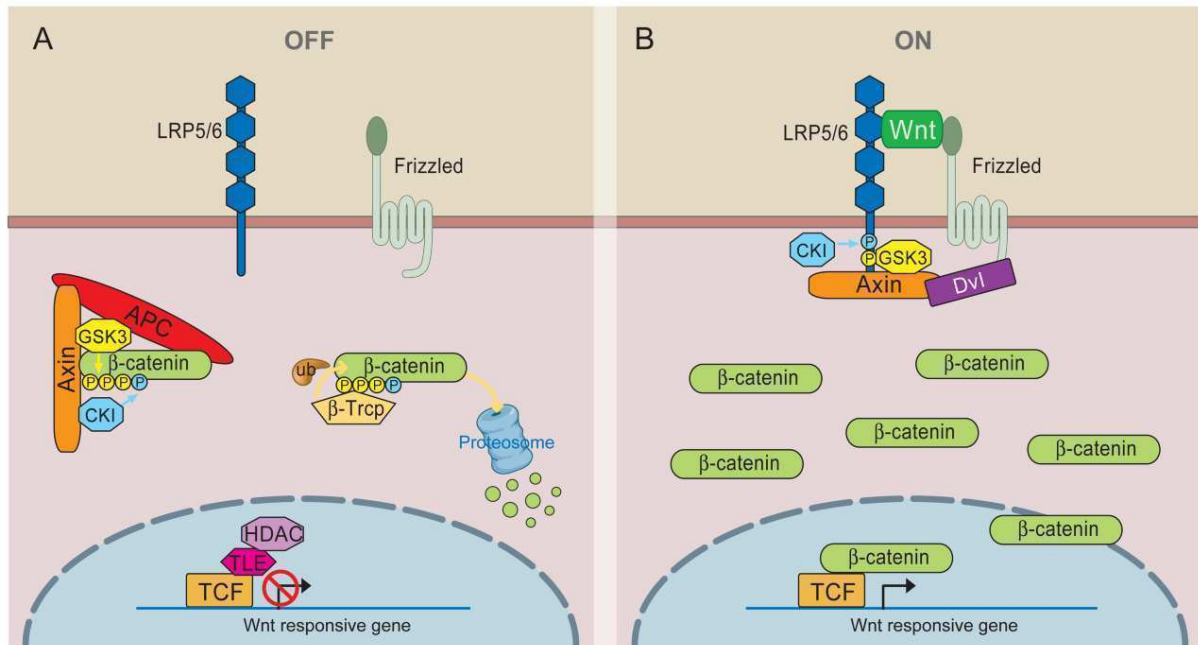
Figure 5: Wnt/β-catenin signaling
A) Wnt-off state: Wnt is absent, therfore cytoplasmic β-catenin forms a complex with axin, APC, GSK3 and CK1 and is phosphorylated by CK1 (blue) and subsequently by GSK3 (yellow). Phosphorylated β-catenin is recognized by the E3 ubiquitin ligase β-Trcp, which targets β- catenin for proteosomal degradation. Wnt target genes are repressed by TCF-TLE/Groucho and histone deacetylases (HDAC).
B) Wnt- on state: Is Wnt ligand present, a receptor complex forms between Fz and LRP5/6. Dvl recruitment by Fz leads to LRP5/6 phosphorylation, and axin recruitment. This disrupts axin-mediated phosphorylation/degradation of β-catenin, allowing β-catenin to accumulate in the nucleus where it serves as a co-activator for TCF to activate Wnt responsive genes. [MacDonald, Tamai and He, 2009]

1.1.7. Forkhead box O transcription factors

The mammalian forkhead box O transcription factor (FoxO) family consists of four members, FoxO1, FoxO3a, FoxO4 and FoxO6 [Clark et al., 1993]. All of these contain a conserved forkhead domain (FKHR) and recognise a consensus Foxo-recognised element (FRE). The sequence of this element is (G/C)(T/A)AA(C/T)AA [Biggs et al., 1999; Furuyama et al., 2000; Gilley, Coffer and Ham, 2003] and present for intance in IGFBP-1 [Barthel, Schmoll, and Unterman, 2005; Cichy et al., 1998], Fas ligand (FasL) , p27[KIP1] [Dijkers, Medema, Pals et al., 2000; Medema et al., 2000], Bim [Dijkers et al., 2000] and MnSOD [Kops et al., 2002]. FoxOs regulate genes that are involved in apoptosis, metabolism, growth, ageing and development [Partridge and Bruning, 2008].
FoxO1 and 3a are ubiquitously expressed, 6 is only found in the brain and 4 has yet not been detected in the brain [Furuyama et al., 2000; Jacobs et al. 2003]. FoxO1 is predominantly

expressed in the adult brain in the in the striatum, dentate gyrus and ventral hippocampus and FoxO3a in the cortex, cerebellum and hippocampus. FoxO6 has been detected in the amygdala, hippocampus and cingulite cortex [Hoekman et al., 2006].

The FoxOs are phosphorylated by AKT, which induces binding of 14-3-3 and therefore nucleus exclusion leading to the termination of the FoxO-mediated transcription. Depending on the stimulus there are other kinases beside to AKT which are able to phosphorylate FoxOs [Huang and Tindall 2007]. For instance FoxO1 can additionally be phosphorylated by dual-specificity tyrosine-phosphorylated and regulated kinase (DYRK). DYRK phosphorylates FoxO1 at Ser329. Whereupon FoxO1 activity is inhibited [Woods et al., 2001]. Additionally glucocorticoid-inducible kinases (SGKs) are able to phosphorylate FoxOs [Brunet et al., 2001]. Furthermore activation of the C-Jun-N-Terminal kinase (JNK) upon oxidative stress leads to nuclear localization of FoxO3a (Lehtinen et al., 2006).

After the exclusion from the nucleus FoxOs are targeted for proteasome-mediated degradation. FoxO1 is polyubiquitilated by e.g. Skp2, the substrate-binding component of the Skp1/culcin 1/F-box protein(SCF^{Skip}) E3 ligase complex. In addition to phosphorylation, acetylation is another posttranslational modification of FoxOs. For example CBP and p300 with their associated proteins like CBP- and p300 associated factor (PCAF) show intrinisic histone acetyl-transferase activity [Li et al., 2003]. Due to acetylation via CBP FoxO transcription factors are inhibited [Daitoku et al., 2004]. Deacetylation is achieved through the silent information regulator 1 (SIRT1), which is a nicotinamide adenine dinucleotide(NAD)-dependent histone deacetylase. Upon stress stimuli SIRT1 forms a complex with acetylated FoxOs and [Brunet et al., 2004; Kitamura et al., 2005] to regulate FoxO mediated transcription via deacetylation.

1.1.8. MAPK signaling

The second main signaling pathway that InR and IGF1R activate is the mitogen activated protein kinase (MAPK) cascade. This pathway is one of the primordial signaling systems nature has used in different permutations to achieve a variety of tasks. This basic arrangement consists of a G-protein working upstream of a core module including three kinases: a MAPK kinase kinase (MAPKKK) that phosphorylates and activates a MAPK kinase (MAPKK) that then activates MAPK. This provides strong signal amplification and besides this allows additional control (Fig.6) [Kolch, 2000].

Is the receptor activated, the IRS proteins get phosphorylated and GRB-2 is feasible to bind [White, 2002]. GRB-2 binds to son of sevenless (SOS), a GDP/GTP exchange factor. SOS is towed to the membrane during this process by the growth-factor-receptor bound protein 2 adapter protein that spots tyrosine phosphate docking sites [McCormick, 1993]. This leads to

the activation of the small G protein RAS and to the recruitment of CRAF (c-raf leukemia viral oncogene) and finally the extracellular signal-regulated kinases (ERK)-1/-2 are activated [Kolch , 2000]. Transcriptional activity is stimulated through activated ERK via direct phosphorylation of ELK-1 member of ETS oncogene family) and FOS (FBJ osteosarcoma oncogene). It is known that ERK-1 and -2 activity is important for long-term potentiation and memory consolidation in the CNS [Sweatt, 2001]. However if ERK-1 and -2 is overactive it might induce cell death in case of oxidative stress or growth factor deprivation [Zhuang and Schnellmann, 2006].
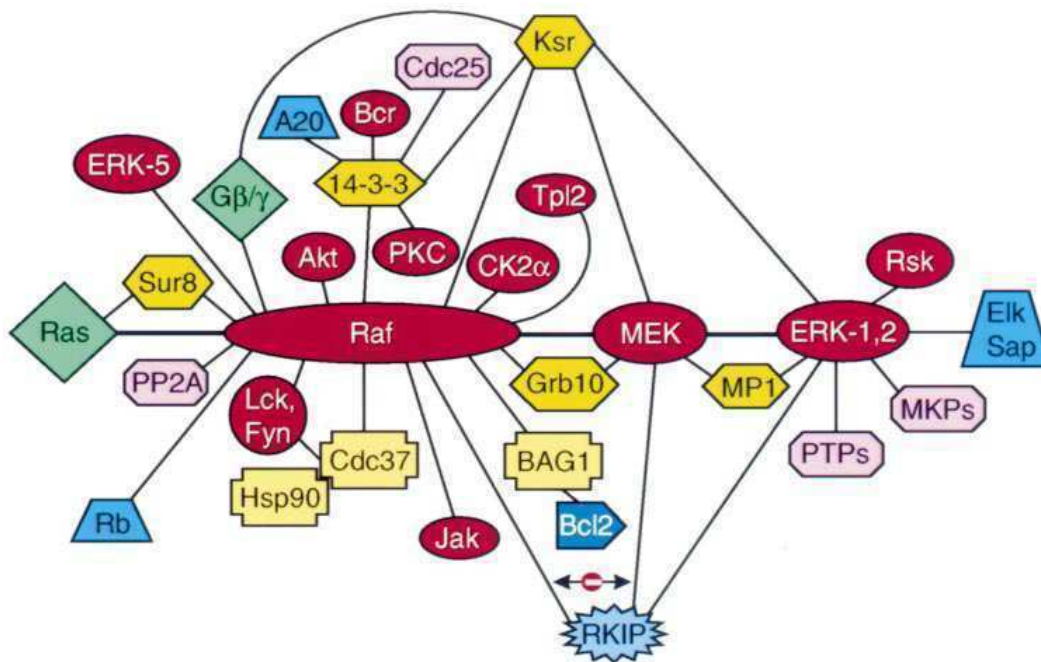
Figure 6: The Multi-protein signaling complexes
Interactions between the proteins are indicated by lines. All possible interactions are shown. Kinases are pictured red; G-proteins green; phosphatases in pink, adapters in dark yellow, chaperones in light yellow, and transcription factors in blue with black letters. The minus symbol indicates that RKIP dissociates the interaction between Raf and MEK. [Kolch, 2000]

1.2. Multiple sclerosis

Multiple sclerosis (MS) is an inflammatory demyelinating disease that attacks the brain, spinal cord and optic nerves in the CNS, but does no affect the nerve roots and peripheral nerves. The pathology appears as follows: 1) primary demyelination with little damage to oligodendrocytes, 2) demyelination and extensive oligodendrocytes loss 3) primary oligodendrocyte loss with secondary demyelination; and 4) activation of macrophages causing non-selective tissue damage, where not only myelin and oligodendrocytes are involved but also astrocytes and axons. Axonal loss is an unstoppable result of MS and might be the pathological correlate of the irreversible neurological impairment of this disease [Ferguson, Matyszak, Esiri and Perry, 1997; Lovas et al., 2000; McGavern et al., 2000; Trapp

et al., 1998]. Interestingly oligodendrocytes progenitors are present in the lesion of MS, but are fail to remyelinate those regions [Scolding 1998; Wolswijk; 1995; Wolswijk; 2000].

Mostly the first clinical symptoms of MS appear between 15 and 50 years of age. However, there are MS cases known not older than 3 or older than seventy years of age [McFarlin and McFarland, Part 1 and 2, 1982]. Females are twice as often affected than males. This disease has usually a relapsing-remitting course where neurologic episodes are repeated and followed by partial or even complete recovery or with periods free of new symptoms. If a patient has relapsing-remitting MS they mostly develop secondary progressive MS, where there is progressive bettering. 10% of MS patients emerge as primary progressive form, which means progressive neurologic deterioration with superimposed reacceleration. MS patients are able to live up to 40 years after onset of the disease [Pender and Greer, 2007]. It is a disease which, is not necessarily life shortening, but it worsens quality of life through deficits of sensormotoric, autonomic and neurocognitive functions [Sospedra and Martin, 2005].

MS is thought to be a CD4$^+$ Th1-mediated disease [McFarland and McFarlin, 1992; Hafler, 2004]. This idea has raised from data of experimental allergic (autoimmune) encephalomyelitis (EAE) experiments. EAE models show similarities with MS to human, because the injections of myelin components into susceptible animals leads to CD4$^+$-mediated autoimmune disease [McFarland and McFarlin, 1992; Zamvil and Steinman, 1990]. Are those CD4$^+$ T cells transferred into a normal healthy animal, they induce EAE in the healthy animal [McFarland and McFarlin, 1992; Zamvil and Steinman, 1990; Pettinelli and McFarlin, 1981]. There are only two known options to transfer EAE, CD4$^+$ T cells and CD8$^+$ T cells, but not via antibodies [Huseby et al., 2001; Sun et al., 2001]. Indirectly this hypothesis is supported by the knowledge that certain HLA class II molecules are the strongest genetic risk factors for MS. However the breakdown of the blood-brain barrier (BBB) and virus-induced demyelination might be a primary and important events in the pathological manifestation of MS [Wekerle, 1993; Fazakerly and Buchmeier 1993]. Alteration of the BBB allows circulating antibodies the entry into the CNS, especially demyelinating antibodies such as anti- myelin oligodendrocyte glycoprotein (MOG) antibodies [Genain et al., 1996; Genain et al., 1999; Linington et al., 1988; Brosman and Raine; 1996]. Activated T cell trigger the release of proinflammatory cytokines, such as TNFα and interferon-γ by inflammatory cells, macrophages and microglia [Brosman and Raine; 1996]. Other mechanisms beside this might be that oligodendrocytes engulf a high iron content and are therefore prone to oxidative stress by reactive oxygen species [Griot, Burget, Vandevelde and Peterhans, 1989]. Neurotransmitter e.g. glutamate can also act negatively on oligodendrocytes and induce demyelination [Matute, 1998; Pitt, Werner and Raine, 2000; Steinman, 2000].

Furthermore a group of zinc-dependent enzymes, the matrix metalloproteinases (MMP) which degrade extracellular matrix components [Yong et al., 1998]. Additionally MBP [Chandler; 1995] is increased in active and chronic MS [Maeda and Sobel; 1996]. Especially MMP-7 and MMP-9 are elevated [Cossins et al., 1997]. It seems that there is more than one mechanism present in the same affected MS lesion [Ludwin; 1997].

Beside the autoimmune hypothesis environmental and genetic MS risk factors have been discussed as influencing factors. For example dietary intake and/ or UV metabolized Vitamin D3 is able to lower the incidence of MS [Ramagopalan et al., 2009]. However this is no explanation for the appearance of MS in regions, where the population is are able to receive Vitamin D through UV metabolism or diet [Yamasaki et al., 1996; Niino et al., 2002; Maghzi et al., 2010]. A genetic explanation or the pathogenesis fails, as genetically similar populations exposed to similar pathogens, e.g. environment, have drastically different incidence of the disease [Benois and Mathis, 2001]. Furthermore another hypothesis proposes, that MS is a disease provoked by dysfunction of lipidmetabolism [Corthal, 2011]. Taken together there are a lot of factors known to be involved, but a comprehensive understanding of the pathogenesis has not yet been reached.

1.2.1. Myelin and its general composition

More than 20 years ago as methods of myelin isolation became available the composition of myelin has been studied intensively. Myelin is the essential constituent of the white matter in the CNS [Notron and Poduslo, 1973; Norton and Poduslo, 1973]. Myelin itself consists of 70% lipids and 30% proteins. Unique is the lipid-to-protein ratio in the myelin membrane, because it is exactly reverse as in other cellular membranes [Martenson, 1992; Morell et al., 1994; Siegel, Albers, Brady and Price; 1994; Juurlink et al., 1997]. This multilayered membrane system enwraps axons with a distinct periodic structure. Oligodendrocytes produce and extent this membrane system in the CNS. Up to 50 axon segments (internodes) can be myelinated by one oligodendrocyte [Hildebrand, Remahl, Persson and Bjartmar, 1993]. Those internodes are separated by short stretches of bare axolemma (nodes of Ranvier) (Fig.7). The myelin internode consists morphologically of compact myelin that built the majority of the internode, and noncompact myelin, which primarily frames the edges of the internode [Soldán and Priko, 2012]. Compact myelin are spiralled sheets around the axons, which consists of two plasma membranes that form a lamellar structure with in turn electron-dense (major dense line) and electron-light (intraperiod lines) layers. The major dense line, are the fused cytoplasmic sites of the membranes, whereas the outsides of the membrane are connected in the intraperiod lines. Cytoplasm is excluded in compact myelin, but extracellular spaces are found at the intraperiod lines. There are also radial components,

which are composed of lines of junctional complexes registered both longitudinally and transversely, across the length of the internode and thickness of the myelin sheath thickness. Noncompact myelin might facilitate the communication between the oligodendrocyte soma and the myelin lamellae possible. Therefore the membrane forms at the inner- (periaxonal), outermost (abaxonal) and lateral (paranodal) edges channel-like tubes [Nave, 2010; Soldán and Pirko I., 2012; Aggarwal, Yurlova and Simons, 2011]

The correct formation and maintance of myelin is important for the functioning of the vertebrate nervous system. Because myelinated nerve fibers allow the rapid, focused signal transduction such as the voluntary and reflex stimulation of locomotory muscles and the perception of external stimuli [Tzakos et al., 2005].
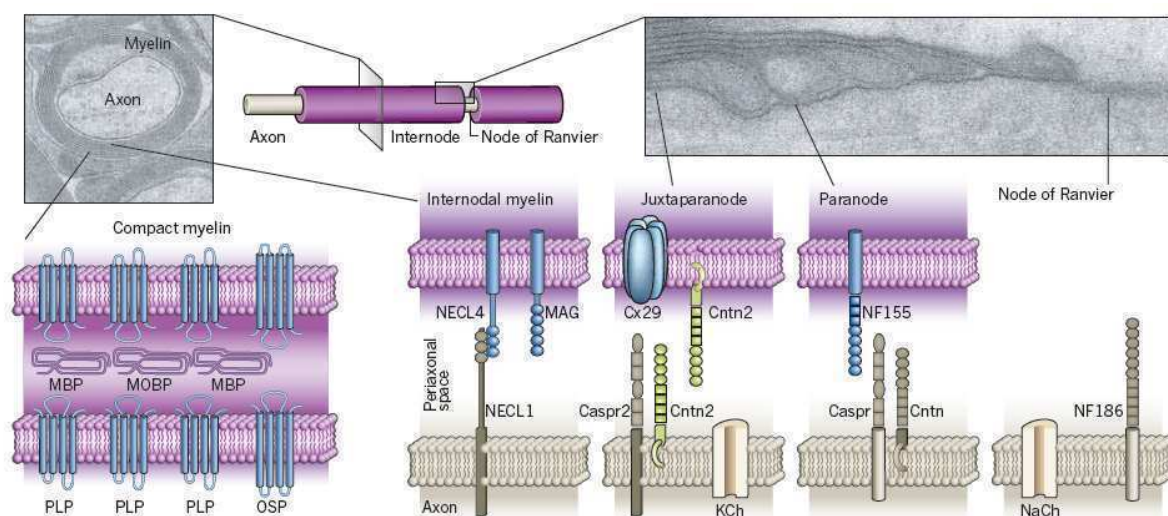
Figure 7: The axon myelin unit
Myelin sheat in cross section (inset: electron micrograph), with its characteristic periodic structure with alternating electron-dense (major dense line) and electron-light (intraperiod line) layers. At the lateral margins, noncompact cytoplasmic loops that abut the axolemma (inset: electron micrograph) and form junctional complexes. This defines distinct structural domains of axon-myelin contact: internode, juxtaparanode, paranode, and node. A cluster Na+ and K+ channels at the node and juxtaparanode. (Caspr, contactinassociated protein; Cntn, contactin; KCh, fast potassium channels; NaCh, voltage-gated sodium channels; NECL, nectin-like protein/synCAM; NF155/186, neurofascin 155kDa/186kDa; Nr-CAM, neuronal cell adhesion molecule) [Nave, 2010].

1.2.1.1. Myelin lipids

Myelin of mammalian species contains cholesterol, phospholipids and glycosphingolipids (GSLs). Those lipids are similar to the lipids found in every cellular membrane, but their ratio is unique for myelin. Cholesterol and GSLs built up to 31% of the total myelin lipids [Jackman, Ishii and Bamsal, 2009]. Myelin membranes are different in their biological properties, e.g. in fluidity and curving, due to the high cholesterol content [Huttner and Zimmerberg, 2001]. Structurally the GSLs found in myelin differ from those in the plasma membranes of other cell types. Headgroups are based on galactose instead of glucose, and

long fatty acids with high degree of oxidation are found [Norton and Poduslo, 1973; Jacque, Bourre, Moreno and Baumann; 1971]. Within the membrane GSLs are differentially located, Galactocerebroside (GalC) for instance is localized within compact and sulfatide in noncompact myelin [Maier, Hoekstra and Baron, 2008]. The biosynthesis is regulated via subcellular compartmentalization. On the cytoplasmasmic face of the endoplasmatic reticulum (ER) the synthesis of GSL is initiated by condensation of L-serine and palmitoyl-CoA and besides this the formation of ceramide via reduction, acylation and desaturation reactions is achieved [Kolter, Proia and Sandhoff, 2002]. After the ceramide has been flipped to the luminal face of the ER, GalCs are formed through the addition of galactose residue. After this a certain amount of GalCs are converted to sulfatide on the luminal face of the Golgi. The GalC and sulfatides reach the outer leaflet of the plasma membrane via vesicular transport [Brown et al., 1993]. The cermaides are the precursors of galactolipids, gangliosides and sphingomyelin [Hannun and Obeid, 2002]. After ceramides are synthesized on the ER cytoplasmic face some of those are transfered to the Golgi cytoplasmic face and glucocerebrosides (GlcC) are formed via addition of a glucose residue [Ichikawa and Hirabayashi, 1998]. Galactose residues are added to GlcC, which are then via a flip transferred to the luminal face of the Golgi. During this transfer lactosylceramide (LacC) are formed [Lannert et al., 1998]. LacC are the precursor for most gangliosides, excluding sialosylgalactosylceramide (GM4) which are processed via sialyltransferases. Similar to the GalCs and sulfatides, gangliosides are transported by vesicular transport to the outer leaflet of the plasma membrane [Farrer and Benjamins, 1992].

1.2.1.2. Myelin proteins

30% of the dry weight of myelin consists of proteins. The most known ones are specific components of myelin and oligodendrocytes. Major CNS myelin proteins are Myelin basic protein (MBP), Proteolipid protein (PLP) as well as its isoform DM20. They account for 22-35% and 30-45% of the total proteins. Furthermore 2',3'-Cyclic nucleotide-3'-phosphatase (CNP) makes up 4-15% of the remaining proteins [Norton and Podulso, 1973; Morell et al., 1972; Deber and Reynolds, 1991; Jahn, Tenzer and Werner; 2009]. Between the remaining proteins is myelin-associated glycoprotein (MAG), which is a myelin glycoprotein at the inner surface of the myelin sheath opposing the axon surface and accounts for less than 1% of the total. Furthermore myelin-associated oligodendrocyte basic protein (MOBP), is exclusively expressed in oligodendrocytes and appears late in myelination. Its location is in the major dense line of compact myelin. Several splice variants exists and the 81 aa isoform is the most abundant in rodent and human myelin [Sospedra and Martin, 2005].

1.2.1.2.1. Myelin basic protein

MBP accounts for ~30% of the total myelin and is one of the major proteins of the CNS. It is found at the cytoplasmic surface of compact myelin membranes where it binds negatively charged lipids, maintaining the major dense line [Privat et al., 1979]. MBP is in fact a family of proteins, as there are a variety of isoforms with different molecular masses. The major isoforms have a molecular mass of 21.5, 18.5, 17 and 14kDa in mice and 21.5, 20.2, 18.5 and 17.2kDa in human [Campagnoni and Macklin, 1988]. Those isoforms are alternative transcripts from the seven exon MBP gene [Roach et al., 1983]. Additionally, the MBP gene contains a larger transcriptional unit [Campagnoni et al., 1993; Grima, Zelenika and Pessac, 1992; Pribyl et al., 1993]. This unit consists of three unique exons spanning region which is 73 kb upstream of the MBP transcriptional start side in mice [Campagnoni et al., 1993]. It is called the Golli-MBP gene and is 195 kb in mice and 179 kb in humans [Campagnoni et al., 1993; Pribyl et al., 1993]. The Golli and the MBP transcripts are regulated differently [Gow, Friedrich and Lazzarini, 1992]. A regulatory element for effective transcription in glial cells, e.g. a MBP promoter region of 256 bp, can drive direct oligodendrocyte specific expression [Goujet-Zalc et al., 1993].

The 17- and 21.5kDa isoform in mice appear earlier in development. While in contrast the 20.2 and 21.5kDa isoforms are expressed mainly during myelinogenesis in human. But both are reexpressed in MS lesions and correlate with the remyelination in those lesions [Capello, Voskuhl, McFarland and Raine, 1997]. Posttranslational modifications of the MBP are as well known, e.g. NH_2-terminal acetylation, citrullination, phosphorylation and methylation. Methylation might be important for the compaction of the membrane during maturation [Campagnoni and Macklin, 1988; Wood and Moscarello, 1989].

Numerous pieces of evidence suggest that MBP might be a good candidate for an autoantigen in MS [Martin, McFaland and McFarlin, 1992]. In MS patients and controls MBP-specific T-cells are described. Due to their activation state in MS patients, proinflammatory phenotype and higher antigen avidity suggest that they have been acitivated in *vivo* [Burns et al., 1983; Richert et al., 1983; Chou et al., 1989; Martin et al., 1990; Pette et al., 1990; Ota et al., 1990; Olsson et al., 1990]. On the other hand mice that express a TCR that is specific for an encephalitogenic peptide of MBP develop as well EAE [Goverman et al., 1993].

1.2.1.2.2. Proteolipid proteins

The gene which encodes for PLP is located on the X chromosome, is 15 kb in size and organized in six exons. PLP and its isoform DM20 are formed by alternative splicing and are therefore coded by the same gene [Morello, Dautigny, Pham-Dinh and Jolles, 1986; Nave,

Lai, Bloom and Milner, 1986]. PLP consist of four hydrophobic α-helices which span the whole tickness of the lipid bilayer, two extracytoplasmic and three cytoplasmic domains (including NH$_2$- and COOH-termini). It is localized at the intraperiodic and major dense line of myelin [Popot, Pham-Dinh and Dautigny, 1991; Weimbs and Stoffel, 1992]. Its extracellular domains form electrostatic interactions with myelin lipids, thereby maintaining the intraperiod line [Griffiths et al., 1998].

In the absence of PLP/ DM20 oligodendrocytes are still able to myelinate axons and assemble compact myelin sheaths, but the ultrastructure of myelin exhibited condensation of the intraperiodic lines correlating with the reduced physical stability. This led to the conclusion, that PLP forms stabilizing membrane junctions after myelin compaction [Boison, Bussow, D'urso, Muller and Stoffel, 1995; Klugmann et al., 1997]. Furthermore the absence of PLP leads to widespread focal axonal swellings, which are followed by axonal degradation associated with impairment of motor performance [Griffiths et al., 1998; Baumann and Pham-Dinh, 2001]. PLP and DM20 is mainly found in the brain, spinal cord and it has been detected in the peripheral lymphoid organs [Seamons, Perchellet and Goverman, 2003; Burno et al., 2002; Klein et al., 2000].

1.2.1.2.3. 2', 3'-Cyclic nucleotide-3'-phosphatase

CNP represents 4% of total myelin proteins. This protein should hydrolyze 2'-3'-cyclic nucleotides into their 2'-derivates, but until now no 2'-3'-cyclic nucleotides has been found in the brain, the function of this enzyme is still obscure [Vogel and Thompson, 1988]. The gene is located on mouse chromosome 11 and 17q21 in humans [Bernier, Colman and D'eustachio, 1988]. The gene consists of four exons which span 17 kb. There are two isoforms of CNP, CNP1 (46kDa) and CNP2 (48kDa). The two isoforms are produced by alternative splicing starting from two transcript start sites. An upstream initiation codon is present in exon 0 and a splice site present in exon 1 [Kurihara et al., 1990]. Moreover two translational start sites can are known for the mRNA encoding the CNP2 isoform, which give rise to additional isoforms [O'Neill et al., 1997].

CNP can be isolated within the myelin fraction, but it is not localized in compact myelin. In Oligodendrocytes CNP can be detected in the soma and in noncompact myelin at the inner and outer tongue processes and in the paranodal loops [Trapp et al., 1988]. It is posttranslational modified via acetylation and phosphorylation [Vogel and Thompson, 1988]. It is known that *in vitro* CNP copolymerizes with tubulin heterodimers and therefore promoting microtubule assembly [Lee et al., 2005]. Furthermore, it links tubulin and actin to membranes [Bifulco et al., 2002; De Angelis and Braun, 1996] by isoprenylation of its C-terminal domain [De Angelis and Braun, 1994; Esposito et al., 2008]. CNP binds RNA and is

able to suppress protein translation [Gravel et al., 2009], which suggests that it is involved in trafficking of specific RNAs to distal parts of the oligodendrocyte at the glia-axonal junction [Edgar et al., 2009]. CNP and PLP are both not essential for myelination, but are required for axonal integrity [Lappe-Siefke et al., 2003]. CNP1-null mutant mice are more severely affected than PLP1-null mice, because their axons degrade just after a few weeks [Edgar et al., 2009].

1.2.2. Myelination and remyelination

Myelination is subdivided in several subsequential steps: 1) migration of oligodendrocytes to the target axons, which the oligodendrocytes are able to recognize; 2) the adhesion process of the oligodendrocyte to the axon; 3) the wrapping of a predetermined number of myelin sheats around the axon and leaving the nodes of Ranvier unmyelinated.

At first the preoligodendrocyte locate along the fiber tracts of the future white matter, still being able to divide. At this time mitoses are still present in the interfascicular longitudinal glial rows. Next the preoligodendrocyte become immature and are ready to start the myelination [Baumann and Pham-Dinh, 2001; Reynolds and Wilkin; 1991]. The onset of myelination might be determined by the degree of neural differentiation and not by the timing of an intrinsic oligodendrocyte differentiation program [Brinkmann et al., 2008]. The signal for the onset of myelination seems to be provided by the activity of neurons [Gyllensten and Malmfors, 1963; Omlin, 1997].

To understand the signaling pathway of myelination and the main players of protein and lipid synthesis, models of remyelination were investigated. In most chronic lesions of MS are enough oligodendrocytes and premyelinating oligodendrocytes, but they fail to remyelinate [Chang et al., 2000, 2002; Lucchinetti et al., 1999; Ozawa et al.,1994; Scolding et al., 1998; Wolswijk, 2000, 2002]. This suggests that the microenviroment of MS lesions does not provide or inhibits the needed signals for remyelination.

1.2.2.1. IGF1R signaling in myelination and remyelination

It is known, that IGF-I is an important survival factor for oligodendrocytes and their precursors (OPCs) [Barres et al., 1992; Mason et al., 2000; McMorris et al., 1986; Ye and D'Ercole, 1999], which stimulate the synthesis of myelin [Roth et al., 1995]. Mice which over express IGF-I show an increased myelin content [Carson et al., 1993; Ye et al., 1995], in contrast, if IGF-I is deleted a strong reduction in myelination and in the numbers of OPCs occur [Beck et al., 1995]. However it has been shown that MS patients and healthy controls have the same IGF-I levels. Furthermore there is a consistent upregulation of IGF-I, IGF1R

and IGFBP-1 and -6 in oligodendrocytes at the edge of demyelinated MS lesions [Wilczak et al., 2008; Gveric et al., 1999]. In cell culture [Kühl et al., 2002] and in transgenic mice over expressing IGFBP-1 [Ye et al., 1995], IGFBP-1 has an inhibitory effect on IGF-I induced cell survival and myelination. The upregulation of IGFBP-1 and -6 might be one of the factors why remyelination fails in MS [Wilczak et al., 2008]. It has been suggested that progesterone might be a good candidate to therapy MS, as it is able to cross the BBB easily and reduces the expression of IGFBP-6 in oligodenrodrocyte cell cultures [Kühl et al., 2003]. Even not investigated in oligodendrocytes, progesterone is known to be a strong inhibitor of IGFBP-1 expression in other cell lines [Davies et al., 2004]. Furthermore progesterone induces remyelination in animal models of toxin-induced CNS demyelination [Ibanez et al., 2004]. On the other hand IGFBP-1 appears to serve as a inhibitor of IGF-I induced differentiation and is able to induce OPC proliferation [Chesik et al., 2010].

Downstream in the IGF1R and InR signaling cascade it has been shown, that IRS-1 is not essential in IGF-I promoted oligodendrocyte development and myelination, and that IRS-2 or IRS-4 might be capable of compensating of the loss of IRS-1 in IRS-1 homozygous transgenic knockout mice (IRS-1 $^{-/-}$) as they were up regulated [Ye et al., 2002]. For IRS-2 homozygous knockout mice (IRS-2 $^{-/-}$) it has been described that IRS-1 is up regulated and increased IGF1R signaling was observed at postnatal day (P)10-14. It seems that IRS-1 is able to compensate the loss of IRS-2, at least partially. But those mice presented less myelin proteins (MBP, PLP and MOBP) at P10, but unchanged qualitatively myelination. Therefore it was reasoned that IRS-2 is critical for appropriate initiation of myelination, but not for myelin maturation. Mice lacking the InR in the brain displayed unchanged myelination, suggesting that the myelination initiation signal is mainly transduced via the IGF1R [Freude et al., 2008].

1.2.2.2. Wnt signaling in myelination and remyelination

As a bypass Wnt signaling seems to be involved in myelination. IRS-2 ($^{-/-}$) mice showed between P5 and week 5 a higher amount of phosphorylated GSK3β (Ser9; p-GSK3β) [Freude et al., 2008]. Additionally other factors of the Wnt signaling cascade are known to be up regulated in EAE mice [Azim and Butt, 2011]. GSK3β inhibition is a major effect in the IGF1R cascade [Frederick et al., 2007], but is also controlled via the Wnt signaling pathway [Fancy et al., 2009; Feigenson et al., 2009]. In the dorsal horn of the spinal cord of EAE mice increased expression of Wnt3a, β-catenin, Wnt5a and its receptor (co-receptor) Ror2 expression have been observed [Yuan et al., 2011]. Furthermore, it has been shown that inhibiting GSK3β results in an increase of OPCs and oligodendrocytes, promoting myelination. Inhibition of GSK3β stimulates OPC proliferation and acts prosurvival and antiapoptotic. Ser9 phosphorylation of GSK3β via the canonical Wnt signaling pathway in

oligodendrocytes regulates nuclear translocation of β-catenin. Wnt3a inhibition reduces oligodendrocyte differentiation, at least in the optic nerve. GSK3β inhibition might be able to overcome the negative effects of Wnt3a by stimulating cAMP response element binding (CREB) [Grimes and Jope, 2001], which activates Bcl2 gene expression to prevent cell death in oligodendrocytes [Saini et al., 2004]. Furthermore, GSK3β inhibition decreases Notch1 signaling, which positively regulates oligodendrocyte differentiation but negatively myelination. These effects are similar during development as well as in the chemically induced de- and remyelination. Therefore GSK3β is a negative regulator of oligodendrocyte differentiation that contributes to inefficient regeneration of oligodendrocytes and myelin repair in demyelination [Azim and Butt, 2011].

1.2.2.3. Fyn kinase in myelination and remyelination

The Src family tyrosine kinase Fyn signaling is known to play a role in promoting oligodendrocyte differentiation, maturation and myelination [Wang et al., 2009]. Fyn is regulated via dephosphorylation of the C-terminal tail residue by protein tyrosine phosphatases (PTPs) [Umemori et al., 1999]. Therefore an essential player and central coordinator, as mice with Fyn deficiency exhibit hypomyelination [Umemori et al., 1994; Sperber et al., 2001]. There is a crosstalk to the IGF1R signaling cascade as Fyn is activated via IGF-I. However other factors activating Fyn are serum withdrawal, β1 integrin stimulation, netrin-1 interaction with the receptor Dcc and antibody-mediated crosslinking of MAG or FcRγ [Umemori et al., 1994,Osterhout et al., 1999; Nakahara et al., 2003; Colognato et al., 2004; Liang et al., 2004; Rajasekharan et al., 2009; Sperber and McMorris, 2001]. Fyn signals to a variety of molecules that are important for oligodondrocyte morphology, regulating cytoskeleton rearrangement and process extensions involving focal adhesion kinase (FAK), Rho GTPases Rho, Rac1, Cdc42, Rho regulators p190 and p250 RhoGAP as well as tau protein [Liang et al., 2004, Hoshina et al., 2007; Wolf et al., 2001; Taniguchi et al., 2003; Klein et al., 2002; Miyamoto et al., 2007].

1.3. Mouse models

The current study investigates the role of IRS-2 over expression in oligodendrocytes and their precursors. For IRS-2 it has bene shown [Freude et al., 2008], that IRS-2 deficiency leads to delayed myelin development, whereas IRS-1 seems to be of minor importance. The influence of increased IRS2 signaling on myelination *in vivo* is unknown. In order to achieve oligodendrocyte specifity the Cre/loxP system under the oligodendrocyte specific CNP

promoter was used [Edgar et al., 2004; Griffiths et al., 1998; Kassmann et al., 2007; Yin et al., 1998].

1.3.1. IRS-2 over-expressing mouse

The transgenic (tg) IRS-2 construct has been cloned into the *rosa26locus* (Fig.8). Since the *rosa26locus* is expressed ubiquitously, a "stop cassette" flanked by loxP sites has been cloned in front of the IRS-2 sequence. The resulting tg IRS-2 (IR) mice were viable. To induce site specific DNA recombination the Cre/loxP system was used. This system was first described in the bacteriophage P1. Necessary for this system is the 34 bp DNA sequence with two 13 bp inverted repeats and the asymmetric 8 bp space region called locus of X-over in P1 (loxP). This sequence targets the site of recombination. In addition the Cre recombinase, a 343 aa monomeric protein, is required for this system. For the *in vivo* study mouse lines carrying the loxP site flanked stop cassette followed by the IRS-2 gene in the *rosa26locus* were used. After deletion of the "stop cassette" using CNP-Cre mice, the IRS-2 mice express transgenic eGFP and overexpress IRS-2.
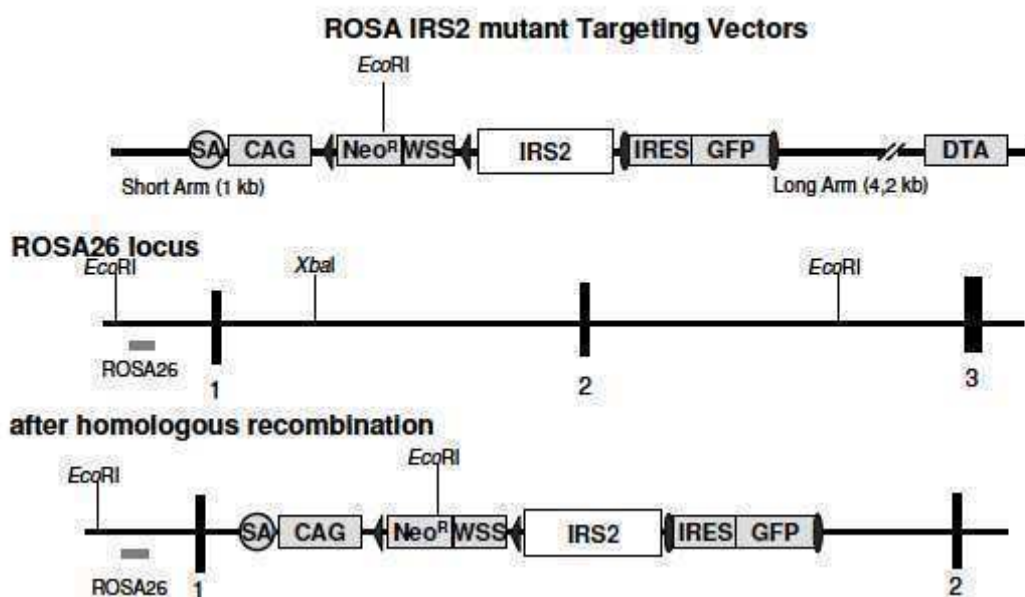
Figure 8: Cre/ loxP targeting strategy for the overexpression of IRS-2 in oligodendrocytes
The upper panel presents the *rosa26* targeting vector included IRS-2 and eGFP, which contains the splice acceptor (SA), the pCMV promoter region (CAG), the loxP sites (tringles) flanked neomycin resistance gene (Neo^R) and westphale stop cassette (WSS), the IRS-2 gene which is followed by the FRT site flanked internal ribosomal entry site (IRES) and enhanced green fluorescent protein (eGFP). After homologous recombination this region is inserted into the Rosa26 locus of the mouse model (lower panel).

1.3.2. CNP promoter driven expression of the Cre recombinase

The enzyme 2′,3′-cyclic nucleotide 3′-phosphodiesterase (CNP) is a widely used marker protein of myelin-forming glial cells [Chandross et al., 1999; Vogel and Thompson, 1988; Sprinkle,1989]. During the development of the brain, CNP is detectable in cells of oligodendrocyte lineage [Yu et al., 1994] and is maintained in mature oligodendrocytes throughout life. CNP is also expressed, at much lower levels, outside the nervous system in subsets of immune cells [Sprinkle et al., 1985], photoreceptor cells [Giulian and Moore, 1980] and the testes [Scherer et al., 1994].

The CNP Cre mice were generated via homologous recombination in R1-ES cells, where a genomic fragment that included most of exons 1-3 of the CNP gene was replaced by the *cre* recombinase gene (Fig.9). The correct clone after puromycin selction was injected into a blastocyst and yielded chimeric mice. Those heterozygous (F1) offsprings were intercrossed to obtain homozygous (F2) mutants. Both heterozygous and homozygous mutant mice were viable and showed no abnormal behaviours during the first month of age [Lappe-Siefke et al., 2003].
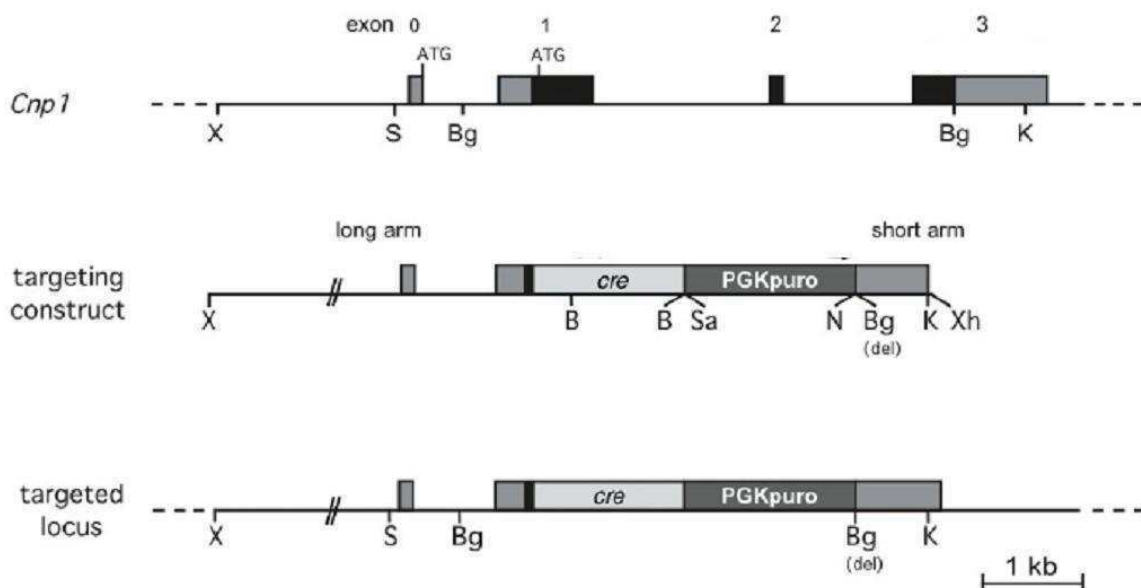
Figure 9: Strategy to include *cre* recombinase
At the top the structure of *CNP1* is shown, with its 4 exons (0-3), the targeted construct is in the middle and the target locus at the bottom. After homologour recombination, the *CNP1* open frame is replaced by cre and a PGK-puromycin selection cassette (PGKpuro).

1.3.3. CNP-Cre mice, a model for multiple sclerosis

It is known, that homozygous CNP deficient (CC $^{-/-}$) mice show normal myelin assembly, whereas the ultrastructure and physical stability are not visibly changed. However, throughout the white matter axons developed abnormal swellings and were progressively lost

leading to premature death mostly before one year of age. But neuronal cell death is not a feature in those mutant mice. Nissl staining of 3,5 month old CC $^{-/-}$ mice revealed that the density of oligodendroglial nuclei in the corpus callosum was unchanged. Additionally, it can not be excluded that axon functions are changed in the motor system of those mice when they reach an older age. Moreover CC $^{-/-}$ showed overall reduction of brain mass after seven month of age. However CC $^{-/-}$ mice showed decreased MBP in whole brain lysate, whereas this could not be seen in purified myelin. Whereas PLP expression showed no developmental delay in 11, 15 and 21 days aged mice. Hence no significant signs of dysmyelination was found [Lappe-Siefke et al., 2003; Nave et al., 2003].

The axonal changes are similar to those in PLP-deficient mice [Griffiths et al., 1998]. Therefore a connection between changed myelin structure and axonal loss is not unlikely [Boison et al., 1995; Rosenbluth, Stoffel and Schiff, 1996; Klugmann et al., 1997; Boison and Stoffel, 1994]. In MS and related animal models, acute white matter lesions are directly linked to axonal loss [Trapp et al., 1998; Wujek et al., 2002]. Therefore it is reasonable that loss of oligodendrocytes within a MS lesion might contribute to axonal demyelination and to the persistent clinical disabilities of MS patients [Lappe-Siefke et al., 2003].

1.4. Aims of the present thesis

The influence of increased IRS-2 signaling on myelination *in vivo* is still unknown. Thus the following thesis aims to investigate the role of IRS-2 over expression in oligodendrocytes *in vivo* and *vitro*. In particular: 1) Does IRS-2 over expression change myelin development; 2) Can IRS-2 over expression alter myelin composition; 3) Influences IRS-2 over expression in oligodendrocytes motor coordination *in vivo.*

2. Material and Methodes

2. Material and Methodes

2.1. Chemicals

Acetic acid	Merck, Darmstadt, Germany
Acrylamide / Bis-acrylamide 30%	Rotiphorese® Gel 30 (37.5/1)
	Carl Roth GmbH + Co. KG, Karlsruhe, German
Agarose	Invitrogen Corporation, Carlsbad CA, USA
Ammonium-persulfate (APS)	AppliChem GmbH, Darmstadt, Germany
Avertin	Sigma-Aldrich Chemie GmbH, Steinheim, Germany
β-mercaptoethanol	Sigma-Aldrich Chemie GmbH, Steinheim, Germany
Bradford reagent	Bio-Rad Laboratories GmbH; Germany
Bromophenol blue	AppliChem GmbH, Darmstadt, Germany
96 % Bovine serum albumin (BSA)	Sigma-Aldrich Chemie GmbH, Steinheim, Germany
Cresyl violet acetate	Sigma-Aldrich Chemie GmbH, Steinheim, Germany
DMSO Dimethyl sulfoxide	Sigma-Aldrich Chemie GmbH, Steinheim, Germany
DTT	Dithiothreitol
	AppliChem GmbH, Darmstadt, Germany
EDTA	Ethylenediaminetetraacetic acid
	AppliChem GmbH, Darmstadt, Germany
Ethanol	AppliChem GmbH, Darmstadt, Germany
Ethidium bromide	Sigma-Aldrich Chemie GmbH, Steinheim, Germany
Geniticin (G418)	Sigma-Aldrich Chemie GmbH, Steinheim, Germany
Glycerol	Glycerin, AppliChem GmbH, Darmstadt, Germany
Glycine	AppliChem GmbH, Darmstadt, Germany
HEPES	Sigma-Aldrich Chemie GmbH, Steinheim, Germany
Hydrogen peroxide	Carl Roth GmbH + Co. KG, Karlsruhe, Germany
Isopropanol	AppliChem GmbH, Darmstadt, Germany
Kanamycin	AppliChem GmbH, Darmstadt, Germany
LB-Agar	Sigma-Aldrich Chemie GmbH, Steinheim, Germany
LB-Medium	AppliChem GmbH, Darmstadt, Germany
LY294002	Promega GmbH, Mannheim, Germany
Methanol 99%	Carl Roth GmbH + Co. KG, Karlsruhe, Germany
Magnesium chloride	Merck, Darmstadt, Germany
NP-40	Polyglycol ether (Nonidet® P40 Substitute) FLUKA
	Chemika/Biochemika Chemie AG, Buchs, Switzerlan
PAP Pen	Abcam plc, UK
PD98059	Sigma -Aldrich Chemie GmbH, Steinheim, Germany

PIPES	AppliChem GmbH, Darmstadt, Germany
PMSF	Phenylmethylsulphonylfluoride
	Sigma-Aldrich Chemie GmbH, Steinheim, Germany
Paraformaldehyde (PFA)	AppliChem GmbH, Darmstadt, Germany
Potassium chloride	Merck, Darmstadt, Germany
Propidiumiodid	Sigma-Aldrich Chemie GmbH, Steinheim, Germany
Sucrose	AppliChem GmbH, Darmstadt, Germany
SDS	Sodium dodecyl sulfate
	AppliChem GmbH, Darmstadt, Germany
Sodium fluoride	Merck, Darmstadt, Germany
Sodium bicarbonate	Carl Roth GmbH + Co. KG, Karlsruhe, Germany
Sodium chloride	Carl Roth GmbH + Co. KG, Karlsruhe, Germany
Sodium orthovanadate	Sigma-Aldrich Chemie GmbH, Steinheim, Germany
Solvent Blue 38	Sigma-Aldrich Chemie GmbH, Steinheim, Germany
TAE	AppliChem GmbH, Darmstadt, Germany
TEMED	N,N,N',N'-Tetramethylethylenediamine
	Sigma-Aldrich Chemie GmbH, Steinheim, Germany
Tris	AppliChem GmbH, Darmstadt, Germany
TritonX-100	AppliChem GmbH, Darmstadt, Germany
Trizol	Invitrogen Corporation, Carlsbad CA, USA
Trypsin	Roche, Mannheim, Germany
TWEEN 20®	Polyoxyethylene (20) sorbitan monolaurate,
	Caesar and Lorentz GmbH, Bonn, Germany
Xylol	AppliChem GmbH, Darmstadt, Germany

2.2. Enzymes

Proteinase K	Fermentas GmbH, St. Leon-Rot, Germany
T4 DNA Ligase	Fermentas GmbH, St. Leon-Rot, Germany
XhoI	Fermentas GmbH, St. Leon-Rot, Germany
BamHI	Fermentas GmbH, St. Leon-Rot, Germany
SspI	Fermentas GmbH, St. Leon-Rot, Germany
GoTaq® Hot Start Polymerase	Promega Corporation, Madison, USA

2.3. Vectors, Primer and supplies

Desoxy-Ribonucleotid-Triphosphate

dNTPs	Fermentas GmbH, St. Leon-Rot, Germany
pCMV-Tag 2C	Agilent Technologies, Santa Clara CA, USA
pCMV-Tag 2B	Agilent Technologies, Santa Clara CA, USA

2.4. Buffer and solution

Solvent blue solution	0.13g Solvent blue 10ml 10% HCL 190ml 96% EtOH
Cresyl violet solution	0.1g Cresyl violet 100ml distilled water 20 drops 10% HCl
5% BSA solution	5g BSA 100ml PBS
0,8% BSA solution	0.8g BSA 100ml PBS
0,5% Triton-X solution	1ml Triton-X (10%) 19ml PBS
SDS-PAGE running buffer	194mM Glycine 25mM Tris 0.1% SDS
4 x SDS sample buffer	250mM Tris-HCl (pH 6.8) 200mM DTT 40% Glycerol 8% SDS 0.01% Bromophenol blue
Stripping solution	62.5mM Tris-HCL pH 6.8 100mM β-mercaptoethanol 2%SDS
TBS buffer (pH 7.6)	137mM NaCl 20mM Tris
TBS-T buffer (pH 7.6)	137mM NaCl 20mM Tris 0.1% Tween 20®
Western Blot antibody solution	137mM NaCl 20mM Tris 5% Western Blocking Reagent (Roche)
Western Blot blocking solution	137mM NaCl 20mM Tris 10% Western Blocking Reagent (Roche)

Western Blot transfer buffer	194mM Glycin 25mM Tris 20% Methanol (99%) 0.05% SDS
DNA loading dye	50% Glycerin 5XTAE
$CaCl_2$ buffer	60mM $CaCl_2$ 15% Glycerin 10mM PIPES pH 7
Tail biopsies lysis buffer	100 mM Tris HCl (pH 8.5), 5 mMEDTA, 0.2% (w/v) SDS, 0.2M NaCl, 500 mg/ml proteinase K)
Cell lysis buffer	50 mM NaCl 50 mM Tris-HCl (pH 7.4) 5 mM EDTA 1 % Nonidet® P40 Substitute
Organ lysis buffer	50 mM HEPES (pH 7.4) 50 mM NaCl 1 % Triton X-100 10 mM EDTA 0.1 M NaF 17 µg/ml Aprotinine 2 mM Benzanidine 0.1 % SDS 1 mM Phenylmethylsulfonyl fluoride (PMSF) 10 mM Na_3VO_4
Nuclear cell lysis buffer	420mM KCl 20mMHEPES 1mM EDTA 0,1mM Na_3VO_4 20% Glycerin
Cytolsolic cell lysis buffer	10mM KCl 20mM HEPES 1mM EDTA 0,1mM Na_3VO_4 10% Glycerin 0,2% NP 40
10x Cathode buffer	1M Tris 1M Tricine 1% SDS pH 8.25
10x Anode buffer	2.1M Tris pH8.9
ECL, Amersham ECLTM Western	

Blotting Detection Reagents	GE Healthcare UK Ltd; England
Fetal bovine serum (FBS)	Invitrogen GmbH; Germany
Phosphate buffered saline 10 fold (pH 7.2)	Invitrogen GmbH; Germany
PageRuler™ Prestained Protein Ladder	Fermentas GmbH, St. Leon-Rot, Germany
Trypsin, 0.25% (1x) with EDTA	Roche, Mannheim, Germany
Western Blocking Reagent	Roche Diagnostics GmbH; Germany
DMEM High Glucose with Glutamax™, 4500mg/L Glucose, Soduim Pyruvate Pen/ Strep	PAA Laboratories GmbH, Cölbe; Germany

2.5. Cells and bacteria

OmniMax	Invitrogen Corporation, Carlsbad CA, USA
OLN-93	Dr. C. Richter-Landsberg (Department of Biology, Molecular Neurobiology, University of Oldenburg, Oldenburg, Germany

2.6. Kits

Qiaprep Spin Maxiprep Kit	Qiagen GmbH, Hilden, Germany
QiAquick Gel Extraction Kit	Qiagen GmbH, Hilden, Germany
Qiaprep Spin Miniprep Kit	Qiagen GmbH, Hilden, Germany
BrdU assay	Millipore, Billerica, MA, USA
METAFECTNE PRO	Biontex Laboratories GmbH, Germany

2.7. Primary Antibodies

2.7.1 Western Blot

-Actin Antibody; Monoclonal mouse antibody detects an epitope conserved in human actin; MP Biomedicals, USA; Item # 69100; Western Blotting Dilution 1:5000

-AKT Antibody; Polyclonal rabbit antibody detects endogenous levels of total AKT1, AKT2 and AKT3 proteins; Cell Signaling Technology, Inc., USA; Item # 9272; Western Blotting Dilution 1:1000.

-β-catenin Antibody; Monoclonal mouse antibody raised against amino acids 680-781 mapping at the C-terminus of β-catenin of human origin; Santa Cruz Biotechnologie, Inc., USA, Item sc-133239tern Blotting Dilution 1:500

-Caspase-3 Antibody; Polyclonal rabbit antibody detects endogenous levels of full length caspase-3 (35kDa) and the large fragment of caspase-3 resulting from cleavage (17kDa); ; Cell Signaling Technology, Inc., USA; Item # 9662; Western Blotting Dilution 1:1000

-CNPase Antibody; Polyclonal rabbit antibody detects human CNPase, Cell Signaling Technology, Inc., USA; Item # 2986; Western; Blotting Dilution 1:500

-Erk Antibody; Polyclonal rabbit antibody detects endogenous levels of total p44/42 MAP kinase (Erk1/Erk2) protein; Cell Signaling Technology, Inc., USA; Item # 9102; Western Blotting Dilution 1:1000

-Fyn Antibody; Polyclonal rabbit antibody detects endogenous levels of total Fyn proteins. This antibody does not cross-react with other Src and Hck family members; Cell Signaling Technology, Inc., USA; Item # 4023; Western; Blotting Dilution 1:500

-GFP (D5.1) Antibidy; Monclonal rabbit antibody detects exogenous GFP; Cell Signaling Technology, Inc., USA; Item # 2959; Western Blotting Dilution 1:1000

-GSK-3β Antibody; Monoclonal rabbit antibody detects endogenous levels of total GSK-3β protein; Cell Signaling Technology, Inc., USA; Item # 9315; Western Blotting Dilution 1:1000

-IGF-1 Receptor β Antibody; Polyclonal rabbit antibody detects endogenous levels of IGF-IR β. Does not cross-react with insulin receptor; Cell Signaling Technology, Inc., USA; Item # 3027; Western Blotting Dilution 1:1000

-IGFBP3 Antibody; Polyclonal goat antibody raised against a peptide mapping the C-terminus of mouse origin; Santa Cruz Biotechnology, Inc., USA, Item: sc-6004, Western Blotting Dilution 1:250

-InRβ Antibody; Polyclonal rabbit antibody detects a peptide mapping at the C-terminus of insulin Rβ (C19) of human origin; Santa Cruz Biotechnology, Inc., USA; Item # sc-711; Western Blotting Dilution 1:1000

-IRS-1 Antibody; Monoclonal rabbit antibody detects C-terminal 14 amino acid peptide ([C]YASINFQKQPEDRQ) of rat liver IRS-1. Rat, mouse and human crossreactivity; Upstate Cell Signaling Solutions, USA; Catalog # 06-248; Western Blotting Dilution 1:1000

-IRS-2 Antibody; Polyclonal rabbit antibody detects endogenous levels of total IRS-2 protein; Cell Signaling Technology, Inc., USA; Item # 4502; Western Blotting Dilution 1:1000

-MBP Antibody; Polyclonal rabbit antibody detects endogenous levels of MBP; Abcam plc, UK, Item: ab40390; Western Blotting Dilution: 1:500

-MMP9 Antibody; Polyclonal rabbit antibody detects full length (proenzyme, 92kDa) human and mouse MMP-9; Cell Signaling Technology, Inc., USA; Item # 2270; Western Blotting Dilution 1:1000

-p27 (C-19) Antibody; Polyclonal rabbit antibody detects the C-terminus of p27; Santa Cruz Biotechnology, Inc., USA; Item #sc-528; Western Blotting Dilution 1:1000

-Phospho-AKT Antibody; Polyclonal rabbit antibody detects endogenous levels of AKT1 only when phosphorylated at Ser473. Also recognizes AKT2 and AKT3 when phosphorylated at the corresponding residues; Cell Signaling Technology, Inc., USA; Item # 9271; Western Blotting Dilution 1:1000

-Phospho-β-Catenin Antibody; Polyclonal rabbit antibody detects endogenous levels of human β-catenin when phosphorylated at Ser33, Ser 37 and Thr41; Cell Signaling Technology, Inc., USA; Item # 9561; Western Blotting Dilution 1:1000

-Phospho-p44/42 MAP Kinase (Thr202/Tyr204) Antibody; Polyclonal rabbit antibody raised against endogenous levels of p44 and p42 MAP Kinase (Erk1 and Erk2) when phosphorylated either individually or dually at Thr202 and Tyr204 of Erk1 (Thr185 and Tyr187 of Erk2); Cell Signaling Technology, Inc., USA; Item # 9101; Western Blotting Dilution 1:1000

-Phospho-GSK-3β (Ser9) Antibody; Polyclonal rabbit antibody detects endogenous levels of GSK-3β only when phosphorylated at serine 9; Cell Signaling Technology, Inc., USA; Item # 9336; Western Blotting Dilution 1:1000

-Phospho-GSK-3α/β (Ser21)/(Ser9) Antibody; Polyclonal rabbit antibody detects endogenous levels of GSK-3α/β only when phosphorylated at serine 21 or 9; Cell Signaling Technology, Inc., USA; Item # 9327; Western Blotting Dilution 1:1000

-Phospho-p70 S6 Kinase (Thr389) Antibody, Polyclonal rabbit antibody detects endogenous levels of p-p70 S6 kinase only when phosphorylated at threonine 389, Cell Signaling Technology, Inc., USA; Item # 9205; Western Blotting Dilution 1:1000

-p70 S6 Kinase Antibody, Polyclonal rabbit antibody detects endogenous levels of p70 S6 kinase, Cell Signaling Technology, Inc., USA; Item # 9202; Western Blotting Dilution 1:1000

-Phospho-PTEN (Ser380/Thr382/383) Antibody, Polyclonal rabbit antibody detects endogenous levels of phosphor-PTEN when phosphorylated at serine 380, threonine 382 and threonine 383, Cell Signaling Technology, Inc., USA; Item #9549; Western Blotting Dilution 1:1000

-PLP Antibody; Polyclonal rabbit antibody detects endogenous levels of PLP; Abcam plc, UK, Item: ab28486; Western Blotting Dilution: 1:500

- PTEN Antibody, Monoclonal mouse antibody detects endogenous levels of PTEN; Thermo Fisher Scientific, Kalamazoo, USA; Item: MS-1601, Western Blotting Dilution 1:1000

-TNFα Antibody; Monoclonal mouse antibody raised against full length recombinant TNFα of rat origin; Santa Cruz Biotechnology, Inc., USA, Item: sc-80383, Western Blotting Dilution 1:250

- Wnt5a Antibody; Polyclonal goat antibody detects endogenous levels of Wnt5a; Santa Cruz Biotechnology, Inc., USA, Item: sc-23698, Western Blotting Dilution 1:250

2.6.2. Immunohistochemistry

- GFAP Antibody, Polyclonal guinea pig detects endogenous levels of GFAP, Synaptic Systems, germany; Item: Cat.No.173004, IHC Dilution 1:200

- GFP Antibody; Polyclonal rabbit antibody detects edogenous levels of GFP and is directed against the entire GFP molecule; Abcam plc, UK, Item: ab290; IHC Dilution: 1:50

- MAC-2 Antibody; Monoclonal mouse antibody detects endogenous levels of MAC-2 (Clone M3/38); Biozol Diagnostica Vertrieb GmbH, Germany; Item # CL8942AP; IHC Dilution 1:100

-MBP Antibody; Polyclonal rabbit antibody detects endogenous levels of MBP; Abcam plc, UK, Item: ab40390; IHC Dilution: 1:500

-PDGFR-α, Polyclonal rabbit antibody detects epitope mapping at the C-terminus of PDGFR-α of human origin, santa cruz biotechnology, inc., USA, Item sc-338, IHC Dilution 1:50

-PLP Antibody; Polyclonal rabbit antibody detects endogenous levels of PLP; Abcam plc, UK, Item: ab28486; IHC Dilution: 1:100

- T-cell CD-3 Antibody; The 17A2 antibody recognizes ε/γ (but not ε/δ) of the CD3 complex. The antibody was purified by affinity chromatography, and conjugated with Alexa Fluor® 488 under optimal conditions.; Biolegend Inc., San Diego, USA; Item # 100210; IHC Dilution 1:50

2.7. Secondary Antibodies

2.7.1. Western Blot

-Anti Goat IgG (whole molecule), peroxidase conjugated; Affinity isolated antigen specific antibody obtained from rabbit anti-goat antiserum by immunospecific purification; Sigma-Aldrich, USA; Item # A5420; Western Blotting Dilution 1:1000

-Anti Mouse IgG (Fab specific), peroxidase conjugated; Developed in goat using purified mouse IgG Fab fragment as immunogen, the antibody is isolated from goat anti-mouse IgG antiserum by immunospecific purification; Sigma-Aldrich, USA; Item # A9917; Western Blotting Dilution 1:15000

-Anti Rabbit IgG, peroxidase conjugated; Developed in goat using purified rabbit IgG as immunogen, the antibody is isolated from goat anti-rabbit IgG antiserum by immunospecific purification; Sigma-Aldrich, USA; Item # A6154; Western Blotting Dilution 1:1000

2.7.2. Imunnohistochemistry

- Anti Rabbit IgG; Developed in goat using purified rabbit IgG as immunogen, the antibody is isolated from goat anti-rabbit IgG antiserum by immunospecific purification; Cy5; Abcam plc, UK, Item: ab6564; IHC Dilution: 1:200

- Anti guinea pig IgG; Developed in goat using purified guinea prg IgG as immunogen, the antibody is isolated from goat anti-guinea pig IgG antiserum by immunospecific purification; Alexa Fluor 488; Life Technologies GmbH, Darmstadt, Germany, Item: A-1073; IHC Dilution 1:200

2.8. Material

-Blotting chamber Trans-Blot® Semi-Dry Transfer Cell
Bio-Rad Laboratories, USA

-Blotting membrane Immun-BlotTM PVDF Membrane for Protein Blotting
Bio-Rad Laboratories, USA

-Blotting paper Whatman® Gel Blotting Paper
Schleicher & Schuell, Germany

-Cover-slips Cover glasses 24 x 50 mm
VWR International GmbH, Germany
-Cover-slips Cover glasses 12 mm

Medishop, Möglingen , Germany

-Culture culture dishes 145cm
Greiner Bio-One GmbH, Frickenhausen, Germany

-Culture culture dishes 10cm
Greiner Bio-One GmbH, Frickenhausen, Germany

-Curix60 AGFA
AGFA Healthcare Corporatio, USA

-iCycler Thermocycler
Bio-Rad Laboratories, USA

-Gewebe-Homogenisator
VWR International GmbH, Germany

- HERA safe
Thermo Fisher Scientific, Deutschland

- SANYO Incubator (MCO-5AC)
SANYO North America Corporation, USA

-Microplate reader Mithras LB 940 multimode microplate reader
Berthold Technologies GmbH & Co. KG, Germany

-Microscope Fluorescence Microscope Olympus IX81
Olympus Deutschland GmbH, Hamburg, Germany

-Microscope slides Microscope slides 76x26 mm
Menzel GmbH &Co KG, Braunschweig, Germany

-Minigel-Twin Gel Electrophoresis Apparatus, Minigel-Twin
Biometra GmbH, Germany

-NanoDrop NanoDropTM Spectrophotometer ND 1000
ThermoFisher Scientific, USA

-Photo-paper Amersham HyperfilmTM ECL
GE Healthcare UK Ltd, England;

-Powerpac Biometra Standard Power Pack P25
Biometra GmbH, Germany

-Research Miroscope Olympus BX51
Olympus Deutschland GmbH, Hamburg, Germany

-Thermomixer
Eppendorf, Hamburg, Germany

-ube Rotator, STUART®
Bibby Scientific Limited, Staffordshire, UK

2.9. Methods

2.9.1. Mice breeding

tg IRS-2 expressing mice were crossed with *CNP* driven Cre recombinase expressing mice (CNPCre) to ensure oligodendrocyte-specific protein synthesis. Mice not containing the transgene IRS-2 or CNPCre were used as controls. These mice were kept in a 12 hour light and dark cycle from 7a.m. to 7p.m. They were fed with standard rodent diet.Tg IRS-2 mice were made by Dr rer. nat. Udelhoven and present a C57BL/6 background back crossed more than 6 generations. CNPCre mice were thankfully provided by Prof Nave, Germany. Experiments with the mice were performed in agreement with the German Laws for Animal Protection and were approved by the local animal care committee and the Bezirksregierung Köln.

2.9.2. Isolation of genomic DNA

Mouse tail biopsies were incubated over night in lysis buffer (tail biopsie lysis buffer and 500mg/ml proteinase K) in a thermomixer at 55°C. The DNA was then precipitated via addition of the equivalent volume of isopropanole. After mixing the lysates were centrifuged at 13.000rpm at room temperature for 15 minutes. Supernant was discarded and 150µl 70% Ethanol was added. The samples were mixed and centrifuged at 13.000rpm at room temperature for 15 minutes. Supernant was discarded, the pellet was dried and resuspended in 100mM TrisHCl pH8.

2.9.3. Polymerase chain reaction (PCR) for genotyping

DNA concentrations of tail biopsies lysis were measured with NanoDrop® ND-100 UV Spectrophotometer at 260nm. After that the DNA was used to genotype mice for expression of *CNP* driven Cre recombinase and IRS-2 over expression in the ROSA 26 locus. Reactions were performed in a Thermocycler PCR machine. All reactions contained not less than 100ng DNA, 25pmol of each primer (Table 1), 25µM dNTP Mix, 4mM $MgCl_2$, 10% DMSO, 1xgoTaq reaction buffer and 1 unit of goTaq DNA polymerase.

Primer	Sequence	Orientation
CNPCre 5´	cccttcttacacagaacacaagct	sense
CNPCre 3´	ccttcttacacagaacacaagct	antisense
CNPCre 5´	accgtcagtacgtgagatatctt	antisense
IRS-2 5´	aatacctttctgggagttctctgctg	sense
IRS-2 5´	gactacaaagatgacgacgataa	sense
IRS-2 3´	ggtgtagtgggcgatcaggtacttgtg	antisense
IRS-2 3´	ggttagcctttaagcctgcccagaa	antisense

Table 1: Primer sequences of CNPCre and IRS-2 constructs.

PCR programms are presented in table 2. Resulting DNA fragments were used for gelelectrophoresis on 2% (w/v) agarose gels (1 x TAE, 0.5 µg/ml ethidium bromide) and separated at 120V.

Programm	Cycle	Degree	Time
CNPCre	single	95°C	4min 10sec
	35 repeats	95°C	30sec
		56°C	5min
		72°C	30sec
	single	72°C	7min
	single	4°C	∞
IRS-2 over expression	single	95°C	4min 40sec
	35 repeats	95°C	30sec
		60°C	1min 30sec
		72°C	2min
	single	72°C	7min
	single	4°C	∞

Table 2: PCR protocols for CNPCre and IRS-2 constructs.

2.9.4. Brain lysates

The whole brain was lysed in organ lysis buffer via a hand homogenizer. Lysates were then mixed on a tube rotator at 4°C for 45 minutes. Afterwards lysates were centrifuged at 13.000rpm at 4°C. The supernant was added into a new tube and the pellet was discarded. Protein levels were measured using the Bradford method. Bradford reagent was diluted 1:5 and 99µl were added to 1µl of each sample in a 96well plate. Standard curve was generated with 0, 1, 2.5, 5 and 10µg of BSA. Detection of protein levels were performed at 600nm via a microplate reader. Protein expression levels were analysed with 100µg protein of lysates in

Laemmli buffer. The samples were denatured at 95°C for 5 minutes and then resolved on SDS-PAGE.

2.9.5. Myelin isolation

Brain myelin was isolated by sucrose density gradient centrifugation as described by Norton (Norton and Poduslo 1973). Briefly, brains were homogenized in 20 lL/mg 0.32 M ice cold sucrose and layered over an equal volume of 0.85 M sucrose. After centrifugation
at 75 000 g for 30 min at 4°C, myelin was collected from the interphase and osmotically shocked with water on ice for 30 min. The myelin fragments were sedimented at 20 000 g for 40 min at 4°C, resuspended in lysis buffer [50 mM Tris-HCl (pH 7.4), 150 mM NaCl, 1% (v/v) NP-40, 5 mM EDTA, 5% (v/v) glycerol,10 lg leupeptin per mL, 10 lg aprotonin per mL, 1 mM phenylmethylsulfonylfluoride and 1 mM Na3VO4]. After centrifugation at 16 000 g for 45 min at 4°C, supernatant was harvested and protein concentration was measured using the method of Bradford (2.9.4).

2.9.6. SDS PAGE

Sodium dodecyl sulfate (SDS) polyacrylamide gel electrophoresis (PAGE) also called SDS-PAGE is used to separate proteins with regard to their molecular size. Proteins are denatured and linearized by heat and anionic detergent SDS. Such samples are negatively charged in proportion to its molecular mass. Samples are supplied to the polyacrylamide gel in a gel apparatus (Minigel-Twin) filled with 1xSDS-PAGE running buffer. An electric current is applied and the negatively charged proteins migrate through the gel with different speed depending on the molecular size of the proteins. Small proteins migrate more easily through the gel while larger proteins migrate more slowly. The stacking gel collects the proteins and the resolving gel seperates the proteins according to their molecular size. The resolving gel shows a contcentration from 8, 10 or 15% acrylamide (Table 5). The different concentrations are dependent on the molecular size of the proteins of interest. 8% resolving gels are used for proteins with high molecular weight and 15% resolving gels are used for small molecular weight proteins.

Chemicals	Stacking Gel	Resolving Gel [8%]	Resolving Gel [10%]	Resolving Gel [15%]
ddH2O	2.74ml	7.14ml	6.34ml	3.5ml
1M TrisHCl	0.5ml			
3M TrisHCl		1.5ml	1.5ml	1.3ml
10% SDS	40ul	120ul	120ul	105ul
30% Acrylamid	680ul	3.2ml	4ml	5.25ml
10% APS	80ul	160ul	160ul	140ul
TEMED	4ul	12ul	12ul	10.5ul

Table 3: SDS-PAGE Gels 8 and 10%(2 mini gels) and 15% (1 mini gel).

Polyacrylamide gels contain the catalyst of polymerization Ammonium-persulfate (APS). N,N,N´,N´-tetramethylethylenediamine (TEMED) is added at last to initiate polymerization. Samples and 10µl PageRuler™ Prestained Protein Ladder is added to the gel. Electrophoresis of samples in the stacking gel is promoted at 120V and in the resolving gel at 150V.

2.9.7. Western Blot

Western Blot is performed to transfer the seperated proteins on the polyacrylamidegel to a polyvinylidene difluoride (PVDF) membrane via electrophoresis with semidry-blotting. An electric current transfers the negative charged proteins from the polyacrylamid gel onto the PVDF membrane (7x9cm). First three transferbuffer soaked whatman papers (7x9cm) were placed on a horizontally localized cathode plate. Then the PVDF membrane was incubated in 99% methanol for 30sec and put onto the whatman papers. After cutting off the stacking gel, the resolving gel is placed on the membrane and covered by three additional transferbuffer soaked whatman papers. Air bubbles were removed by carefully rolling over the stack with a pipette. Then the anode plate is placed on top of the stack. These two electric plates are close to each other because only seperated by the stack to provide a high field strength (V/cm) for the protein transfer.

The transfer was performed with an electric current of about 200 milli-ampere (mA). The time of transfer was dependent on the molecular mass of the proteins of interest. Proteins with a size up to 100kDa were transferred for 1 hour, proteins with a higher molecular mass for 1.5 hours. Afterwards the gel and whatman papers were discarded and the membrane was incubated in blocking solution (10% western blocking solution in 1xTBS) for 1 hour at room temperature to saturate vacant membrane protein binding sites. Then the membrane was incubated with the primary antibody to detect the protein of interest (antibody in 5% western blocking solution in 1xTBS) over night at 4°C. Subsequently the membrane was washed four times every 15 minutes with 1xTBS consisting of 0.1 % TWEEN 20® (TBS-T). These

processes were performed on a rocker at room temperature and removed unbound antibodies.

After that the membrane was added to the secondary antibody solution (antibody in 5% western blocking solution in 1xTBS) for 1 hour. The secondary antibody is conjugated to horseradish peroxidase (HRP) via protein cross-linking. Afterwards the membrane was washed four times for each 15 minutes with TBS-T. Enhanced chemiluminescence (ECL) assay was used to detect proteins of interest with photographic film. β-actin served as loading control. For phosphorylated proteins the unsphosphorylated form of the protein served as loading control.

The HRP conjugated to the secondary antibody catalyzes the oxidation of luminol which causes light emitting. This light is detected using a photograph film. For this detection membrane is incubated in two detecting reagents (Amersham ECL™ Western Blotting Detection Reagent), which are mixed. Afterwards the membrane was covered with plastic foil and placed into a metal cassette. In a darkroom the membrane was exposed to a photosensitive film (AmershamTM Hyperfilm ECL). The time of exposure depended on the intensity of emitted light and lasted from 10 seconds to 30 minutes. Then the film was developed (CURIX60, Agfa-Gevaert, Sepestraat, Belgium).

In some cases the PVDF membrane was cleared from antibodies, "stripping" to be incubated with an antibody detecting another protein. This was performed once for each blot to obtain proper protein detection. The membrane was incubated in stripping solution at $60^{\circ C}$ for 20 minutes in a shaking water-bath. Then the membrane was washed for four times in TBS-T followed by blocking (10% western blocking reagent in 1xTBS) for 1 hour at room temperature. Afterwards another primary antibody could be added to the membrane.

2.9.8. Histology

CC mice were crossed with tg IRS-2 mice. Those mice were anesthetized and transcardially perfused with physiological saline solution and then with 4% paraformaldehyde (PFA) in 0.1M phosphate-buffered saline (PBS pH7.4). Brains were incubated in 4% PFA over night and then for three days in 20% sucrose in PBS pH7.4 at 4°C. Then brains were frozen in tissue-freezing medium (Jung Tissue Freezing Medium; Leica Microsystems, Wetzlar, Germany). These samples were axially sectioned via Research Cryostat Leica CM3050 S (Leica, Wetzlar, Germany) harvest on slides and stored at -80 °C.

2.9.8.1. Immunohistochemistry

Frozen sections were dried at room temperature and with the PAP pen a hydrophobic barrier through was drawn around the section on the slide. Afterwards the slides were rinsed 2-3 times in PBS to remove frozen mounting media. The slides were then incubated for 10min in 5% Triton-X and washed for 3 times in PBS for 5min. The primary antibody diluted in 0.8% BSA was then put on the sections and incubated for 18h at RT. Afterwards the slides washed again in PBS 3 times for 5min and incubated with the secondary antibody diluted in 0.8% in BSA for 2h at RT. The slides were then dried and mounted in Fluoromount (Sigma Aldrich, Cat. No. F4680, USA).

2.9.8.2. Histological stainings

2.9.8.2.1. Combinational staining of Klüver-Barrera

Frozen sections were dried at room temperature and then washed with distilled water for 30 seconds. Afterwards sections were stained for 2h at 56°C in Solvent blue-solution, which was diluted 1:4 in 96% Ethanol and incubated at room temperature (RT) for 2min in 96% Ethanol, 2min in 0,01% NaOH (1M) and 1 min in distilled water. Then the sections were stained for 6min at 56°C in Cresyl violet -solution. Finally sections were differentiated in 96% Ethanol and dehydrated in 100% isopropanol, both for 2min. Slides were dried and mounted in Entellan (Merck, Catalog # 1079610100, Darmstadt, Germany).

2.9.8.2.2. Nissl staining

Frozen sections were dried at room temperature and then washed with water for 30 seconds. Afterwards sections were stained in Nissl staining solution (0.1% Cresyl violet in distilled water) for 20 minutes followed by an additional washing step in water for 30 seconds.. Then sections were incubated in 40%, then 70%, 95% and at last in 100% ethanol for up to 10 minutes. Afterwards slides were incubated in Xylol for 5 minutes and additionally in fresh Xylol for 2 minutes. Slides were dried and mounted in Entellan (Merck, Catalog # 1079610100, Darmstadt, Germany).

2.9.9. Behavioral studies

Behavioural studies were performed to test whether an oligodendrocyte specific over expression of IRS-2 cause any changes in behaviour and motor coordination. For the

following tests Wildtype (WT), CNPCre (CC), IRS-2 (IR) and IRS-2 overexpressing (IRCC) male and female mice were used.

RotaRod

Mice were placed on a rotating wheel with different speeds and the time was measured until the mice fell off the wheels. First the mice had to learn to run on the wheels. After this period the measurements were performed at 4, 8, 16rpm and accelerated speed.

Trunk-curl

The Trunk-curl is an analysis of motor coordination. Mice were lifted about 30cm in the air by the tail presence or absence of a trunk curl is noted.

2.10. Transformation and Plasmid isolation

Transformation of $CacI_2$-competent *Escherichia coli* (Omnimax) was performed to amplify a specific vector in shaking culture of 100ml LB-medium followed by isolation of the Plasmid (Qiaprep Spin Maxiprep Kit, Qiagen GmbH, Hilden, Germany) or to separate single bacteria colonies on a agar plate. Both medium and agar plate contain the specific antibiotic to guarantee bacteria growth which include the vector with the specific antibiotic resistance gene.

For transformation of $CacI_2$-competent *E. coli* bacteria were incubated at $4^{\circ}C$ with 7µl of the ligation reaction added for 25 minutes. After that a heat shock is performed at $42^{\circ}C$ for 1.5 minutes. Then bacteria were harvested at 4°C for 5 minutes followed by addition of 400µl of LB-medium. Bacteria were then shaked at 37°C for one hour. Afterwards the bacteria were plated on an agar containing kanamycin 25µg/ml and incubated at 37°C overnight in a bacteria incubator (BINDER GmbH, Tuttlingen, Germany).

The next day single bacteria colonies were picked and each added to single tubes with LB-medium (kanamycin 25µg/ml) and shaken in a bacteria shaker (INFORS AG, Bottmingen, Switzerland) at 37°C overnight.

Plasmids were isolated using the Qiaprep Spin Miniprep Kit (Qiagen GmbH, Hilden, Germany) according to the protocol of the manufacturer. The plasmids of the single bacteria clones were digested with BamHI and XhoI at 37°C for 1h to identify plasmids which contain the target gene. These plasmids were sequenced via T3 and T7 sequencing primers (Eurofins MWG Operon, Ebersberg, Germany). Plasmids of clones which showed disruptions of the target gene, e.g. like frame shifts were again transformed into $CacI_2$-competent *E. coli,*

grown in 100ml shaking LB-medium culture followed by isolation of the plasmid (Qiaprep Spin Maxiprep Kit, Qiagen GmbH, Hilden, Germany) to obtain an increased amount of suitable DNA for further transfection.

Generation of Cacl$_2$-competent *E. coli*

Cacl$_2$-competent *E. coli* were grown in 100ml LB-medium at 37°C overnight in a bacteria shaker (INFORS AG, Bottmingen, Switzerland). Then 2ml were added to new 200ml LB-medium and shaken at 37°C until the culture reached an OD$_{600}$ of 0.4. Measurements were performed with NanoDrop. The bacteria culture was incubated at 4°C for 10 minutes to stop growth. Then the culture was centrifuged at 3000rpm at 4°C for 5 minutes. The supernant was discarded and bacteria were resuspended in 100ml CaCl$_2$-buffer. Afterwards this suspension was incubated at 4°C for 25 minutes and then centrifuged at 3000rpm and 4°C for 4 minutes. The supernant was discarded and the pellet was resuspended in 5ml CaCl$_2$-buffer. Bacteria were separated in 100μl aliquots and harvested at -80°C.

2.11. Generation of stably expressing cells

pCMV-Tag 2C vector containing mouse derived IRS-2 and the pCMV-Tag 2B containing human derived IRS-1 (2μg), were linearized with 4 Units SspI for 2 hours at 37°C. Transfection of OLN93 cells was performed via Metafectene according to the protocol of the manufacturer. OLN93 cell transfected with the empty vector were used as controles (EV). Cells were treated with selection medium containing 2mg/ml G418 (Sigma-Aldrich Chemie GmbH, Steinheim, Germany) for two days after transfection. Single cells were separated on 96-well plates after 2 weeks of selection with G418 and cultured in 0,3mg/ml G418. Cell clones were tested for expression of IRS-2 and IRS-1, positive clones were used for further experiments. After that cells were grown without G418.

2.12. PCR T7 Primer

DNA concentrations were measured with NanoDrop® ND-100 UV Spectrophotometer at 260nm. After that the targeted DNA was tested for amplification. Reactions were performed in a Thermocycler PCR machine. All reactions contained not less than 100ng DNA, 25pmol of each primer (Table 1), 25μM dNTP Mix, 4mM MgCl$_2$, 10% DMSO, 1xgoTaq reaction buffer and 1 unit of goTaq DNA polymerase.

Primer	Sequence	Orientation
T7-Promotor	taatacgactcactataggg	sense
T3-Promotor	attaaccctcagtaaaggga	sense

Table 4 : Primer sequences of CNPCre T7-Promotor sequence.

PCR programm is shown in table 5. Resulting DNA fragments were used for Gelelectrophoresis on 2% (w/v) agarose gels (1 x TAE, 0.5 µg/ml ethidium bromide) and separated at 120V.

Programm	Cycle	Degree	Time
T7-Promotor	single	95°C	5min
	40 repeats	95°C	1min
		56,5°C	45sec
		72°C	5min
	single	72°C	10min
	single	4°C	∞

Table 5: PCR protocol for T7-Promotor PCR

2.13. Cell lysates

For whole cell lysates, cells were twice washed with PBS and then incubated at -80°C for 30 minutes. After that cell lysis buffer was added to the cells (100µl for 10cm plates and 150µl for 15cm plates). Then cells were scraped from the culture dishes via cell scraper (Greiner Bio-One GmbH, Frickenhausen, Germany), incubated at 4°C for 30 minutes and needeled. Afterwards cell lysates were centrigufed at 13.000rpm and 4°C for 30minutes. Supernant was added into a new tube and the pellet was discarded. The protein concentration was measured using the Bradford method.

2.14. Proliferation assay

Proliferation assay was performed with 100.000 cells per well of each cell line. For IRS-1 and IRS-2 stably overexpressing cells 2 clones were analyzed. First cells were counted using the Neubauer Zählkammer and 1000 cells were put into a well of a 96-well plate. The next day cells were starved in a medium without FBS for 3 days to stop cell proliferation. After that a medium with 10% FBS was added for 48 hours. For inhibition of the PI3K and MAPK pathway the following inhibitors were used (LY294002: PI3K-inhibitor: 20µM; PD98059: MAPK-inhibitor: 50µM) and were added next for 12h, before BrDU was put onto the cells for

12h. Subsequently the proliferation assay (BrdU assay, Millipore, Billerica, MA, USA, item #HCS201) was performed according to the protocol of the manufacturer.

2.15. Cell differentiation

To promote differentiation, OLN-93 cells were seeded at low density on 15cm plates (0.6 x 10^6 cells) and cultured in DMEM with 10% FCS. After overnight attachment, cells were gently washed and subsequently cultured in serum-free DMEM for 6 days [Van Meteeren et al., 2005]

3. Results

3. Results

Multiple sclerosis (MS) is an inflammatory demyelinating disease that attacks the brain, spinal cord and optic nerves in the CNS, but skips the nerve roots and peripheral nerves of the peripheral nervous system (PNS). Axonal loss is an unstoppable result from MS and might be the pathological correlate for the irreversible neurological impairment of this disease [Ferguson, Matyszak, Esiri and Perry, 1997; Lovas et al., 2000; McGavern et al., 2000; Trapp et al., 1998]. However oligodendrocytes progenitors are present in MS lesions but they fail to remyelinate the affected regions [Scolding 1998; Wolswijk; 1995; Wolswijk; 2000].

Oligodendrocytes support axonal function and survival throughout life, independent of myelin function [Trapp et al., 1998; Wujek et al., 2002]. The InR/ IGF1R-signaling cascade is known to be an fundamental player in myelination, as it acts as a survival factor for oligodendrocytes as well as their OPCs [Barres et al., 1992; Mason et al., 2000; McMorris et al., 1986; Ye and D'Ercole, 1999] and stimulates the synthesis of myelin [Roth et al., 1995]. Animal studies showed that over expression of IGF-I increases myelin content [Carson et al., 1993; Ye et al., 1995] and deletion of IGFI strongly decreases myelination and the number of OPCs [Beck et al., 1995].

As the IRS proteins are important signaling molecules in the IR/ IGF1R our group investigated their role for myelination. Previous work showed, that IRS-2 is critical for appropriate initiation of myelination, but not for myelin maturation and IRS-1 can only partly compensates for the loss of IRS-2. Furthermore IRS-2 knockout mice displayed a smaller brain size compared to their littermates, which might reflect myelination as well. On the other hand mice lacking the InR revealed no changed or altered myelination, so that the myelination initiation signal is mainly transduced via the IGF1R [Freude et al., 2008].

Wether increased IRS-2 signaling impacts myelination *in vivo* is still unknown. Thus the following thesis aims to elucidate the influence of IRS-2 on myelination and the InR-/ IGF1R signaling in oligodendrocytes.

Therefore we generated mice which own a floxed westphale stop cassette that regulates an IRS-2 gene in the Rosa26 locus (IR). These mice were crossed with mice expressing the CNP driven Cre recombinase (CC) to guarantee an oligodendrocyte-specific over expression of IRS-2 (IRCC) (Fig. 10).

CNP ($^{-/-}$) are known to show normal myelin assembly, whereas the ultrastructure and physical stability are not visibly changed. Aside throughout the white matter axons developed abnormal swellings and were progressively which leaded to premature death mostly before one year of age. Additionally, it can not be excluded that axon functions are changed in the motor system of those mice during aging. Therefore those mice present a usable MS model [Lappe-Siefke et al., 2003].
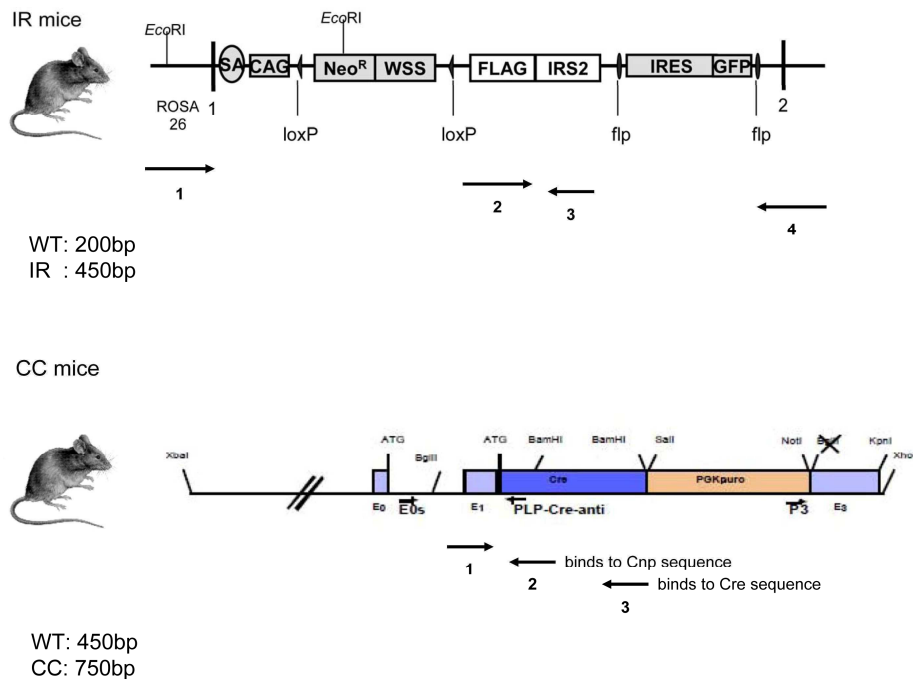
Figure 10: Breeding strategy of oligodendrocyte-specific over expressing IRS-2 mice.
Mice with IRS-2 inserted in the *Rosa26 locus* were crossed with CNP promoter driven Cre recombinase expressing mice. Presented below are the locations of the PCR Primers, those generate an allele specific PCR.

3.1. Validation of IRCC mice

The IRS-2 insert in the Rosa26 locus was detected via the IRS-2 specific PCR (2.9.3.). Primer 1 and 2 bind forward and 3 and 4 reverse to the DNA sequence. As 1 and 4 bind onto the sequence of the *Rosa26 locus*, the result is a WT specific PCR fragment (Fig.10). Similary primer 2 and 3, as this sequence does not exist in WT mouse the fragment is particular detectable in transgenic mice. The amplified fragment of IR shows a size of about 450bp and of a WT mouse 200bp (Fig.11A). For the CC mouse was as well an allele specific PCR was designed. Here Primer 1 binds forward in the DNA sequence of the CNP gene and 2 reverse. Primer 2 binds in case the CNP gene is not deleted (due to insertion of Cre recombinase). The Cre recombinase is detected via Primer 3, which binds in a reverse orientation (Fig.11). Therefore two bands result in heterozygous mice, a WT fragment about 450bp and the transgenic fragment about 750bp (Fig. 11A).

A

B

C
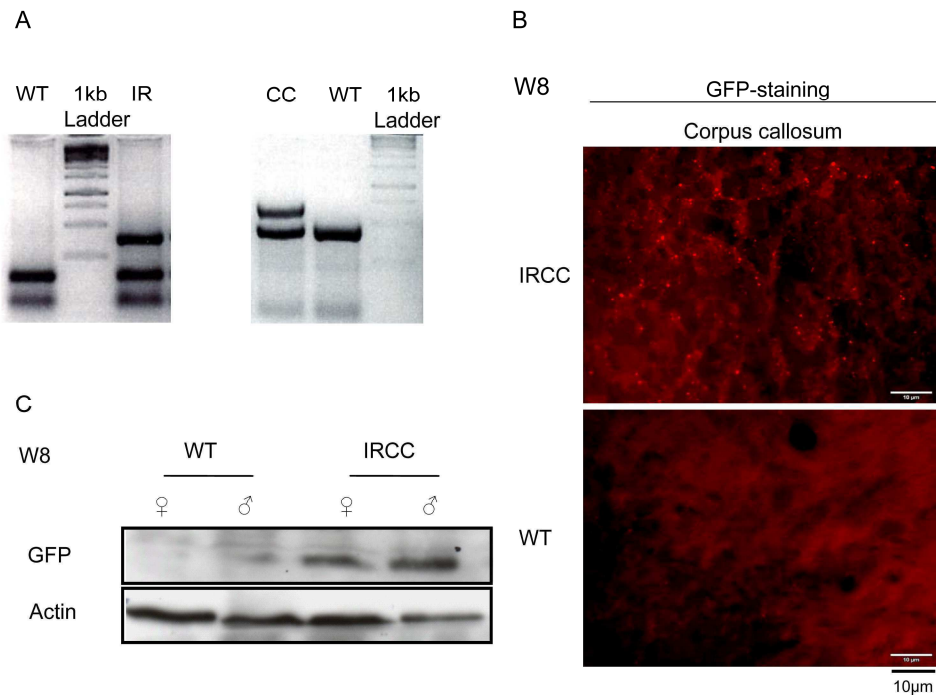
Figure 11: Validation of IRCC and CC mice.
(A) IR and CC specific PCR products separated on a 2% agarose gel (2.9.3.). The IR transgenic fragment shows a size of about 450bp, whereas the WT is about 200bp. CC transgenic fragment is 750bp and the WT 450bp.
(B) Immunological staining of eGFP in the corpus callosum of 8 week old IRCC mice and wild type mice as controls, show an eGFP expression in IRCC but not in the WT mouse.
(C) Western-Blot detection of eGFP of 200µg whole brain lysate of 8 week old mice shows an eGFP expression in male and female IRCC mice and none in female and male WT mice (12 SDS-PAGE gel).

Immunohistochemical staining (Fig. 11B) showed an expression of eGFP in IRCC mice in the corpus callosum. There was no eGFP detected in the WT mouse brains. Expression of eGFP was proven in both genders (Fig. 11C).

3.2. Characterisation of IRCC mice

Previously, it has been shown using IRS-2 ($^{-/-}$) mice that IRS-2 plays a critical role in appropriate initiation of myelination, but not in myelin maturation. Therefore IRCC mice were analyzed in an age-dependent manner detecting changes of morphology, structure, myelin specific protein expression and InR/ IGF1R signaling in the brain. Furthermore motorcoodination, body weight and body brain ratio was as well probed.

3.2.1. Body weight and brain body ratio of IRCC mice

The body weight, length and brain weight were measured over the time from day 5 until day 140 of all different genotypes and both genders to evaluate the body mass index (BMI) and the brain body ratio of the mice.

The BMI was similar in all genotypes of female mice from 5days up to 140 days of age. All four genotypes showed an increase of the BMI from 17,4 at day 5 to 23,6 at day 140 (Fig.12).

Figure 12: BMI of female mice.
BMI of female WT (n=5-15; blue), CC (n=5-19; orange), IR (n=3-14; green) and IRCC (n=3-17; pink) until 140days (40weeks) of age.

Male mice showed compared to female mice a higher BMI. The timely pattern is similar to female mice, a drop until 15,7 at day 14 which is followed by a gain to 29,5, at day 140 (Fig.13).

Figure 13: BMI of male mice.
BMI of male WT (n=5-26; blue), CC (n=7-13; orange), IR (n=6-14; green) and IRCC (n=4-12; pink) until 140days (40weeks) of age.

Next the brain body ratio of all different genotypes during postnatal development was investigated to detect any genotype-specific changes during development. Female mice of all genotypes showed a similar plot, which starts at about 6.5%, followed by a decrease and a stagnancy from 35 days until 140 days up to about 2% (Fig. 14).

Brain Body Ratio Female Mice
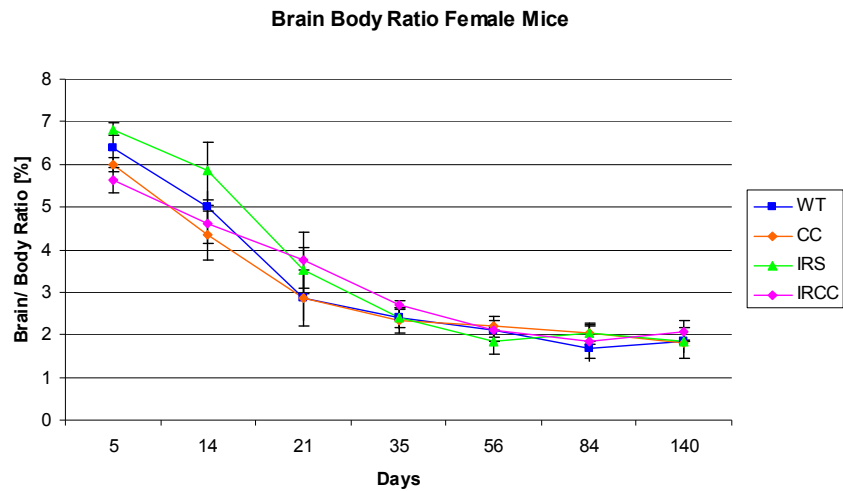
Figure 14: Brain body ratio of female mice
Body brain ratio of female WT (n=5-15; blue), CC (n=5-19; orange), IR (n=3-14; green) and IRCC (n=3-17; pink) until 140days (40weeks) of age.

Male mice of all genotypes indicated the same pattern as the female mice. However at 5 days of age WT, IR and IRCC mice start around 6.5%, whereas CC mice displayed a reduced brain body ratio by 4,2%. Going further down with age in all genotypes demonstrated the same course as females (Fig. 15).
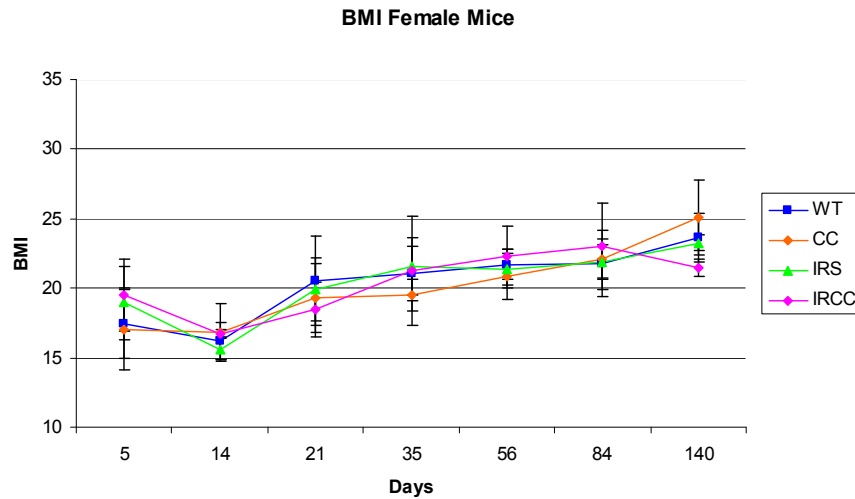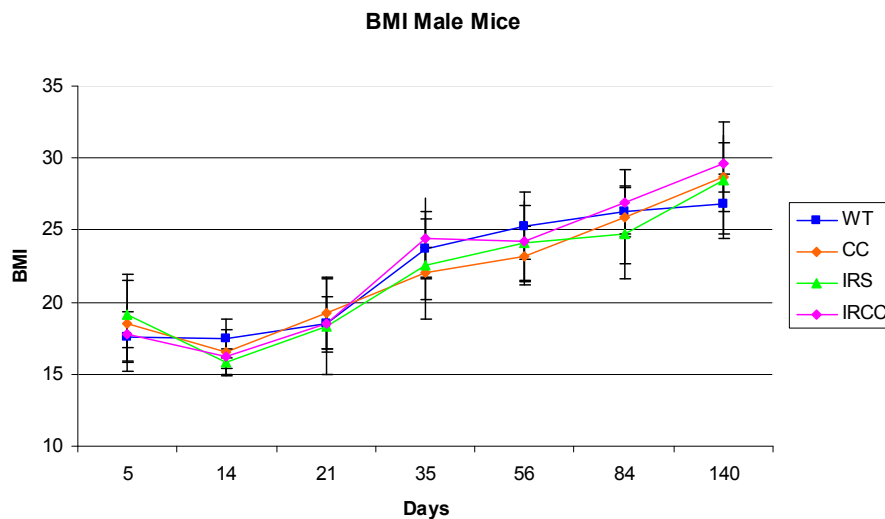
Brain Body Ratio Male Mice
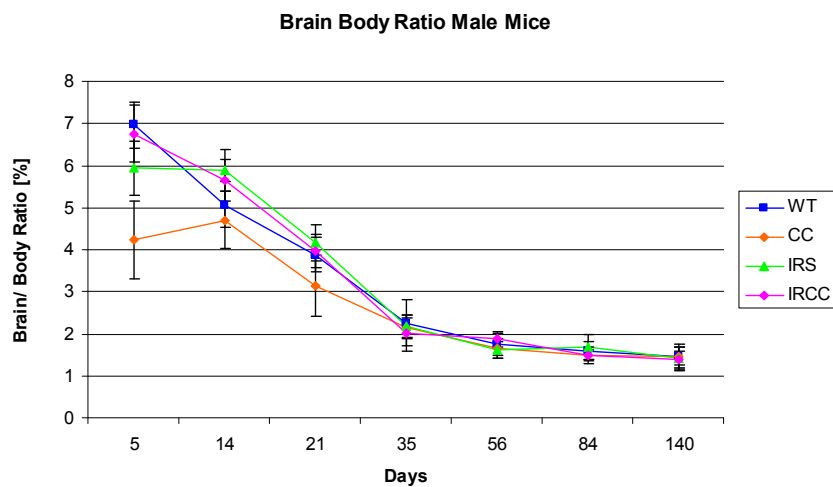
Figure 15: Body brain ratio of male mice.
BMI of male WT (n=5-26; blue), CC (n=7-13; orange), IR (n=6-14; green) and IRCC (n=4-12; pink) until 140days (40weeks) of age.

3.2.2. Behaviour of IRCC mice

Motor coordination was investigated via RotaRod. A mouse was put on a rotating wheel with different speed and the time was measured until the mouse falls down. This gives a hint whether the specific mouse displays an affected motor coordination. For this test adult mice (week 12) were tested (Fig.16). Female CC ($^{-/-}$) (homo CC) mice showed a reduced ability to stay on the rod at 16rpm. However no differences were observed comparing the other genotypes.

Accelerating wheel speed did not result it any alternations of IRCC mice. In male mice CC and CC ($^{-/-}$) mice showed a tendency to decrease performance at 16rpm. At accelerating speed no differences between the different genotypes were observed.
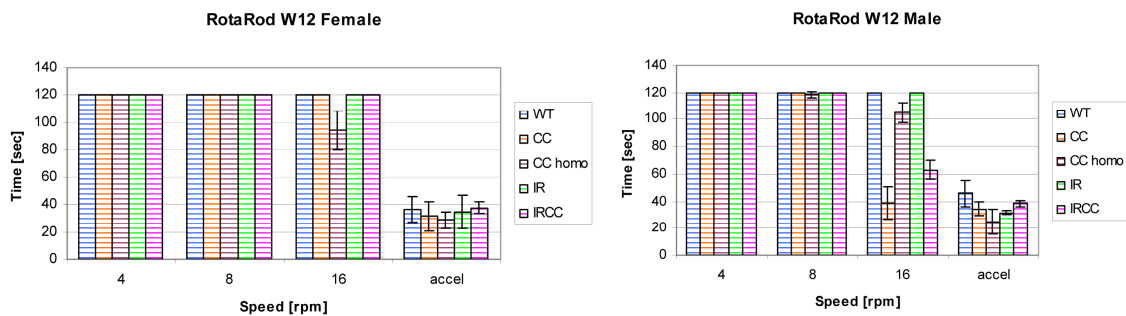
Figure 16: RotaRod of 12 weeks old mice
The RotaRod test male and female WT (n=3, blue), CC (n=3, orange), CC homozygous (CC homo; n=3, red), IR (n=3, green) compared to IRCC animals (n=3, pink). Animals were 12 weeks old.

Additionally neuromuscular functions were measured via grip strength. An individual mouse grabbed a trapeze with its forepaws, and then a horizontal backwards pull was applied until the pulling force overcomes its grip strength. Maximal grip strength was measured.

Female CC, CC ($^{-/-}$) and IRCC mice displayed an decrease in grip strength compared to IR and WT mice. No differences were observed within the different male genotypes (Fig. 17).
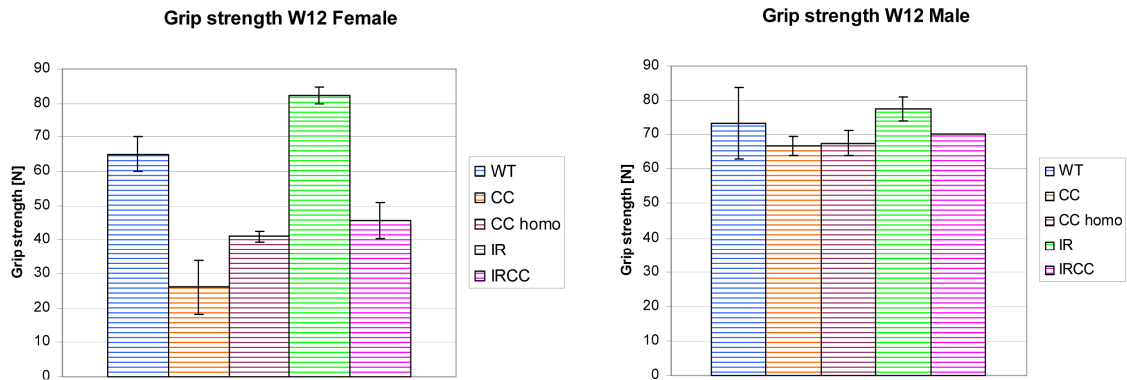
Figure 17: Grip strength of 12 weeks old mice
The Grip strength of male and female WT (n=3, blue), CC (n=3, orange), CC homozygous (CC homo; n=3, red), IR (n=3, green) compared to IRCC animals (n=3, pink). Animals were 12 weeks old.

Due to the lack of enough female and male mice of week 40, individual mice off all genotypes and genders were observed during the Trunk-curl. The Trunk-curl is the ability of mice to bring the upper body up and a sit up movement when held by the tail. Whereas twisting the upper body sideways is not defined as a Trunk-Curl.

Female and male WT and IR mice were able to bend properly upwards (Fig.18). CC and CC homo mice of both genders did not manage to move their body upwards and stretch their hind paws backwards, whereas the CC homo mice compared to the CC mice showed a stronger phenotype. IRCC mice of both genders displayed similar behaviour as the CC mice, but less severe compared to CC homo mice.

W40
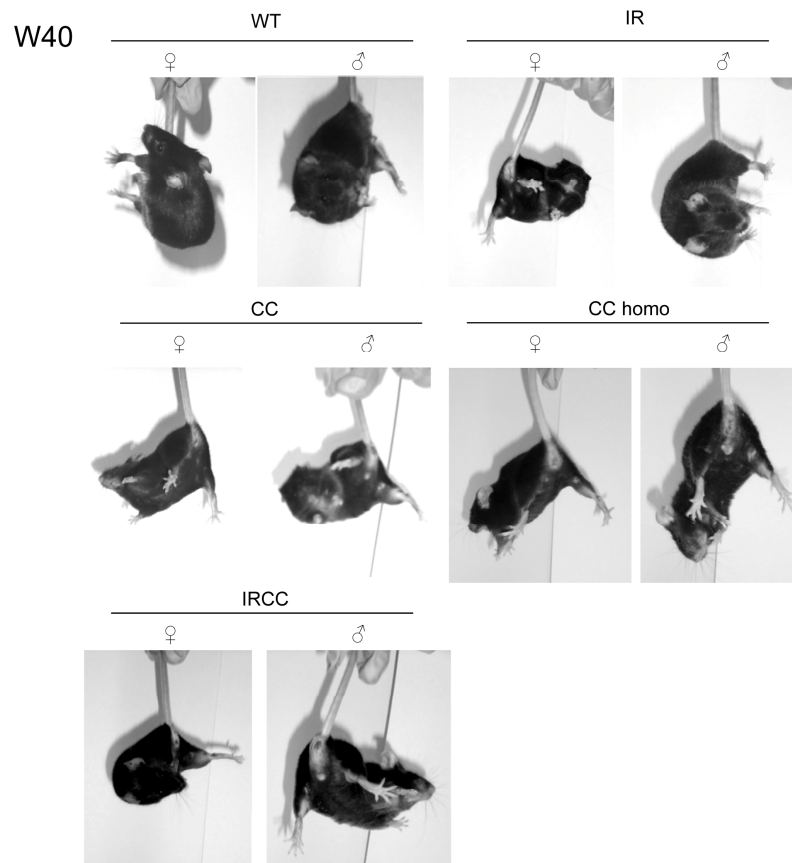
Figure 18: Trunk-curl of 40 weeks old mice
The Trunk-curl test analyses the ability of the mouse to bend upwards, when held downwards. Tested were female and male WT, IR, CC, CC homo and IRCC mice at week 40.

3.2.3.1. Morphological and structural brain analysis of IRCC mice

Perfused brains for female and male mice of all genotypes were sliced in coronal sections and examined in respect to changes in morphology and structure of the brain.

Nissl-staining stains the negatively charged RNA blue and highlights important structural features of neurons. The Nissl substance appears dark blue as it represents the granular cytoplasmic reticulum and ribosomes, which gives the cytoplasm a mottled appearance. DNA present in the nucleus is stained blue. The second method, Klüver-Barrera-staining is a combination to demonstrate myelin and Nissl substance respectively. Myelin and phospholipids appear blue to green whereas cells and cell products are pink to violet.

Slices of week 12 mice of all genotypes showed no difference in morphological and structural appearance of the brain. There were no discrepancies in the structure of the white (as corpus callosum) or grey matter (as cerebellum). Equally myelin and phospholipids staining via Klüver-Barrera-staining displayed no differences between the different genotypes. The white matter, as the corpus callosum displayed no structural or morphology changes (Fig. 19).

Figure 19: Nissl-staining and Klüver-Barrera-staining of W12 mice
Perfused brains were sliced coronoal in 20µm slices. Those were stained by Nissl-staining and Klüver-Barrera-staining. Shown are brain slices of male WT, CC and IRCC mice. The left row give an overview and the enlargement focuses onto the corpus callosum.

Going downwards in age week 8 female and male mice of all genotypes demonstrated no structural abnormalities compared to each other. Nissl-staining and Klüver-Barrera-staining showed the same appearance of white and grey matter, in the hippocampal formation, the corpus callosum and the cerebral cortex. There were no age dependent morphological chances in the formation of the different brain regions, as the corpus callosum, hippocampal formation and cerebral cortex indicated an unaltered brain development (Fig. 20).
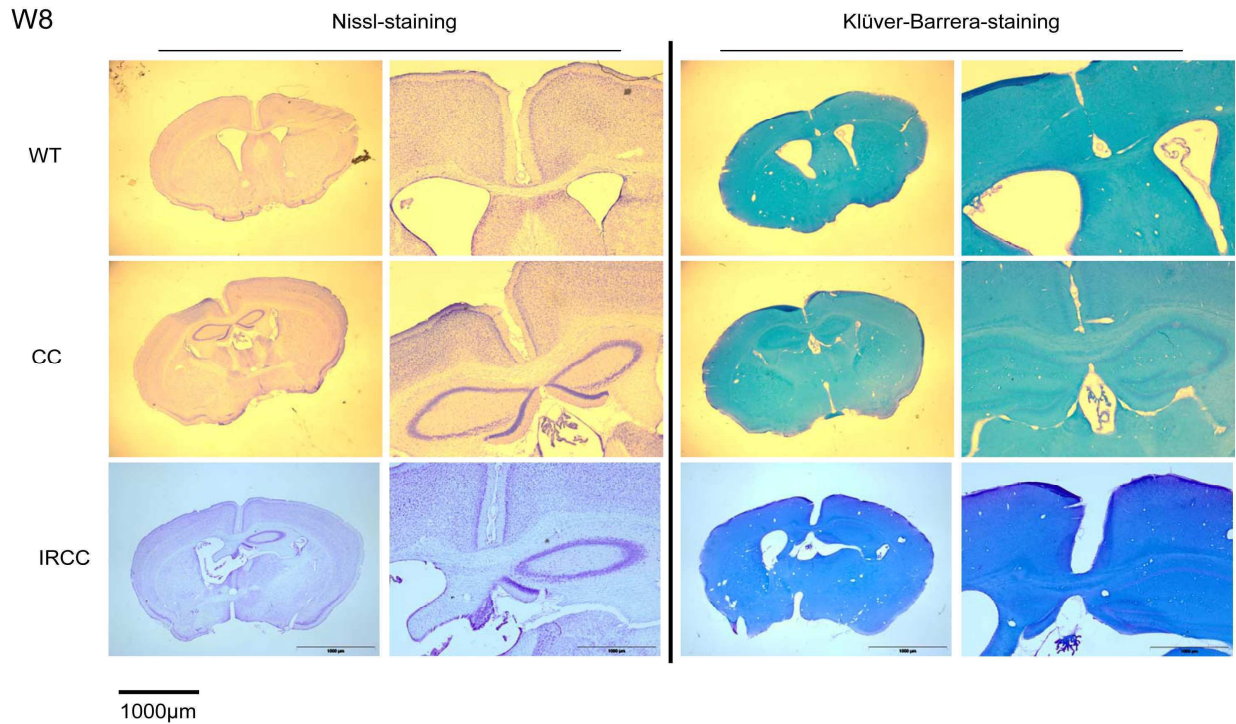
Figure 20: Nissl-staining and Klüver-Barrera-staining of W8 mice
Perfused brains were sliced coronoal in 20µm slices. Those were stained by Nissl-staining and Klüver-Barrera-staining. Shown are brain slices of male WT, CC and IRCC mice. The left row give an overview and the enlargement focuses onto the corpus callosum.

Sections of female and male mice of all genotypes at week 5 revealed no structural or morphological changes as well. The corpus callosum was completely normal structured in all genotypes. There were no differences in the cortex or the hippocampal formation detected. Morphologically and structurally all brains were not altered, due to the transgenic IRS-2 over expression or heterozygous CNP gene deletion (Fig. 21).
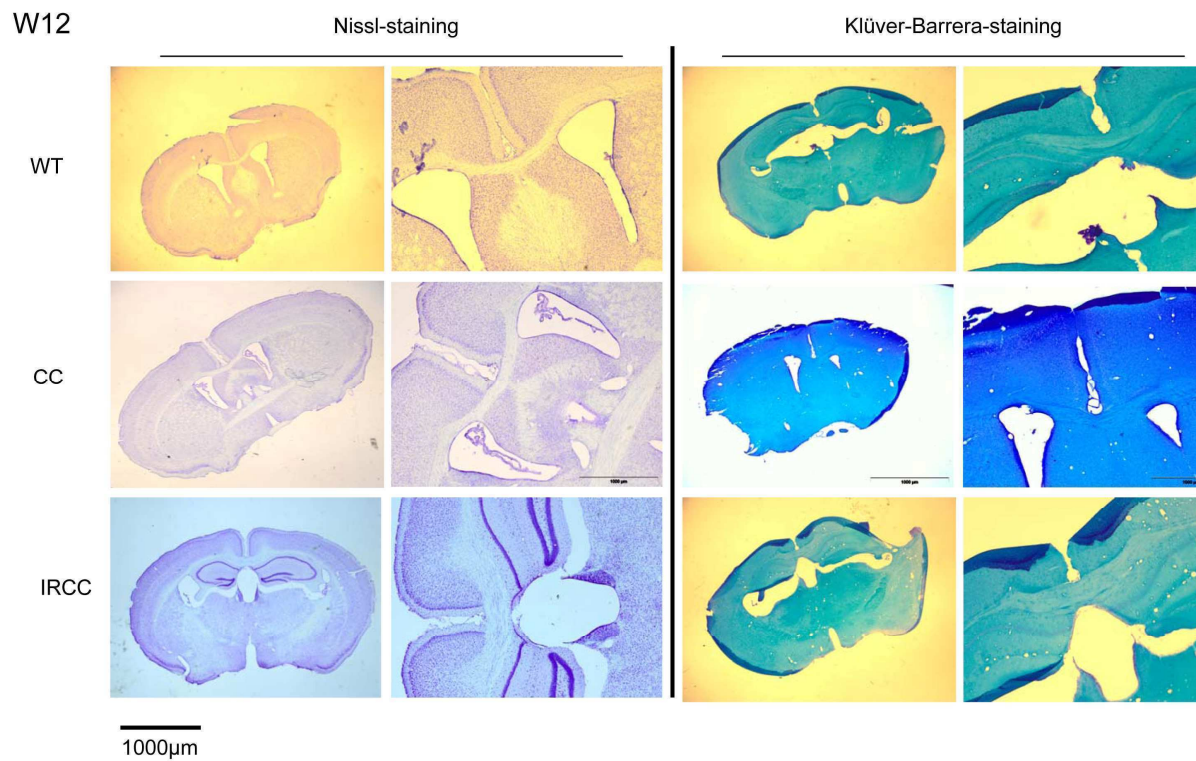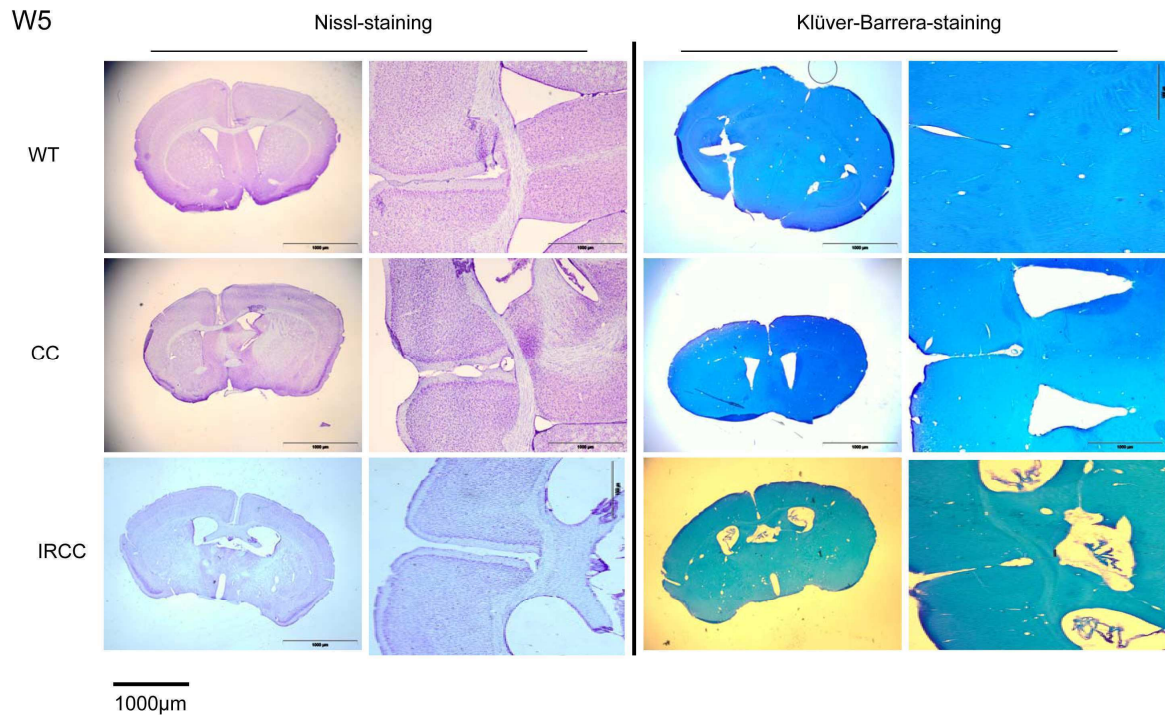
Figure 21: Nissl-staining and Klüver-Barrera-staining of W5 mice
Perfused brains were sliced coronoal in 20µm slices. Those were stained by Nissl-staining and Klüver-Barrera-staining. Shown are brain slices of male WT, CC and IRCC mice. The left row give an overview and the enlargement focuses onto the corpus callosum.

3.2.3.1. Immunohistochemical analysis of myelination in IRCC mice

Histochemically no differences were observed (Fig.10-12) in all genotypes at week 12, 8 and 5. As those staining methods can give only a general impression about morphology and structure, those brain slices were also immunohistochemically stained against two myelin specific Proteins, MBP and PLP. Those should give the opportunity to get a more detailed insight into the structure of myelination in the brain of WT, CC and IRCC mice.

However, staining using antibodies against MBP and PLP revealed in CC and IRCC mice compared to the WT no differences at the age of week 12. The corpus callosum showed the same protein expression pattern in all genotypes (Fig.22).
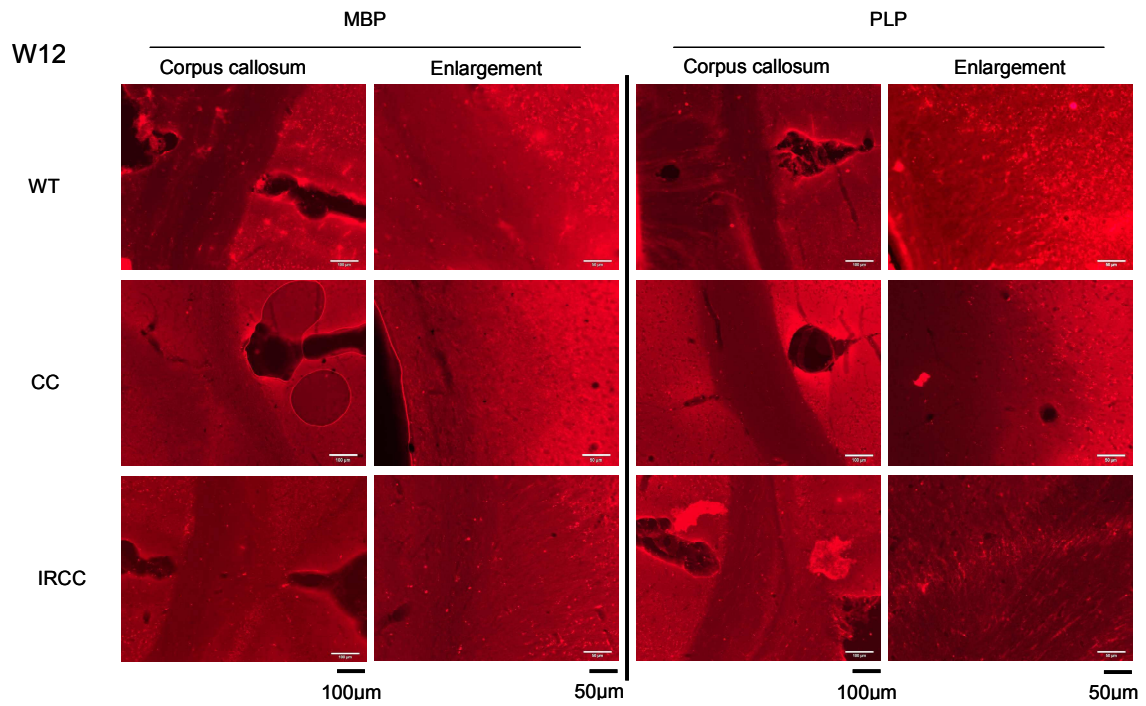
Figure 22: Immunohistochemical staining of MBP and PLP at the age of 12 weeks
Perfused brains were sliced coronoal in 20µm slices. Those were stained using antibodies against MBP (1:500) and PLP (1:100). Shown are brain slices of male WT, CC and IRCC mice.

At week 8 brains of female and male mice of all genotypes were immunohistochemically stained using antibodies of the proteins MBP and PLP. Staining against MBP and PLP revealed no differences in CC and IRCC mice compared to the WT (Fig.23).
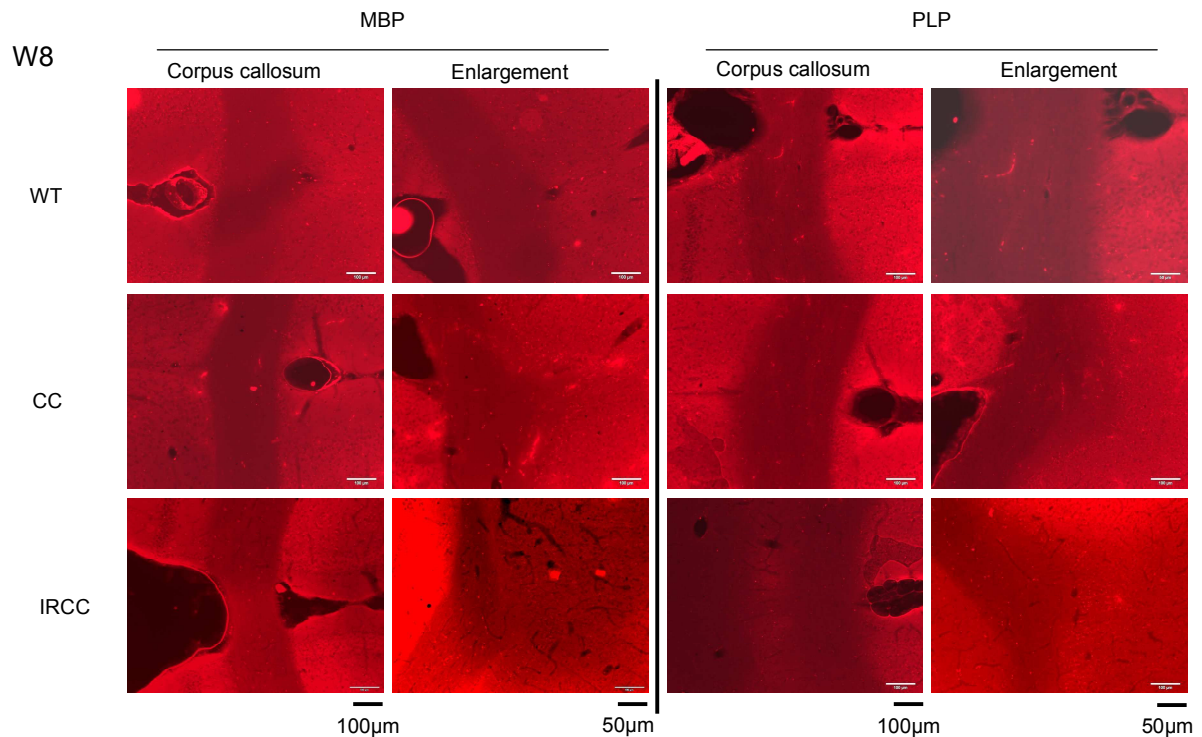
Figure 23: Immunohistochemical staining of MBP and PLP at the age of 8 weeks
Perfused brains were sliced coronoal in 20µm slices. Those were stained using antibodies against MBP (1:500) and PLP (1:100). Shown are brain slices of male WT, CC and IRCC mice.

5 weeks old brains of female and male mice all genotypes were immunohistochemically stained using antibodies of the proteins MBP and PLP. MBP as well as PLP staining revealed no changes of protein expression or distinctions in the white matter structures like corpus callosum, compared to thedifferent genotypes (Fig.24).

Heterozygous knockout of CNP as well as the oligodendrocyte over expression of IRS-2 showed no effect on MBP and PLP expression in the brain (Fig.22-24)
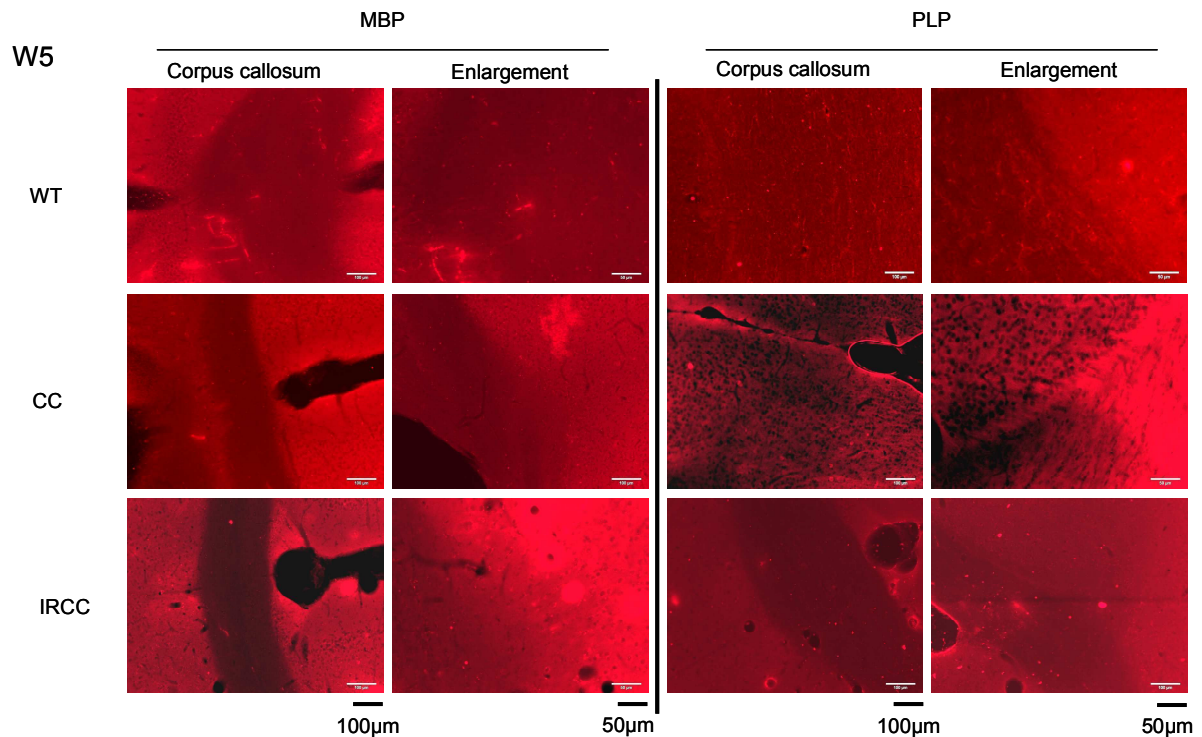
Figure 24: Immunohistochemical staining of MBP and PLP at the age of 5 weeks
Perfused brains were sliced coronoal in 20µm slices. Those were stained using antibodies against MBP (1:500) and PLP (1:100). Shown are brain slices of male WT, CC and IRCC mice.

3.2.4. Quantity of myelin specific proteins

Mice of all four genotypes were sacrificed at different time points, to investigate myelin protein composition. Out of those brains, myelin was isolated via sucrose density gradient centrifugation as described by Norton (Norton and Poduslo 1973) (2.9.7) and analysed via SDS-PAGE and Western Blot to get a more detailed insight into myelin protein composition.

Comparison of CNP amount in the four different genotypes showed a strong reduction in the expression in female and male IRCC mice at the age of 20 weeks. Female and male WT, IR and CC mice displayed the same amount of CNP. Heterozygous CC mice of both genders displayed the same protein level of CNP at this time point when compared to WT and IR mice.

PLP and its splice variant DM20 as well as MBP did not show any differences between the genotypes (Fig.25).

Coomassie staining of the SDS-PAGE gel displayed an equal gel loading.

Figure 25: Myelin specific protein expression of mice 20 weeks of age
Myelin was isolated using a sucrose gradient centrifugation and separated via 15% SDS-PAGE gel. Detection of
of CNP, PLP/DM20 and MBP was performed using 50µg protein lysate of female and male WT, IR, CC and IRCC
mice at 20 weeks of age. Coomassie staining was performed as loading control of the SDS-PAGE gels.

Analysis of week 12 old mice showed no changes in CNP protein expression level in all four genotypes and both genders. Heterozygous Female and male CC mice did not display reduced CNP content at this timepoint compared to WT, IR and IRCC mice of both genders. PLP, DM20 and MBP protein amount in female and male mice of all genotypes diplayed no difference (Fig.26)

Coomassie staining of the SDS-PAGE gel showed an equal loading.

Figure 26: Myelin specific protein expression of mice 12 weeks of age
Myelin was isolated using a sucrose gradient centrifugation and separated via 15% SDS-PAGE gel. Detection of
of CNP, PLP/DM20 and MBP was performed using 50µg protein lysate of female and male WT, IR, CC and IRCC
mice at 12 weeks of age. Coomassie staining was performed as loading control of the SDS-PAGE gels.

Myelin isolation of 8 weeks old mice showed the same CNP protein content in all gebotypes. Heterozygous CC mice, did not display a reduced CNP content at this time point in isolated myelin samples compared to WT, IR and IRCC mice of both genders.

PLP and DM20 protein amount in all genders and genotypes was the same. The protein quantity of MBP indicated equal expression levels in all lines (Fig.27).

Coomassie staining of the SDS-PAGE gel displayed an equal loading of the protein samples of the two genders and different genotypes.

Figure 27: Myelin specific protein expression of mice 8 weeks of age
Myelin was isolated using a sucrose gradient centrifugation and separated via 15% SDS-PAGE gel. Detection of
of CNP, PLP/DM20 and MBP was performed using 50µg protein lysate of female and male WT, IR, CC and IRCC
mice at 8 weeks of age. Coomassie staining was performed as loading control of the SDS-PAGE gels.

At 5 weeks of age isolated myelin of female and male WT, IR, CC and IRCC mice displayed an equal expression level of CNP.

Protein amount of PLP, DM20 and MBP in isolated myelin showed no strong alterations at this time point in both genders and in all four genotypes (Fig.28).

Coomassie staining of the SDS-PAGE gel revealed equal loading of isolated myelin proteins.

Figure 28: Myelin specific protein expression of mice 5 weeks of age
Myelin was isolated using a sucrose gradient centrifugation and separated via 15% SDS-PAGE gel. Detection of of CNP, PLP/DM20 and MBP was performed using 50µg protein lysate of female and male WT, IR, CC and IRCC mice at 5 weeks of age. Coomassie staining was performed as loading control of the SDS-PAGE gels.

Isolated myelin at week 3 of female and male WT, IR, CC and IRCC mice displayed a slight reduced amount of CNP in both genders of WT mice compared to IR, CC and IRCC mice. CNP amount of female and male IR, CC and IRCC mice compared to each other was similar. Heterozygous CNP mice had the same CNP content as female and male IR and IRCC mice at this time point.

PLP and DM20 protein expression was in female mice of all genotypes the strongest and displayed to be similar.

Female mice expressed more protein of the 21.5kDa MBP isoform, which is known to appear earlier in development of mice. IRCC mice of both genders mice showed to have the highest protein levels of all MBP isoforms (21.5, 18.5, 17, 14kDa). The expression level of the 18.5 and 17kDa isoform in CC mice is nearly similar to the one in IRCC mice.

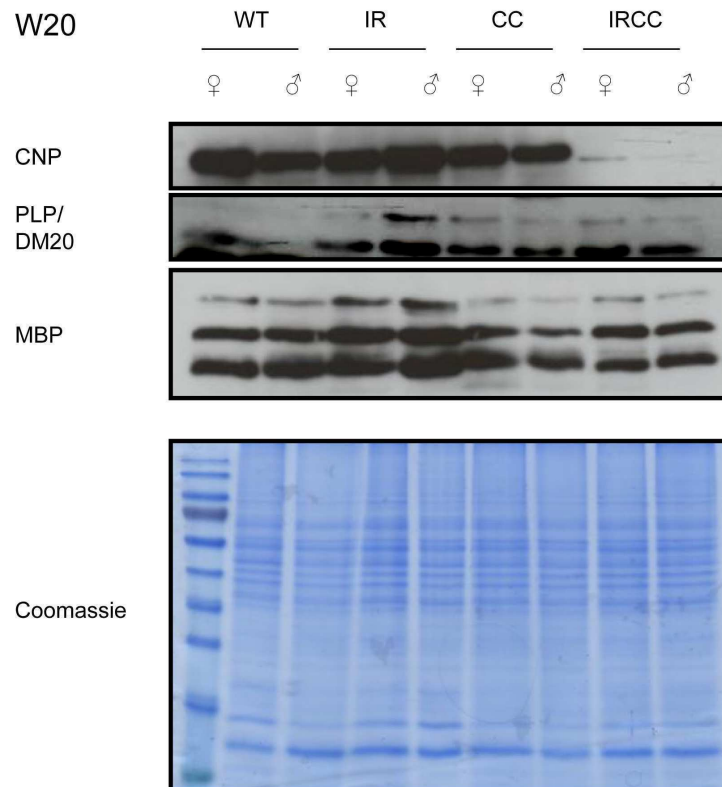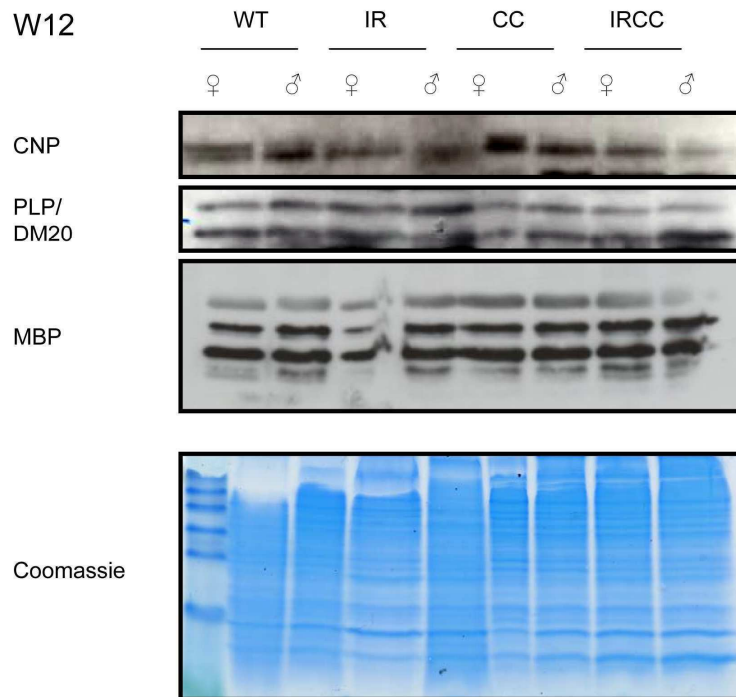Coomassie staning of the SDS-PAGE gel revealed a equal loading (Fig.29).
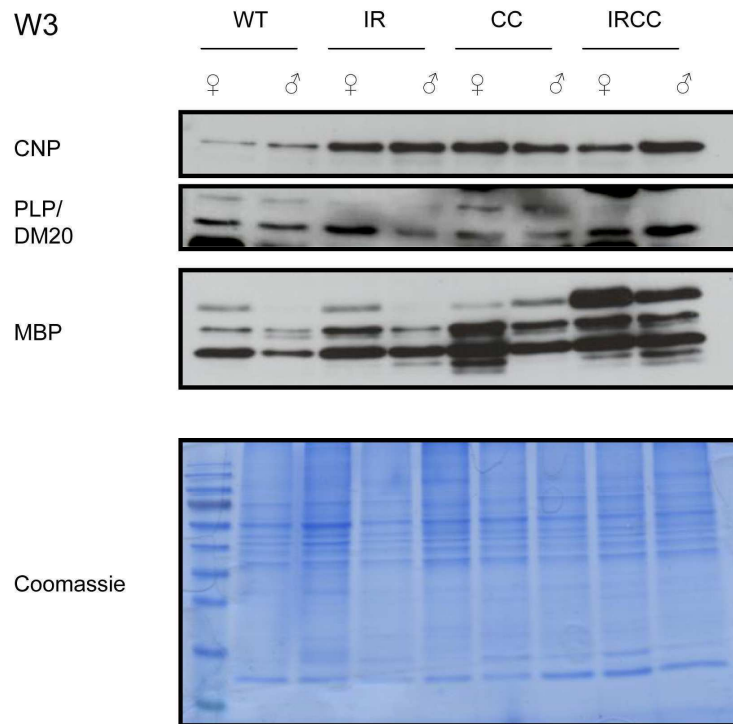
Figure 29: Myelin specific protein expression of mice 3 weeks of age
Myelin was isolated using a sucrose gradient centrifugation and separated via 15% SDS-PAGE gel. Detection of of CNP, PLP/DM20 and MBP was performed using 50µg protein lysate of female and male WT, IR, CC and IRCC mice at 3 weeks of age. Coomassie staining was performed as loading control of the SDS-PAGE gels.

At day 5 of age CNP abundance in isolated myelin showed slight variations which were not dependent on the genotype.

DM20 protein levels was not detectable, even when 500µg protein amount were loaded.

Protein content of MBP isoforms were similar in both genders of WT, IR and IRCC mice. Male CC and WT displayed elevated levels of the 18.5, 17 and 14kDa isoform. The other mice indicated comparable amount of the 18.5, 17 and 14kDa isoform.

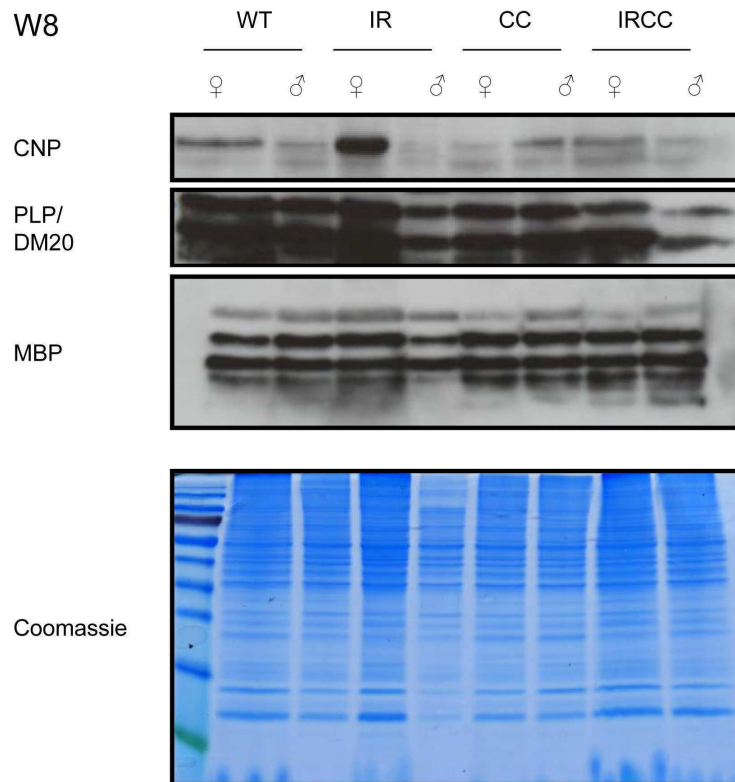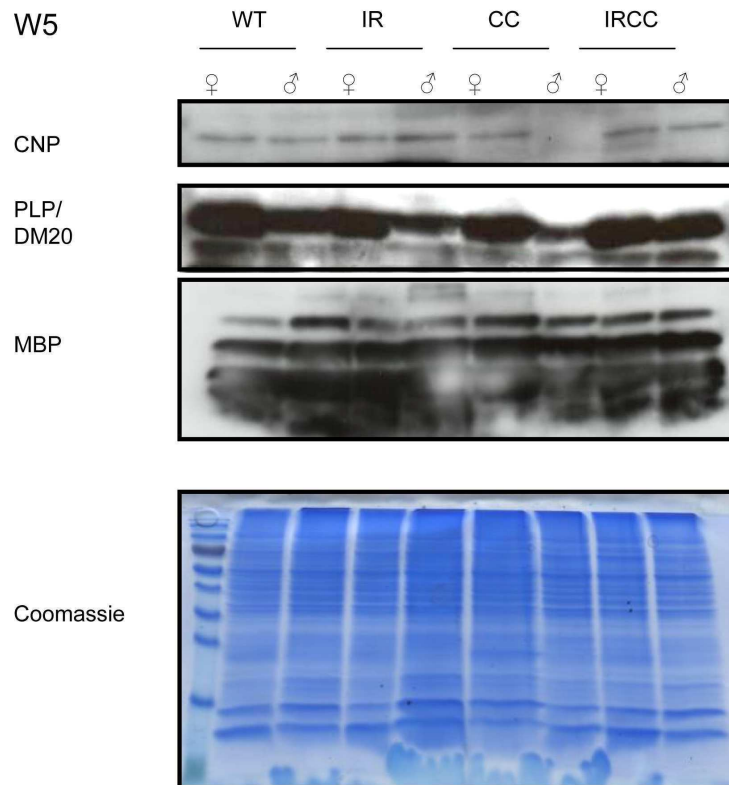Coomassie staning of the SDS-PAGE gel revealed equal protein content (Fig.30).
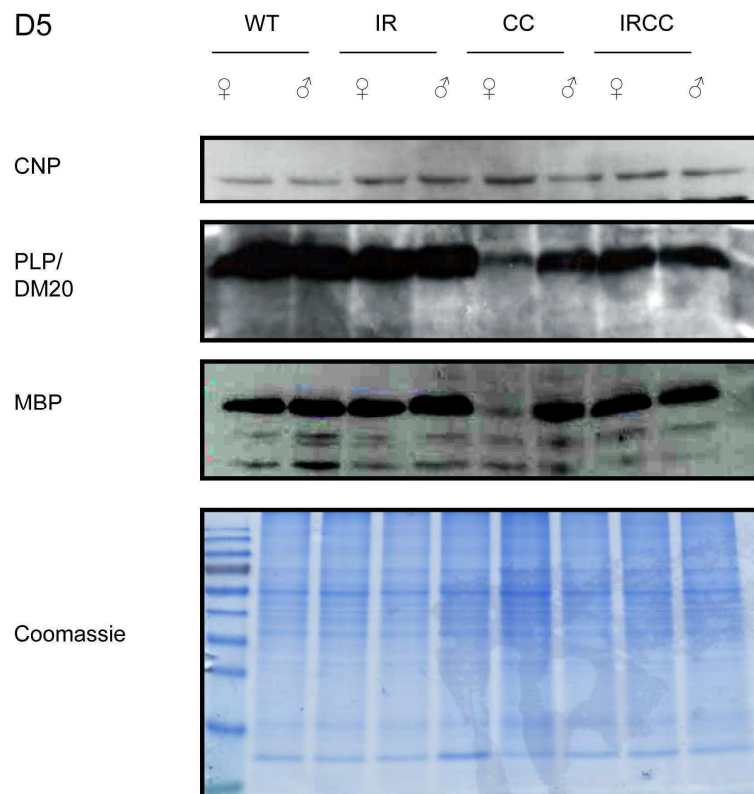
Figure 30: Myelin specific protein expression of mice 5 days of age
Myelin was isolated using a sucrose gradient centrifugation and separated via 15% SDS-PAGE gel. Detection of of CNP and MBP was performed using 50µg and PLP/ DM20 using 400µg protein lysate of female and male WT, IR, CC and IRCC mice at 5 days of age. Coomassie staining was performed as loading control of the SDS-PAGE gels.

3.2.5. InR/ IGF1R signaling in IRCC mice

The InR and IGF1R signaling pathway, as well as myelin specific proteins and some components of the Wnt signaling pathway were analysed time dependently in female and male WT, IR, CC and IRCC mice via western-blot.

At the age of week 20 the expression of the IGF1R was similar in female and male WT, CC, IR and IRCC mice. The expression levels of InR were comparable to each other in both genders and all four genotypes. The protein GFP was as expected only found in female and male IRCC mice and the actin control showed equal loading of protein amount (Fig.31 A).

Downstream of the InR and IGF1R, it could be observed at this time point that AKT phosphorylation showed no difference between the genotypes. AKT protein amount was euqal in both genders and all four genotypes.

ERK 1 and 2 phosphorylation was not different between the genotypes. ERK 1 and 2 protein amount was similar in all genotypes.

GSK3α and β phosphorylation showed no differences between female and male mice of the different genotypes, as well as GSK3β expression (Fig 31 B).

In chronic MS especially MMP-7 and MMP-9 protein levels are elevated [Cossins et al., 1997]. Next to this activated T cells trigger the release of proinflammatory cytokines, such as TNFα and interferon-γ by inflammatory cells, macrophages and mikroglia in MS [Brosman and Raine; 1996]. Therefore, inflammatory protein expression levels of MMP-9 and TNFα were as well analysed.

MMP-9 protein amount was similar in WT, CC, IR and IRCC mice. TNFα content was equal in female and male WT, IR and female CC mice. In male CC and female IRCC mice, but more pronouced in male IRCC mice protein expression of TNFα was sightly upregulated (Fig. 31C).

W20
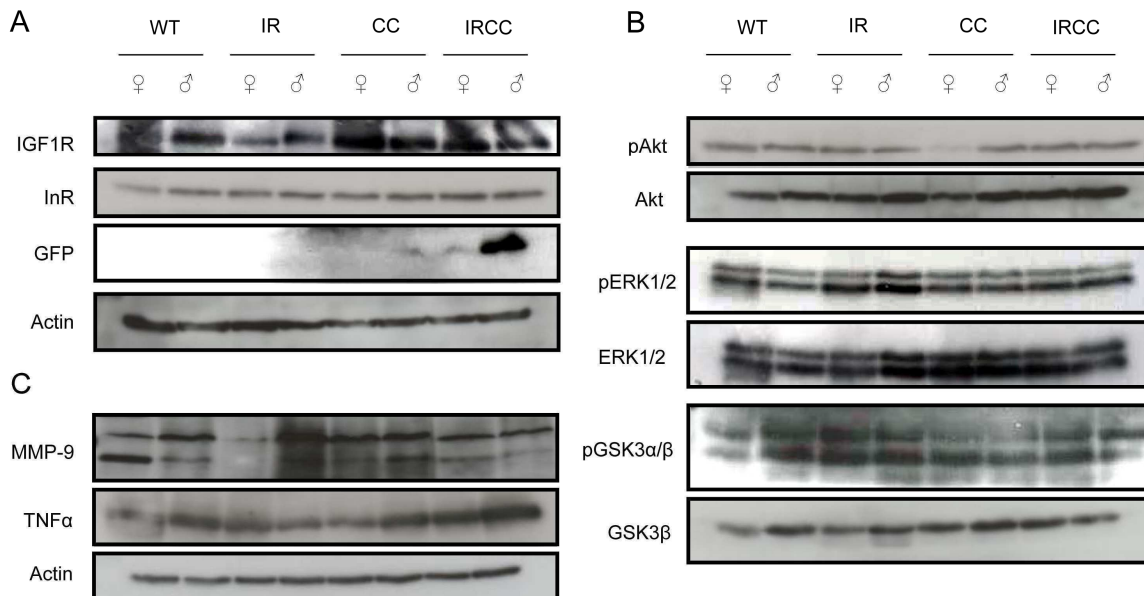
Figure 31: InR/ IGF1R signaling pathway and inflammatory proteins in female and male WT, IR, CC and IRCC mice at 20 weeks of age
(A) IGF1R, InR and GFP expression levels are shown. Actin served as control.
(B) Phosphorylation of AKT (pAKT, Ser473), ERK1/2 (pERK1/2, Thr202/Tyr204) and GSK3αβ (pGSK3α, Ser 21/pGSK3β, Ser9) are shown. As control served unphosphorylated protein level of AKT, ERK1/2 and GSK3β
(C) MMP-9 (upper band) and TNFα protein expression are shown. Actin served as control.
100 μg of total proteins were used and separated via 10% SDS-PAGE in A, B and C.

Myelin specific protein expression and the analysis of Fyn kinase, which is known to be involved in myelination, in mice at 20 weeks of age showed an equal expression of the unphosphorylated active form of the Fyn kinase in female and male mice of all four genotypes.

CNP expression levels were similar in male WT, female CC, IR and IRCC mice of both genders (Fig. 32).
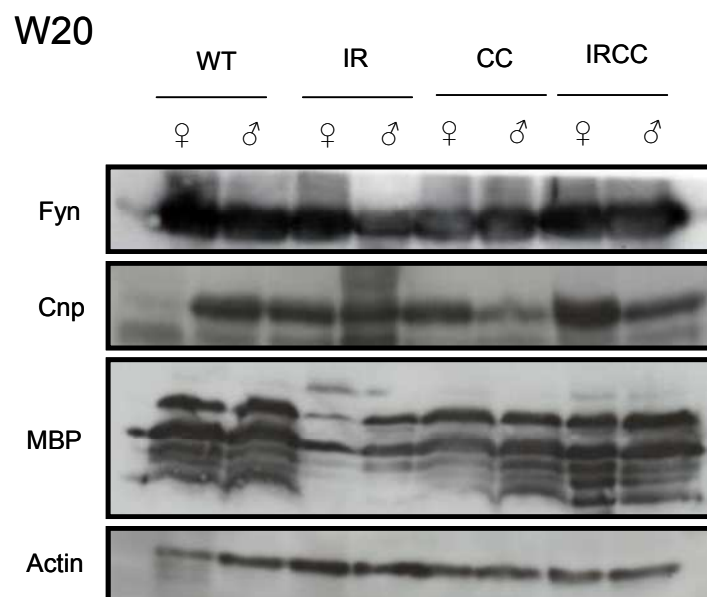
Figure 32: Myelin specific protein and Fyn kinase expression in female and male WT, IR, CC and IRCC mice at 20 weeks of age.
Fyn kinase, CNP, and MBP expression levels are shown. Actin served as control. 100µg of total protein were used and separated via 10% and 15% SDS-PAGE gel.

Analysis of protein expression of proteins of the Wnt signaling pathway showed similar β-Cat phosphorylation in male CC, female and male IR and IRCC mice.

Wnt5a, the opponent of Wnt3 in the Wnt signaling cascade, expression was equal in both genders and all genotypes at 20 weeks of age. Actin protein levels were all equal of all genotypes (Fig.33).

W20
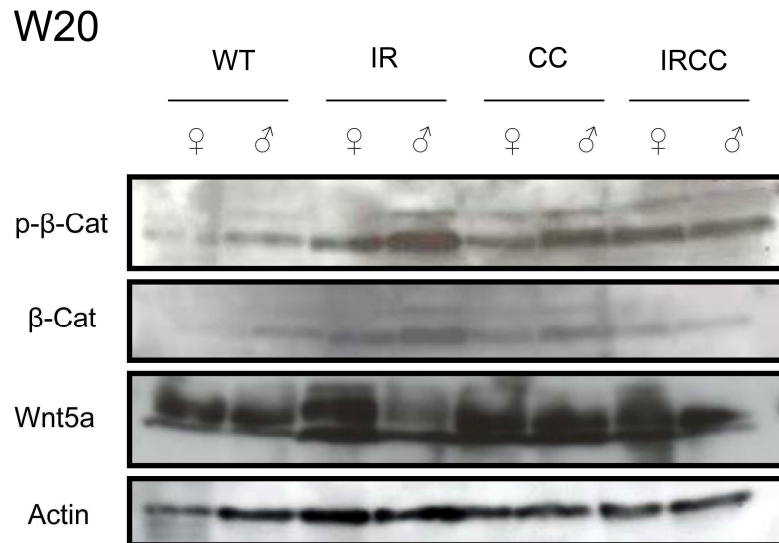
Figure 33: Wnt signaling pathway in female and male WT, IR, CC and IRCC mice at 20 weeks of age. Phosphorylation of β-Catenin (p-β-Cat, Ser33, Ser 37 and Thr41), β-Catenin and Wnt5a protein levels are shown. Actin served as control. 100µg of total protein were used and separated via 10% SDS-PAGE gel.

InR and IGF1R signaling pathway analysis of mice at week 12 of age, showed similar protein expression of IGF1R in male WT, female and male IR and CC mice. Reduced protein content could be found in female WT, female and male IRCC mice compared to the other mice.

InR expression levels were identically in female and male mice of all genotypes.

GFP protein was only detectable in female and male IRCC mice. Control of protein loading, i.e. actin content was equal in both genders and all genotypes (Fig.34 A).

Phosphorylation of AKT and AKT protein content showed no differences.

ERK1 and 2 phosphorylation was similar in female WT, female CC, female and mal IR and IRCC mice. ERK1 and 2 protein amount as control showed equal ERK1 and ERK2 concentrations.

Phosphorylation of GSK3β were similar in both genders and all genotypes. GSK3β protein amount was unaltered (Fig.34 B).

MMP-9 protein expression was increased in female and male CC and IRCC mice compared to the other genotypes.

TNFα, showed increased expression levels in female WT, female IR and both genders of IRCC mice in respect to the other genotypes.

Control of equal protein loading revealed similar gel loading of all samples (Fig.34 C).

W12
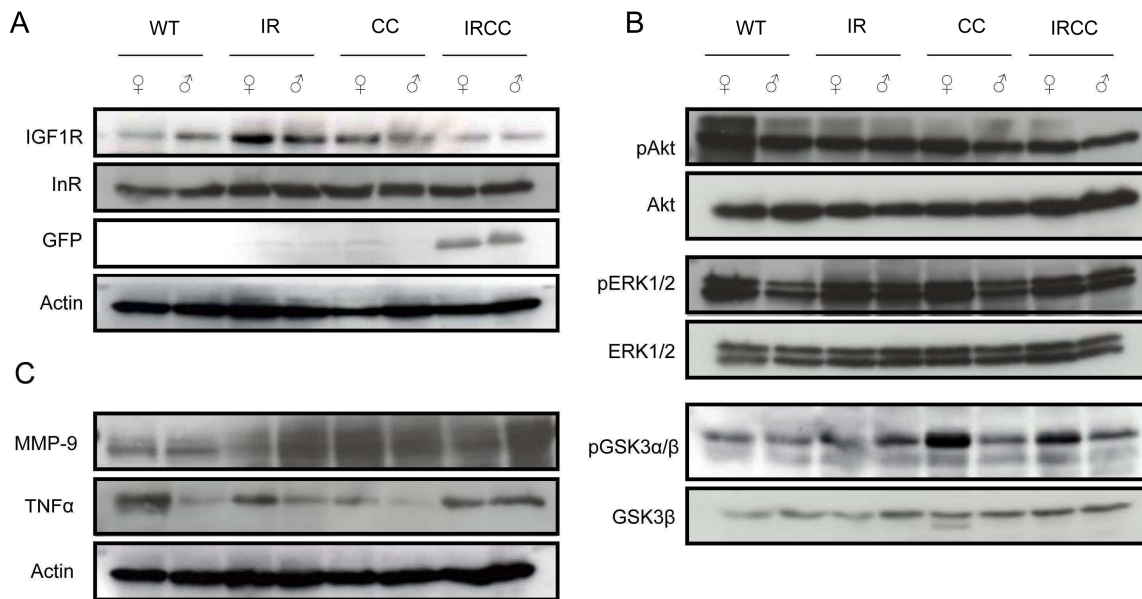
Figure 34: InR/ IGF1R signaling pathway in female and male WT, IR, CC and IRCC mice at 12 weeks of age
(A) IGF1R, InR and GFP expression levels are shown. Actin served as control.
(B) Phosphorylation of AKT (pAKT, Ser473), ERK1/2 (pERK1/2, Thr202/Tyr204) and GSK3αβ (pGSK3β, Ser9) are shown. As control served unphosphorylated protein level of AKT, ERK1/2 and GSK3β
(C) MMP-9 and TNFα protein expression are shown.
Actin served as control.100 µg of total proteins were used and separated via 10% SDS-PAGE in A, B and C.

Analysis of Fyn kinase expression revealed no differences in the protein expression.

The myelin specific protein CNP was similar expressed in both genders of WT, IR and female CC mice, with an increase in male CC and the lowest in female and male IRCC mice.

Protein amount of MBP was unaltered in both genders and in those four genotypes.

Expression levels of PLP compared in female and male mice of WT, IR, CC and IRCC showed no changes due to gender or genotype.

Protein loading control, i.e. actin indicated equal loading of protein amount (Fig. 35).

W12

Figure 35: Myelin specific protein and Fyn kinase expression in female and male WT, IR, CC and IRCC mice at 12 weeks of age.
Fyn kinase, CNP, MBP and PLP expression levels are shown. Actin served as control. 100µg of total protein were used and separated via 10% and 15% SDS-PAGE gel.

Protein amount of IGF1R and InR was similar in both genders of WT, IR, CC and IRCC mice. GFP protein expression was only found in female and male IRCC mice and protein loading reveals equal protein quantity (Fig. 36 A).

Downstream of the InR/ IGF1R signaling cascade AKT phosphorylation was similar in both genders of WT, IR, CC and IRCC mice. AKT protein content was similar in both genders and all genotypes.

ERK1 and 2 phosphorylation was unchanged in female and male mice of all genotypes, as well as ERK1 and 2 protein levels.

GSK3α/β phosphorylation showed no variations. GSK3β protein concentration was equal in both genders and all genotypes (Fig. 36 B).

MMP-9 expression levels were similar in female and male mice of all genotypes. TNF α protein expression was identical in female and male WT, IR and IRCC mice, reduced in both genders of CC mice. Actin protein content displayed to be unaltered in female and male mice of all genotypes (Fig. 36 C).

W8

A

B

C

Figure 36: InR/ IGF1R signaling pathway in female and male WT, IR, CC and IRCC mice at 8 weeks of age
(A) IGF1R, InR and GFP expression levels are shown. Actin served as control.
(B) Phosphorylation of AKT (pAKT, Ser473), ERK1/2 (pERK1/2, Thr202/Tyr204) and GSK3αβ (pGSK3β, Ser9) are shown. As control served unphosphorylated protein levels of AKT, ERK1/2 and GSK3β
(C) MMP-9 and TNFα protein expression is shown. Actin served as control.
100 µg of total proteins were used and separated via 10% SDS-PAGE in A, B and C.

Fyn kinase protein expression was equal in female and male WT, IR, CC and IRCC mice. Myelin specific protein expression, as CNP and MBP revealed similar protein expression throughout both genders and all genotypes. PLP protein content was equal in female and male WT, IR and CC mice and slightly decreased in both genders of IRCC mice. DM20 protein expression levels were similar in female and male WT, CC and IRCC mice, and marginally reduced in both genders of IR mice.

Actin Western Blot revealed equal protein loading of female and male samples of all genotypes (Fig. 37).

W8

Figure 37: Myelin specific protein and Fyn kinase expression in female and male WT, IR, CC and IRCC mice at 8 weeks of age.
Fyn kinase, CNP, MBP and PLP expression levels are shown. Actin served as control. 100µg of total protein were used and separated via 10% and 15% SDS-PAGE gel.

InR and IGF1R signaling pathway analysis of mice at week 5 of age using Western Blots, showed similar protein expression of IGF1R in male WT, female and male IR, IRCC and female CC mice. Reduced protein content was found in female WT and male CC mice compared to the other genotypes and genders.

InR expression levels were similar in females and males of all genotypes.

GFP protein was only found in female and male IRCC mice.

Control of protein loading, i.e. actin content was equal in both genders of all genotypes (Fig.38 A).

AKT phosphorylation was in female and male mice of all genotypes similar. AKT protein content showed no difference.

ERK1 and 2 phosphorylation was unaltered in all genotypes as well as ERK1 and 2 protein amount.

GSK3α/β phosphorylation was similar in both genders and all genotypes. GSK3β protein amount as control of protein loading was unchanged in all genotypes as well (Fig.38 B).

Protein content of MMP-9 displayed no consistent changes within the different genotypes.

TNFα, showed increased expression levels in female and male WT and IR mice. Reduced levels could be found in both genders of CC and IRCC mice.

Control of equal protein loading showed similar protein content of each sample (Fig.38 C).

W5
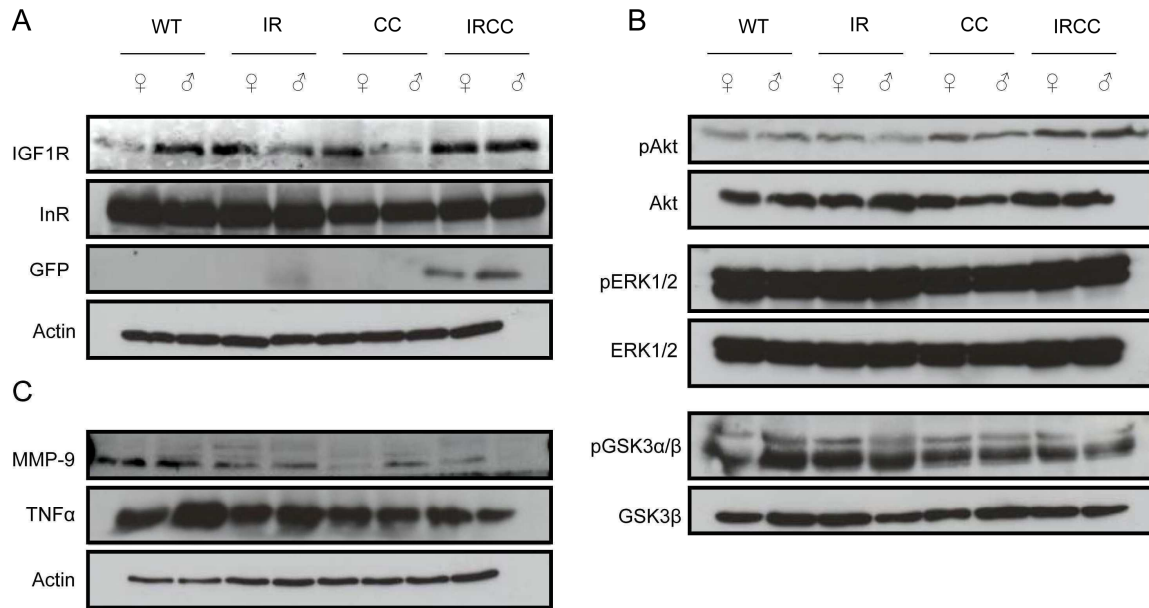
Figure 38: IR/ IGF1R signaling pathway in female and male WT, IR, CC and IRCC mice at 5 weeks of age
(A) IGF1R, InR and GFP expression levels are shown. Actin served as control.
(B) Phosphorylation of AKT (pAKT, Ser473), ERK1/2 (pERK1/2, Thr202/Tyr204) and GSK3αβ (pGSK3β, Ser9) are shown. As control served unphosphorylated protein level of AKT, ERK1/2 and GSK3β
(C) MMP-9 and TNFα protein expression is shown. Actin served as control.
100 µg of total proteins were used and separated via 10% SDS-PAGE in A, B and C.

Analysis of myelin specific protein expression and Fyn kinase, revealed similar expression levels in females and males of all genotypes.

Myelin specific proteins as CNP showed equal protein levels in all genotypes.

MBP protein content was similar in female and male WT, IR and female CC mice, a bit lower levels were found in male CC and both genders of IRCC mice.

PLP and DM20 protein expression was equal in female and male WT, IR and CC mice, and slightly increased in both genders of IRCC mice (Fig. 39).
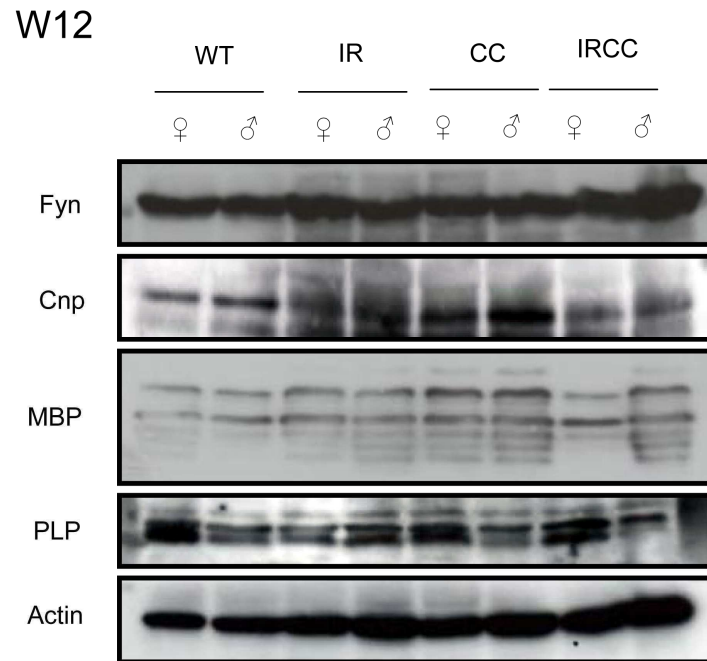
Figure 39: Myelin specific protein and Fyn kinase expression in female and male WT, IR, CC and IRCC mice at 5 weeks of age.
Fyn kinase, CNP, MBP and PLP expression levels are shown. Actin served as control. 100µg of total protein were used and separated via 10% and 15% SDS-PAGE gel.

InR and IGF1R signaling pathway analysis of mice at week 5 of age, showed similar protein expression of IGF1R in female and male mice of WT, IR, CC and IRCC.

InR expression levels were similar in female and male mice of all genotypes.

GFP protein was only detected in female and male IRCC mice.

Control of protein loading, i.e. actin content was equal in samples of both genders and all genotypes (Fig.40 A).

AKT phosphorylation was equal in female and male WT, IR, CC and IRCC mice. AKT protein content showed no differences.

ERK1 and 2 phosphorylation was unaltered in female and male mice of all genotypes. ERK1 and 2 protein served as control and indicated equal loading.

GSK3α/β phosphorylation was similar in female and male WT and CC mice and slightly higher in female and male IR and IRCC mice. GSK3β protein amount as control of protein loading was unchanged (Fig.40 B).

Protein content of MMP-9 was equal in all genotypes. Furthermore TNFα, showed decreased expression levels in female and male IRCC mice, whereas similar expression in female and male WT, IR and CC mice. Control of equal protein loading displayed to be similar (Fig.40 C).
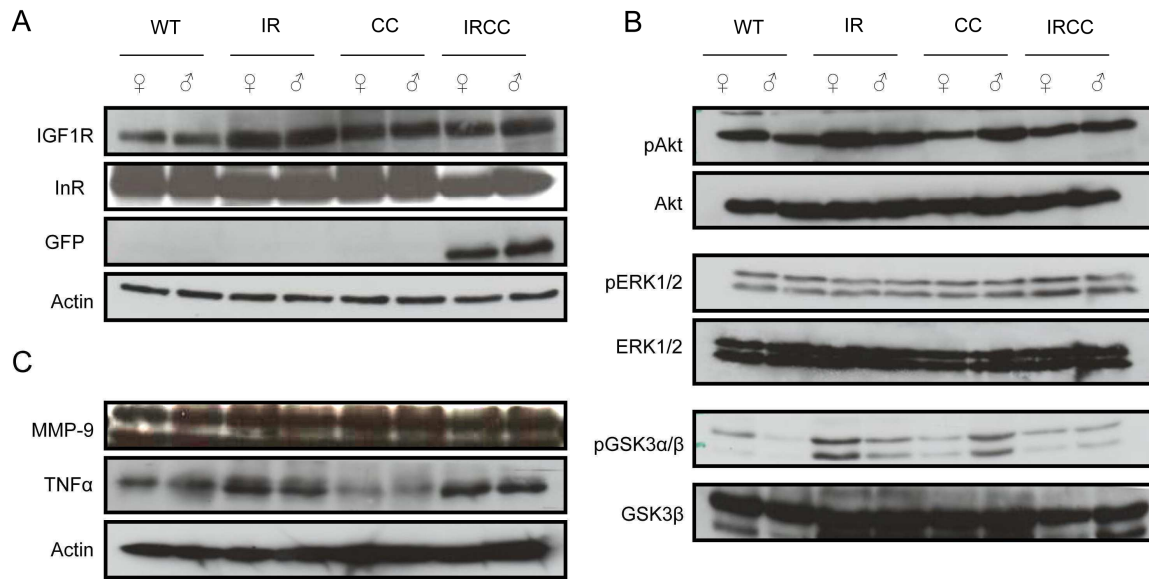
W3
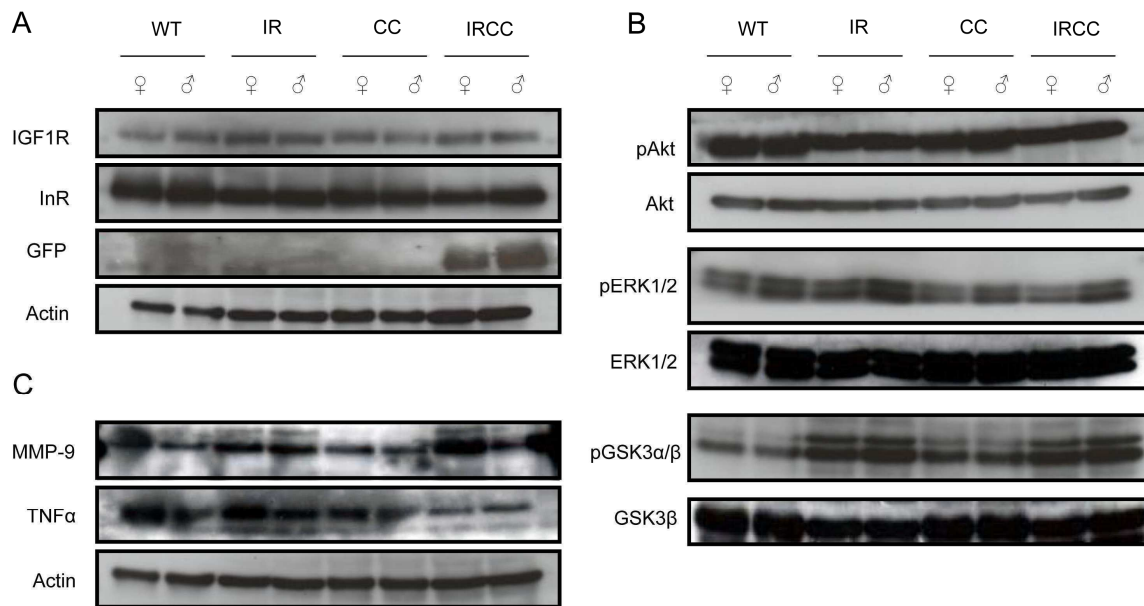
Figure 40: InR/ IGF1R signaling pathway in female and male WT, IR, CC and IRCC mice at 3 weeks of age
(A) IGF1R, InR and GFP expression levels are shown. Actin served as control.
(B) Phosphorylation of AKT (pAKT, Ser473), ERK1/2 (pERK1/2, Thr202/Tyr204) and GSK3αβ (pGSK3β, Ser9) are shown. As control served unphosphorylated protein level of AKT, ERK1/2 and GSK3β
(C) MMP-9 and TNFα protein expression are shown. Actin served as control.
100 µg of total proteins were used and separated via 10% SDS-PAGE in A, B and C.

At 3 weeks of age Fyn kinase was equally expressed in both genders and genotypes.

Myelin specific proteins, as CNP showed a slightly reduced expression in female and male WT and IR mice compared to female and male CC and IRCC mice.

MBP protein levels were similar without difference between the genotypes.

PLP and DM20 analysis revealed a unaltered protein content in female and male mice of all genotypes.

Actin protein amount as control of protein loading was unchanged (Fig.41).
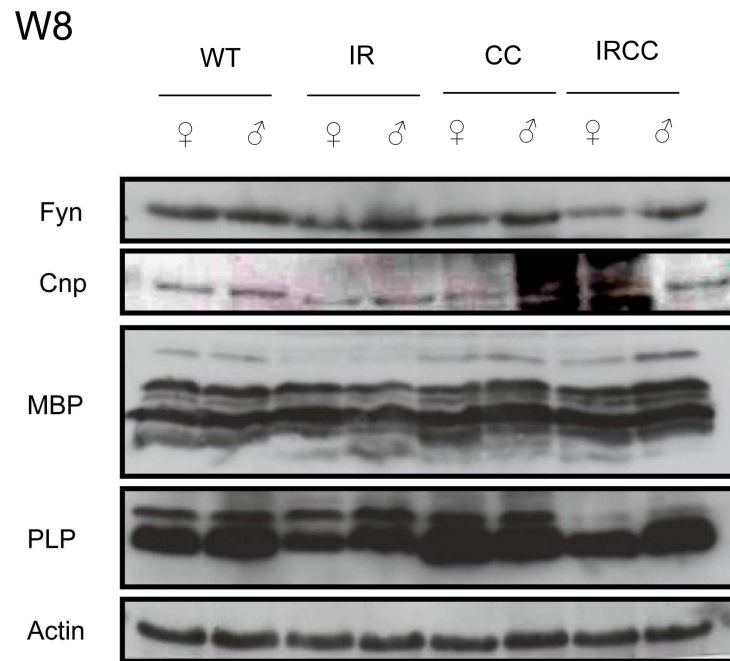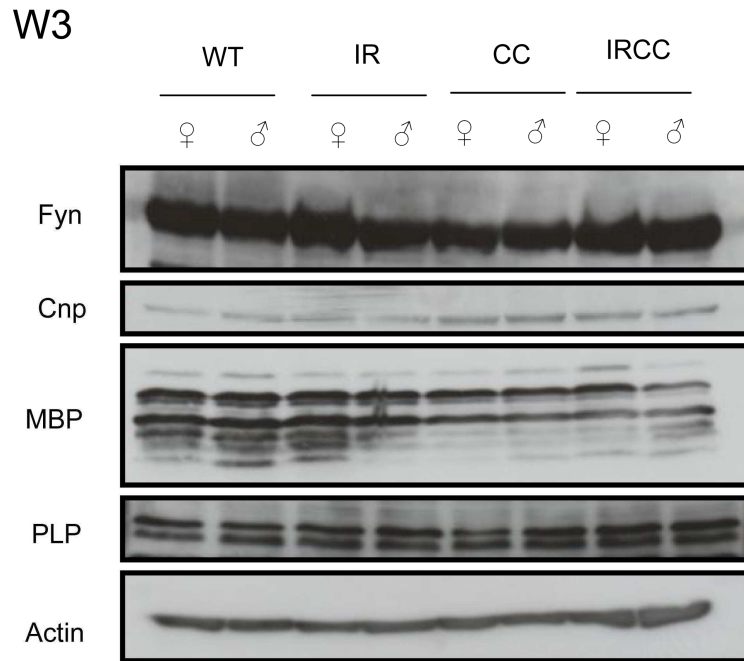
Figure 41: Myelin specific protein and Fyn kinase expression in female and male WT, IR, CC and IRCC mice at 3 weeks of age.
Fyn kinase, CNP, MBP and PLP expression levels are shown. Actin served as control. 100µg of total protein were used and separated via 10% and 15% SDS-PAGE gel.

Analysis of InR and IGF1R signaling in the brain of 5 days old mice, showed slightly higher expression levels of IGF1R in female and male CC mice compared to the other genotypes.

InR expression levels were similar in female and male mice of all genotypes.

GFP was only detectable in female and male IRCC mice.

Actin Western Blot showed equally loading of the gel (Fig. 42 A).

AKT phosphorylation was unchanged in both genders of all genotypes. AKT protein levels showed to be the same in all tested samples.

ERK 1 and 2 phosphorylation was unaltered in both genders of all genotypes. ERK 1 and 2 protein level displayed no alterations in female and male mice of the four genotypes.

Phosphorylation of GSK3α/β was similar in both genders and all genotypes. GSK3β protein concentration as control of protein loading was unchanged (Fig.42 B).

MMP-9 levels were shown to be equal in female and male WT, IRCC and male CC mice, in contrast lower in female and male IR and female CC mice.

Furthermore TNFα, showed similar expression levels in female and male of the four genotypes.

Western Blot using actin antibodies proofed equal loading (Fig.42 C).

D5
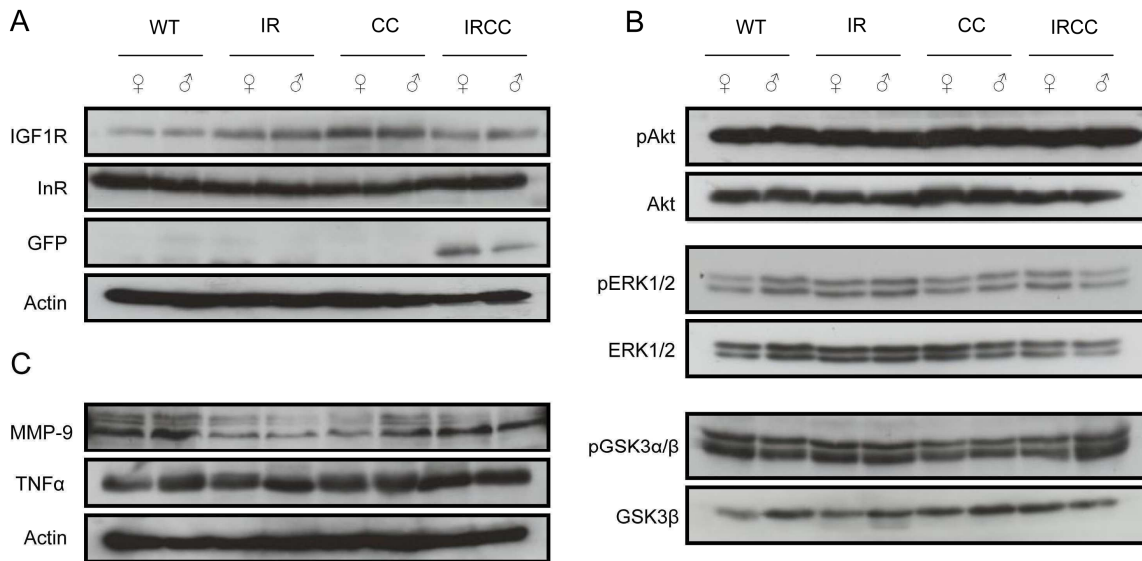
Figure 42: InR/ IGF1R signaling pathway in female and male WT, IR, CC and IRCC mice at 5 days of age
(A) IGF1R, InR and GFP expression levels are shown. Actin served as control.
(B) Phosphorylation of AKT (pAKT, Ser473), ERK1/2 (pERK1/2, Thr202/Tyr204) and GSK3αβ (pGSK3β, Ser9) are shown. As control served unphosphorylated protein level of AKT, ERK1/2 and GSK3β
(C) MMP-9 and TNFα protein expression are shown. Actin served as control.
100 µg of total proteins were used and separated via 10% SDS-PAGE in A, B and C.

Fyn kinase protein expression levels were similar in female and male WT, CC and IRCC mice and slightly lower in both genders of IR mice.

CNP protein expression was equal in both genders of the different genotypes.

There were no differences in MBP expression depending on the genotypes.

PLP and DM20 protein expression levels were equal in female and male mice of the four genotypes.

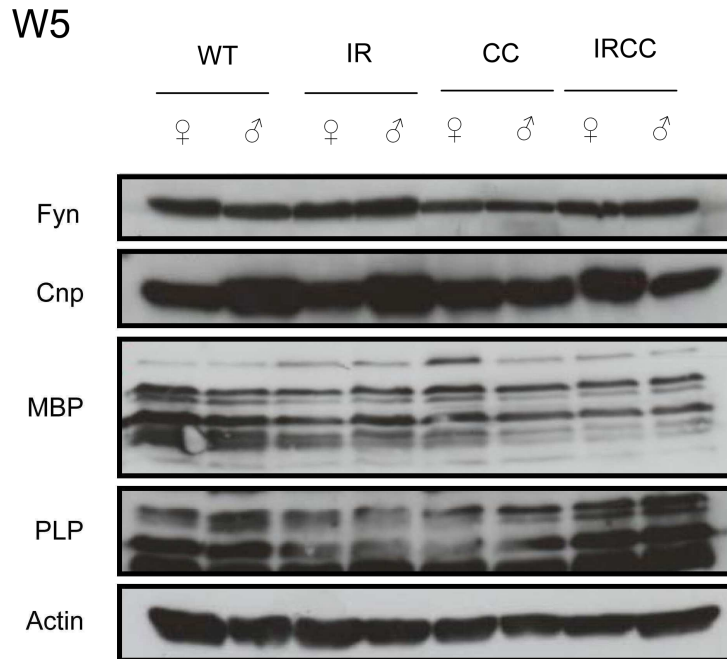Actin Western Blot, as control of protein loading revealed equal loading (Fig. 43).

D5
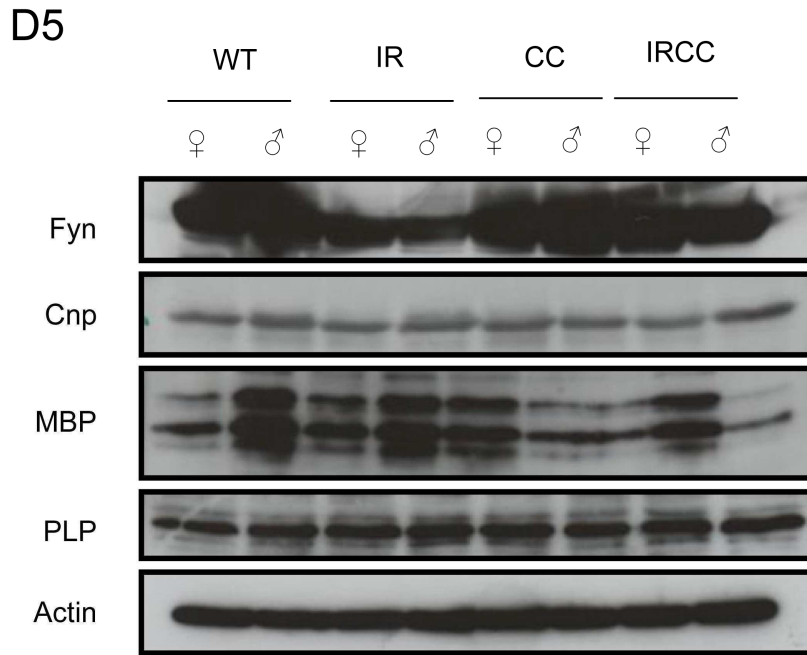
Figure 43: Myelin specific protein and Fyn kinase expression in female and male WT, IR, CC and IRCC mice at 5 days of age.
Fyn kinase, CNP, MBP and PLP expression levels are shown. Actin served as control. 100µg of total protein were used and separated via 10% and 15% SDS-PAGE gel.

Phosphorylation of β-Cat, β-Cat and Wnt5a protein expression showed no differences depending on genotype.

Actin protein concentration revealed equal loading (Fig. 44).

D5
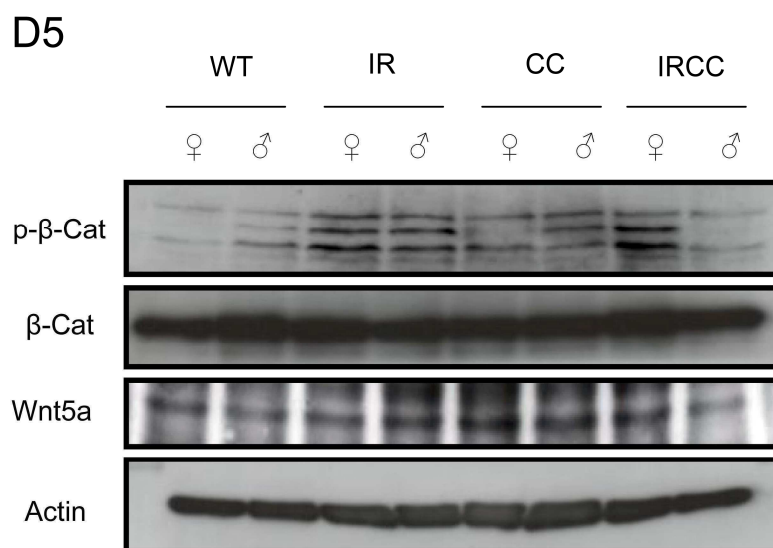
Figure 44: Wnt signaling pathway in female and male WT, IR, CC and IRCC mice at 5 days of age.
Phosphorylation of β-Catenin (p-β-Cat, Ser33, Ser 37 and Thr41), β-Catenin and Wnt5a protein levels are shown. Actin served as control. 100µg of total protein were used and separated via 10% SDS-PAGE gel.

3.2.6. Inflammatory analysis of IRCC mice

The protein expression of inflammatory proteins determined by Western Blot analysis revealed slightly different expression of TNFα and MMP-9 in the different genotypes. Therefore immunohistochemical analysis of perfused brains of female and male WT and IRCC mice were done. The different inflammatory cells were detected using immunohistochemistry in the brains of 12 and 8 weeks old mice.

GFAP staining was more intensed in IRCC mice compared to WT mice. However staining intensity was stronger at 8 than in 12 weeks old IRCC mice. In WT mice only weak GFAP staining was detected in white and grey matter of 12 and 8 weeks old mice.

However, all genotypes showed, as expected strong GFAP staining around the vessels and at brain surfaces (Fig.45).
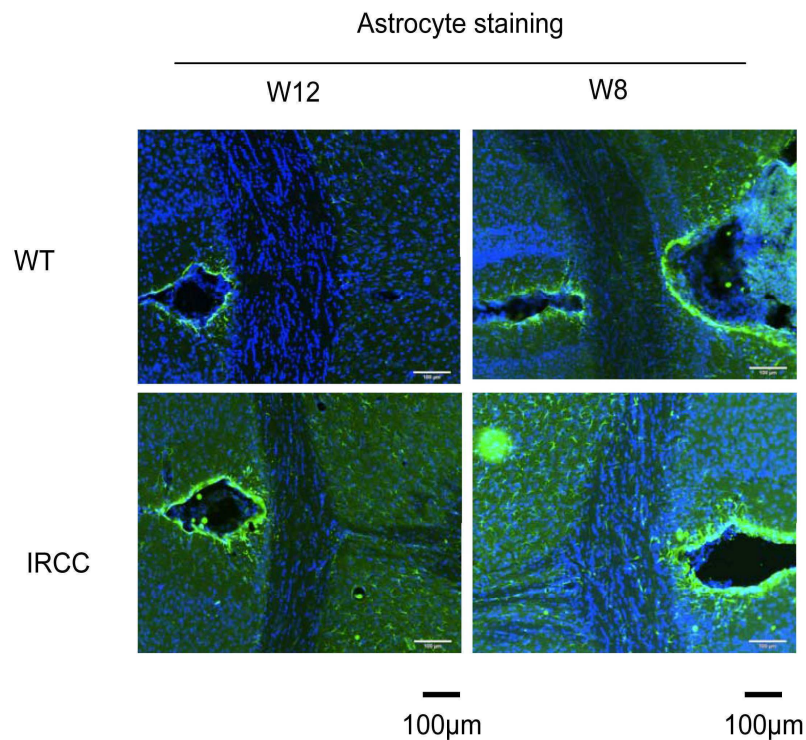
Fig 45: Immunohistochemical staining using GFAP antibodies of week 12 and 8 mice
Perfused brains were sliced 20µm coronoally. Those were stained using antibodies against GFAP (1:200), a common astrocyte marker and DAPI (1:1000), which stains cell nuclei. Shown are brain slices of male WT and IRCC mice focused onto the corpus callosum.

In addition to the analysis of astrocyte expression other inflammatory cells, as macrophages and T-Cells were investigated in perfused brains of 12 week old male and female WT and IRCC mice. Furthermore, NG2 cells, which are a new class of glial cells, known to be able to differentiate in oligodendrocytes as well as neurons, where probed.

Macrophage staining revealed in WT and IRCC mice no differences. In both mice brains resting and differentiating macrophages were detected, but as expected in low numbers.

NG2 staining displayed no visible NG2 cell in both genotypes in the areas inverstigated.

T-cell staining showed nearly no detectable T-cell in the brain of WT and IRCC mice (Fig.46).
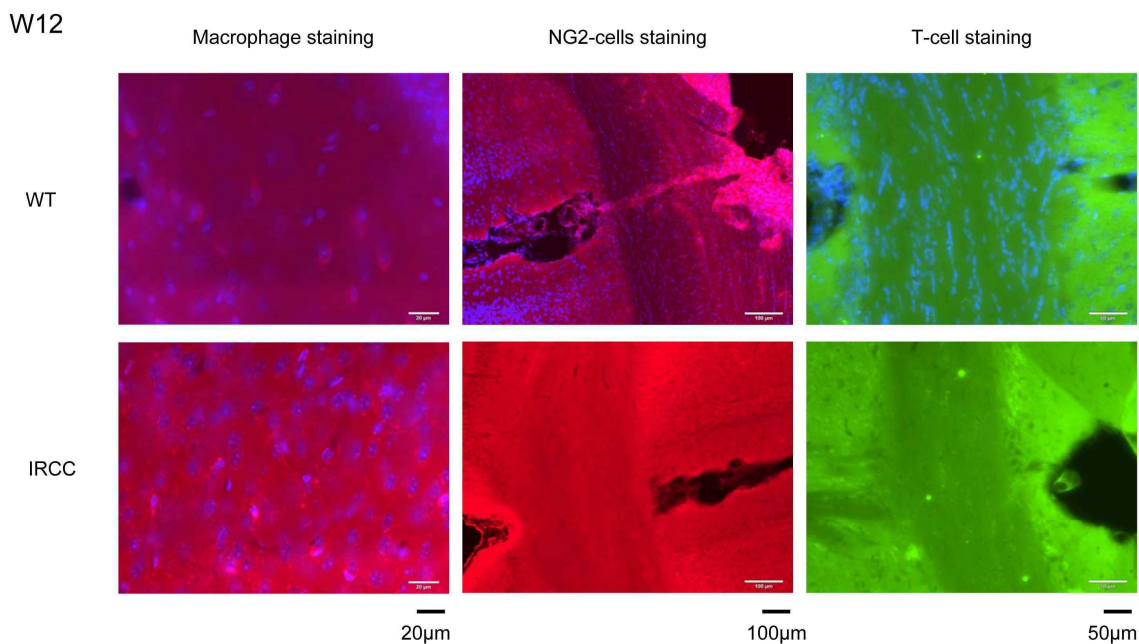
Figure 46: Immunohistochemical staining of macrophages, NG2-cells and T-cell in 12 week old WT and IRCC mice
Perfused brains were sliced 20µm coronoally. Those were stained with antibodies against MAC- 2 (1:100), a common macrophage marker, PDGFR-α, a NG2-cell marker (1:50), CD-3 antibody, a T-cell marker (1:100) and DAPI (1:1000), which stains cell nuclei. Shown are brain slices of male WT and IRCC mice focused onto the corpus callosum.

3.3. *In vitro* analysis of stably over expressing IRS-1 and IRS-2 OLN-93 cells

For *in vitro* studies the permanent cell line (OLN-93), derived from spontaneously transformed cells in primary rat brain glial cultures were stably transfected with pCMV-Tag-2 B including human derived IRS-1 and pCMV-Tag 2C mouse derived IRS-2. Vectors were linearized and then transfected into the OLN-93 cells. 2 days after transfection cells were selected with G418. Single cell clones were grown and tested for target expression. For all experiments 2 clones of each IRS cell line (IRS-1, 1+; IRS-2, 2+) were used. Wild-type (OLN) cells and cells transfected with the empty vector (EV) served as controls. Cell lines were

analysed in respect to changes in morphology, proliferation, IR/IGF1R signaling as well as expression of myelin proteins.

3.3.1. Over expressing IRS-1 and IRS-2 OLN-93 cells

ONL-93 cells were tested for stably transfection of pCMV-Tag-2 B (EV) , pCMV-Tag-2 B IRS-1 (1+) and pCMV-Tag 2C IRS-2 (2+) via PCR (Fig. 47 A and B). The T7 Primers bind onto the pCMV sequence and result in a 250kb DNA product. The EV, the IRS-1 and IRS-2 over expressing ONL-93 cells displayed the pCMV specific 250kb DNA product.

The proof of over expression was performed via Western Blot analysis. 1+ and 2+ cells presented a strong IRS-1 (Fig. 47 C) and IRS-2 (Fig. 47 D) protein expression signal. Western Blot for actin proofed equal loading (Fig. 47 C and D).
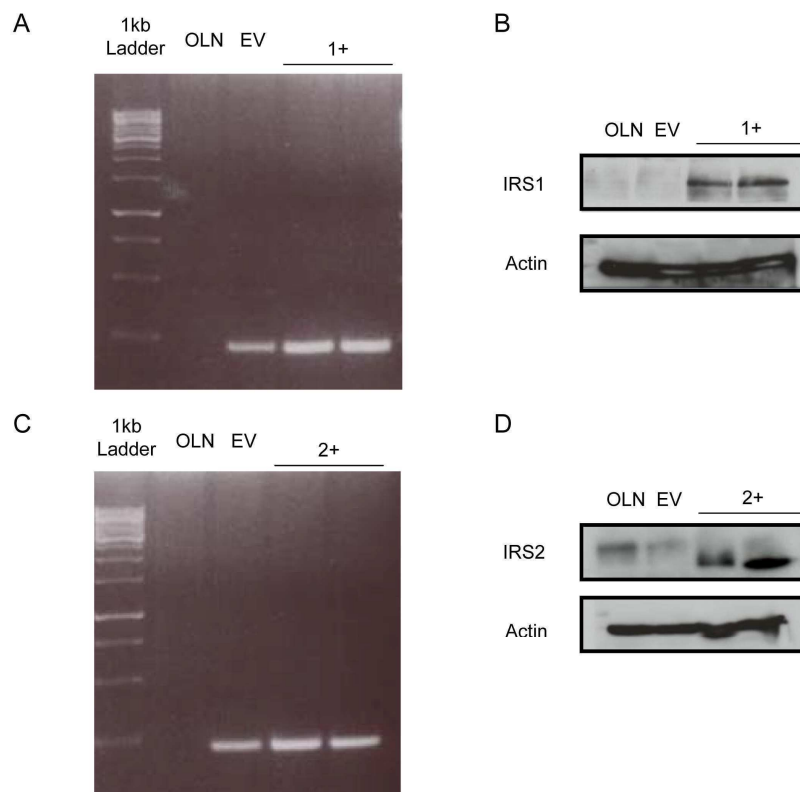
Figure 47: Detection of stably over expressing IRS-1 and IRS-2 OLN-93 cells
(A) T7 Primers specific PCR separated on a 2% agarose gel (2.9.3.). The pCMV fragment shows a size of about 250bp, whereas untransfected cells display no PCR product.
(B) Western-Blot detection of IRS-1 in 400µg whole cell lysate shows an elevated expression of IRS1 in stably transfected cells and basal protein content in untransfected (OLN) and stably transfected with pCMV-Tag-2 B (EV) separated on a 10% SDS-PAGE gel.
(C) T7 Primer specific PCR separated on a 2% agarose gel (2.9.3.). The pCMV fragment shows a size of about 250bp, whereas untransfected cells display no PCR product.
(D) Western-Blot detection of IRS-2 in 400µg whole cell lysate shows an elevated of IRS2 in stably transfected cells and basal protein content in untransfected (OLN) and stably transfected with pCMV-Tag-2 C (EV) separated on a 10% SDS-PAGE gel.

3.3.2. Morphological Characterization of stably over expressing IRS-1 and IRS-2 OLN-93 cells

OLN-93 are a permanent cell line derived from spontaneously transformed cells of primary rat brain glial cultures [Richter-Landsberg and Heinrich, 1996]. Those cells were analysed in respect to morphological changes due to IRS-1 or IRS-2 over expression.

Undifferentiated OLN-93 (OLN) cells as well as the EV cells presented when grown in low density a bipolar cell body with long thin extensions (Fig.48, both pictures left panel).

If grown under serum deprivation cell bodies displayed a globular appearance. The long thin extensions get longer and built up complex connections between the different cell bodies (Fig.48, both pictures right panel).
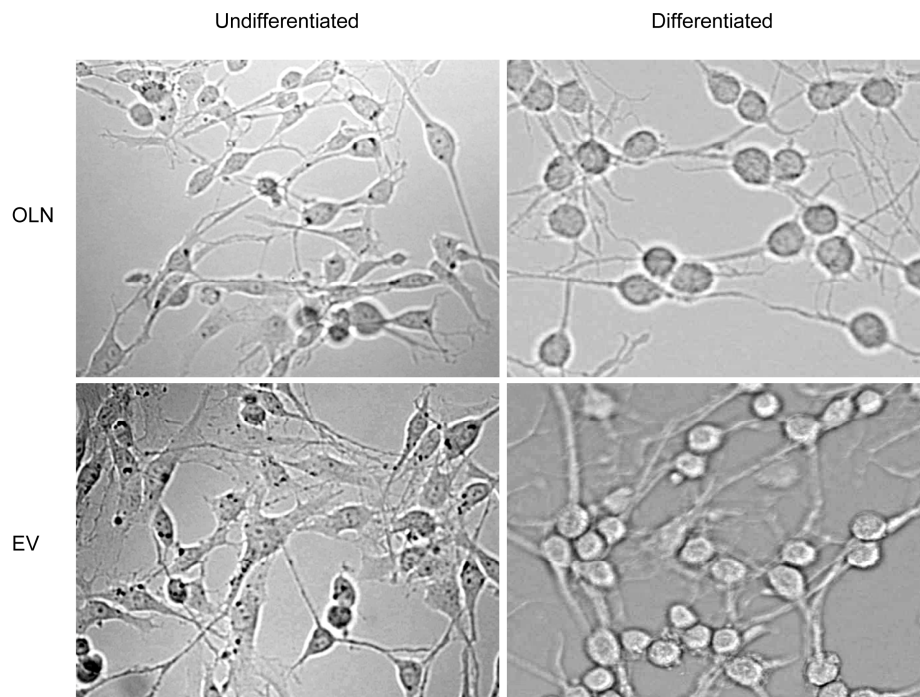
Figure 48: Phase-contrast micrographs of differentiated and undifferentiated OLN-93 (OLN) and pCMV-2C (EV) cells
Cells were cultured in FCS (10%)-containing and FCS free medium, seeded on uncoated plastic dishes and photographed after 1 day (undifferentiated) and 6 days (differentiated). Pictures represent 100x extension.

Undifferentiated IRS-1 over expressing cells (1+) (Fig.49, both pictures left panel). displayed the same bipolar structure as the OLN and EV cells (Fig.49, both pictures left panel) and showed the same thin extensions.

Interestingly 1+ cells in the differentiated state form more complex networks compared to WT cells (Fig.49, both pictures right panel; Fig.48, both pictures right panel).
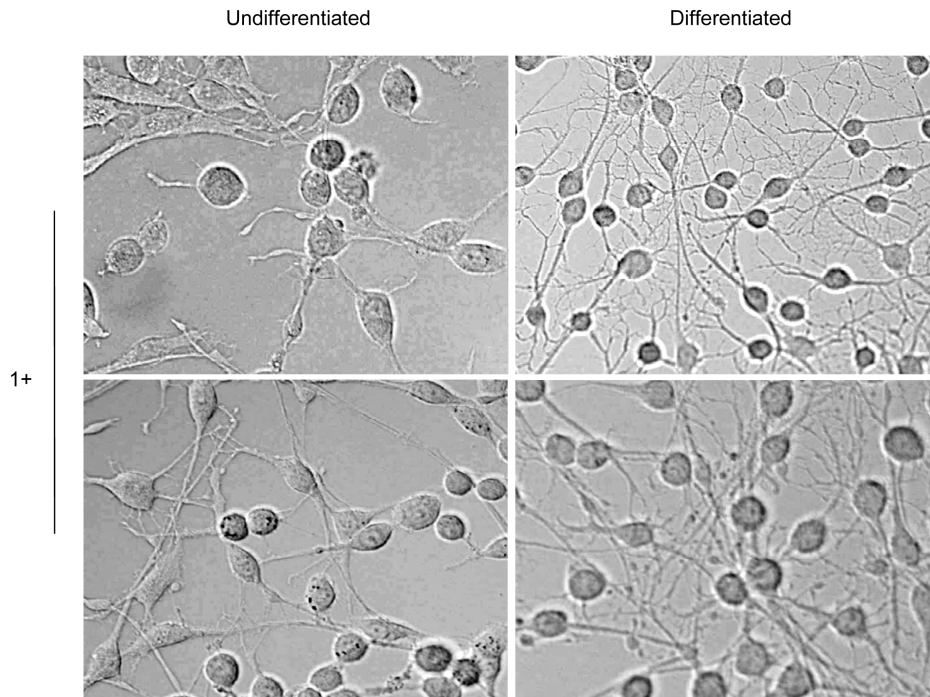
Figure 49: Phase-contrast micrographs of differentiated and undifferentiated pCMV-Tag-2 B-IRS1 stably transfected cells
Cells were cultured in FCS (10%)-containing and FCS free medium, seeded on uncoated plastic dishes and photographed after 1 day (undifferentiated) and 6 days (differentiated). Pictures represent 100x extension.

Undifferentiated IRS-2 over expressing cells (2+) (Fig.50, both pictures left panel). displayed the same bipolar structure as the OLN and EV cells and in contrast indicated a reduced ability to built up long thin extensions (Fig.48, both pictures left panel).

When differentiated, 2+ cells showed globular cell bodies (Fig.49, both pictures right panel), displayed longer extensions compared to the undifferentiated 2+ cells. Those extensions in contrast to the OLN and EV cells were shorter and not so numerous (Fig.50, both pictures right panel; Fig.48, both pictures right panel).
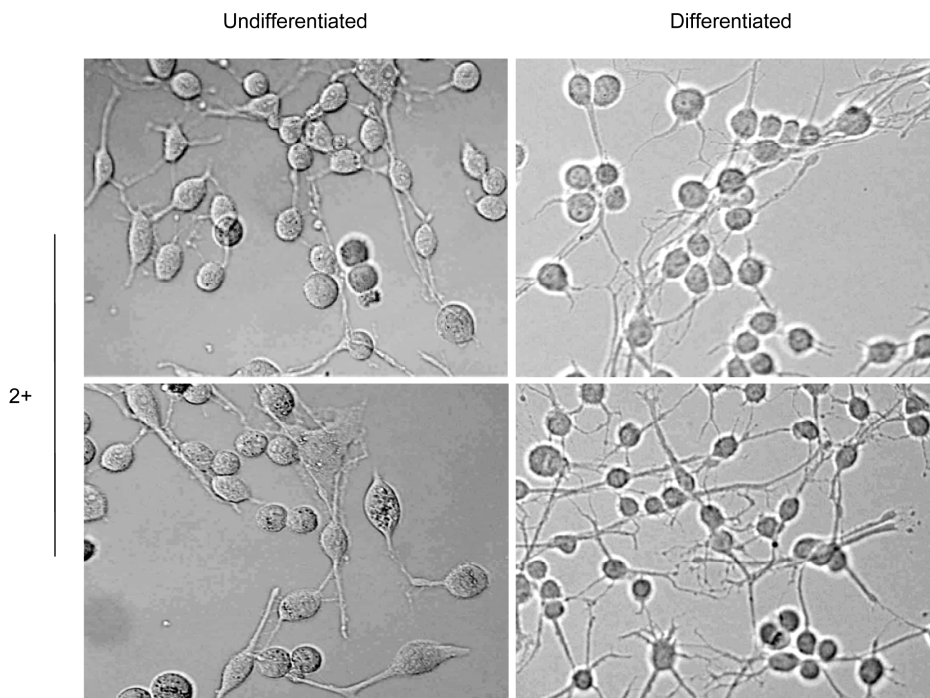
Figure 50: Phase-contrast micrographs of differentiated and undifferentiated pCMV-Tag-2 C-IRS-2 stably transfected cells
Cells were cultured in FCS (10%)-containing and FCS free medium, seeded on uncoated plastic dishes and photographed after 1 day (undifferentiated) and 6 days (differentiated). Pictures represent 100x extension.

3.3.3. Proliferation of stably over expressing IRS-1 and IRS-2 OLN93 cells

In order to analyse, whereas IRS-2 (2+) or IRS-1 (1+) over expression in OLN-93 cells does change cell proliferation, BrdU proliferation assays where performed. In addition cells were treated with inhibitors for either the PI3K (LY294002) and MAPK (PD98059) to elucidate the role of the different branches of the InR/ IGF1R signaling cascade for proliferation.

For the proliferation assay, cells were straved for 72h to stop proliferation. Then proliferation was initiated with 10% FCS for 48h, inhibitors were incubated for 12h and BrdU was added for another 12h. As controls empty vectors (EV) and non transfected OLN-93 cells (OLN) were used. Proliferation was measured via BrdU incorporation.

However, no significant difference in proliferation of 1+ and 2+ cells compared to control cells were detected during this experimental approach (Fig. 51).
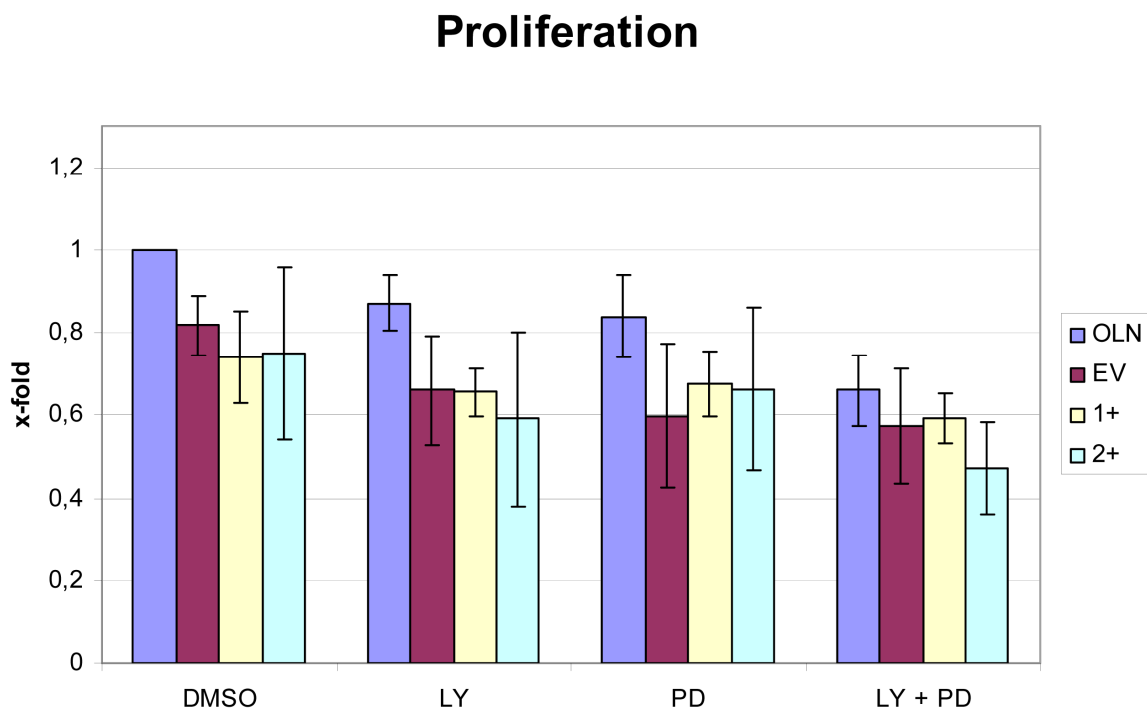
Figure 51: Proliferation of stably over expressing IRS-1 and IRS-2 OLN-93 cells
Poliferation analysis of stably over expressing IRS-1 (yellow) and IRS-2 (green) OLN-93 cells performed via BrdU incorporation assay. Empty vector controls (EV) (red) and untransfected OLN-93 (OLN) were used as control cell lines. Cells were starved (72h) and proliferation was induced by adding 10%FCS, inhibitors (20µM LY:PI3K-inhibitor; 50µM PD: MAPK-inhibitor) were added for 12h, cells were incubated for 12h with BrdU. DMS0 was used as controls, as the inhibitors were solved in DMS0.

3.3.4. Protein expression in stably over expressing IRS-1 and IRS-2 OLN-93 cells

In terms in protein expressions of the InR/ IGF1R signaling pathway in undifferentiated and differentiated IRS-1 (1+) and IRS-2 (2+) over expressing OLN-93, empty vector (EV) and non transfected OLN-93 (OLN) cells were characterized.

Undifferentiated 1+ cells showed increased IRS-2 levels and due to IRS-1 over expression an elevated IRS-1 protein content in contrast to OLN and EV cells. IGF1R levels were raised in contrast to InR, which was reduced, compared to OLN and EV cells. Actin used as loading control was unchanged (Fig.52, left panel, first row).

Differentiated 1+ cells showed decreased IRS-2 and IRS-1 protein expression compared to differentiated OLN and EV cells. IGF1R protein amount was elevated. InR levels were similar. Protein loading was controled via actin Western Blot (Fig 52, left panel, second row).

Undifferentiated 2+ cells displayed increased IRS-2 and IRS-1 protein expression compared to OLN and EV cells. IGF1R protein amount was elevated and InR levels were similar compared to OLN and EV cells. Actin protein levels were euqal (Fig. 52, right panel, first row).

Differentiated 2+ cells showed unaltered IRS-2, IRS-1, IGF1R and InR protein expression levels. Actin protein concentrations were similar (Fig. 52, right panel, right row).
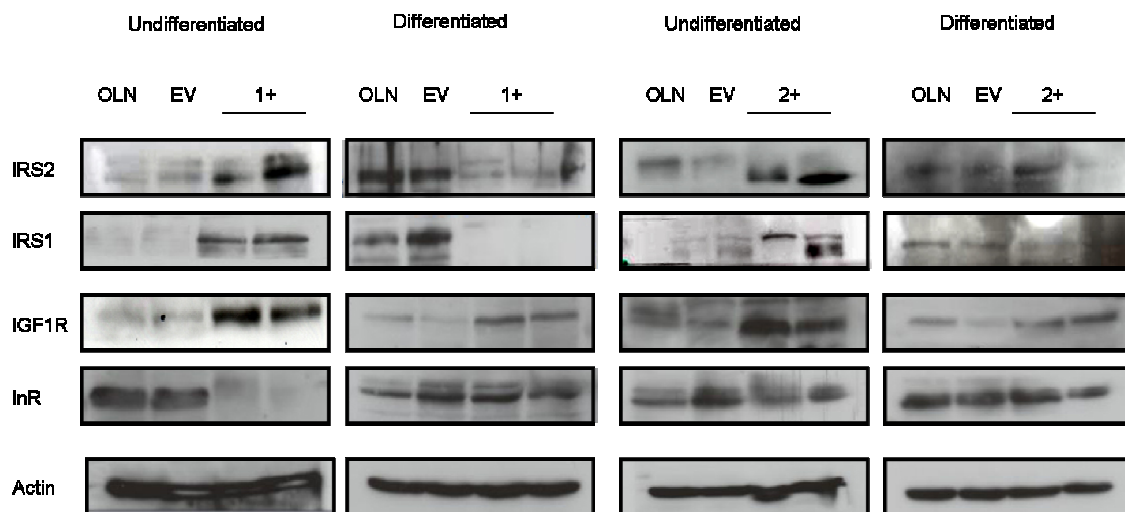
Figure 52: InR/ IGF1R signaling pathway in undifferentiated and differentiated over expressing IRS-1 and IRS-2 OLN-93 cells
IRS-2, IRS-1, IGF1R and InR expression levels are shown. Actin served as control. 400 µg of total proteins were used and separated via 10% SDS-PAGE gel.

Activation of the PI3K and MAPK pathway was analysed via phosphorylation of AKT, ERK1/2 and GSK3α/β.

Undifferentiated 1+ cells displayed an elevated AKT phosphorylation, whereas phosphorylation of ERK1/2 and GSK3α/β was equal compared to OLN and EV cells. Protein content of AKT, ERK1/2 and GSK3β showed no changes indicating identical gel loading (Fig. 53, left panel, first row).

Differentiated 1+ cells demonstrated similar phosphorylation of AKT, ERK1/2 and GSK3α/β compared to OLN and EV cells. Protein levels of AKT, ERK1/2 and GSK3β were unchanged (Fig. 53, left panel, second row).

Undifferentiated 2+ cells revealed the same phosphorylation of AKT, ERK1/2 and GSK3α/β as OLN and EV cells. Protein levels of AKT, ERK1/2 and GSK3β were unchanged (Fig. 53, right panel, first row).

Differentiated 2+ cells showed reduced phosphorylation of AKT, equal ERK1/2 and GSK3α/β phosphorylation. Protein expression levels of AKT, ERK1/2 and GSK3β were similar (Fig. 53, right panel, second row).
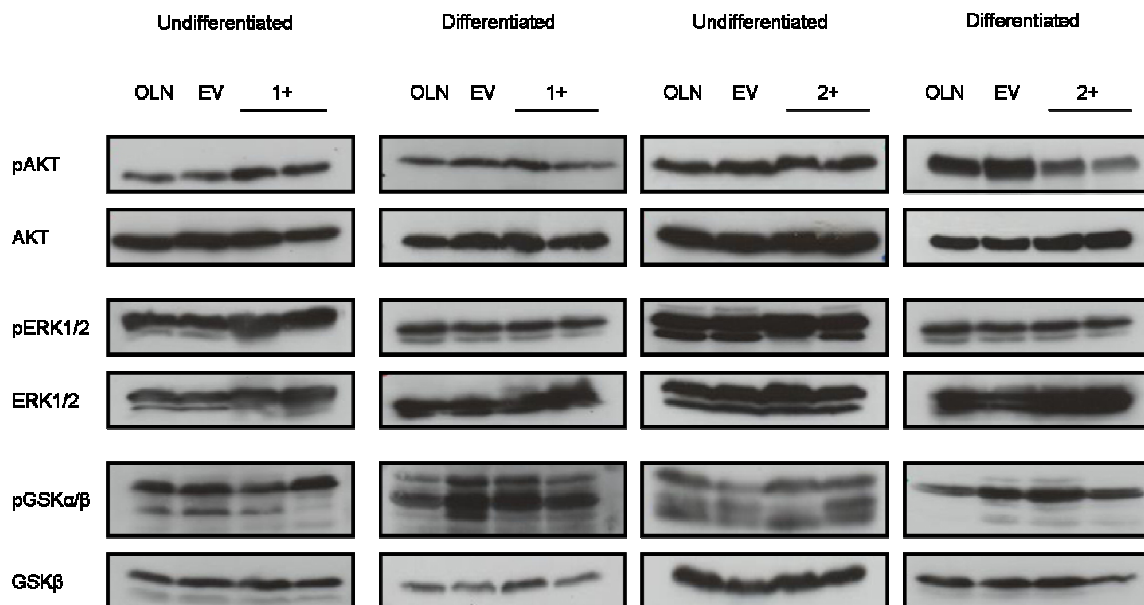
Figure 53: Downstream signaling of the IR/ IGF1R signaling pathway in undifferentiated and differentiated over expressing IRS-1 and IRS-2 OLN-93 cells
Phosphorylation of AKT (pAKT, Ser473), ERK1/2 (pERK1/2, Thr202/Tyr204) and GSK3αβ (pGSK3β, Ser9) are shown. As control served unphosphorylated protein level of AKT, ERK1/2 and GSK3β. Actin served as control. 400 µg of total proteins were used and separated via 10% SDS-PAGE gel.

Different serine kinases such as p70S6 (S6K; p70) induce a dissociation and inactivation of the PI3K, due to phosphorylation of the serine residues at the C-terminus of IRS-1. Furthermore the abunance of phosphatase and tensin homolog deleted on chromosome ten (PTEN) was analysed. PTEN reverses the phosphorylation of $PI_{3,4,5}P$ to generate $PI_{4,5}P$.

Western Blot of lysates of undifferentiated 1+ cells showed equal signals for pP70, p70, pPTEN and PTEN. Actin protein content was unchanged (Fig. 54, left panel, left row).

Differentiated 1+ cell showed unchanged phosphorylation of pP70 (upper band), p70, pPTEN and PTEN signals comparable in all samples tested. Actin protein content was alike (Fig. 54, left panel, second row).

Furthermore, undifferentiated and differentiated 2+ cells revealed similar pP70, p70, pPTEN and PTEN signals when compared to WT and EV cells in Western Blot analysis. Actin showed equal protein content (Fig. 54, right panel, first row; Fig. 54, right panel, second row).
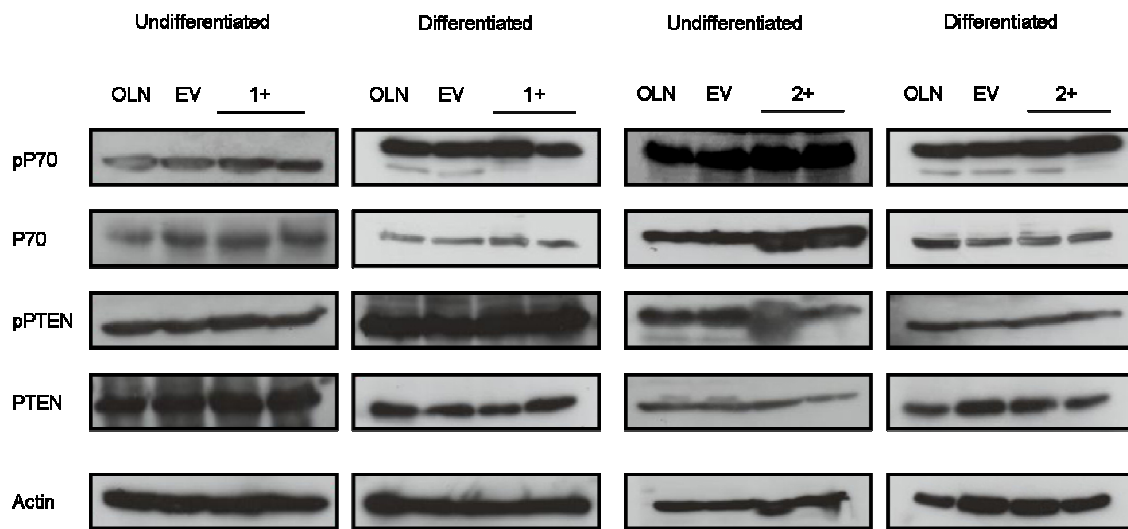
Figure 54: S6 kinase and PTEN expression in undifferentiated and differentiated over expressing IRS-1 and IRS-2 OLN-93 cells.
Phospho-p70 S6 kinase (Thr389), p70 S6 kinase, phospho-PTEN (Ser380/Thr382/383) and PTEN expression levels are shown. Actin served as control. 400 µg of total proteins were used and separated via 10% SDS-PAGE gel.

Next cell cycle arrest and apoptosis was analysed. The cell cycle inhibitor p27 is a member of the Cip/Kip family of CDK inhibitors and causing cell cycle arrest. To investigate whether apoptosis was induced cleavage of Caspase 3 was detected using Western Blots.

Undifferentiated 1+ cells revealed elevated p27 protein levels as well as Caspase 3 (upper band) and cleaved Caspase 3 (lower band) compared to OLN and EV cells. Actin Western Blot showed equal gel loading (Fig. 55, left panel, first row).

Differentiated 1+ cells demonstrated increased p27 and similar Caspase3, cleaved and uncleaved, protein expression (Fig. 55, left panel, right row).

Undifferentiated 2+ cells displayed identical p27 and Caspase 3, cleaved and uncleaved, protein levels compared to OLN and EV cells. Actin protein content was equal (Fig. 55, right panel, first row).

Differentiated 2+ cells revealed increased p27 and equal Caspase 3, cleaved and uncleaved, levels as compared to OLN and EV cells. Actin protein amount was unchanged (Fig. 55, right panel, second row).
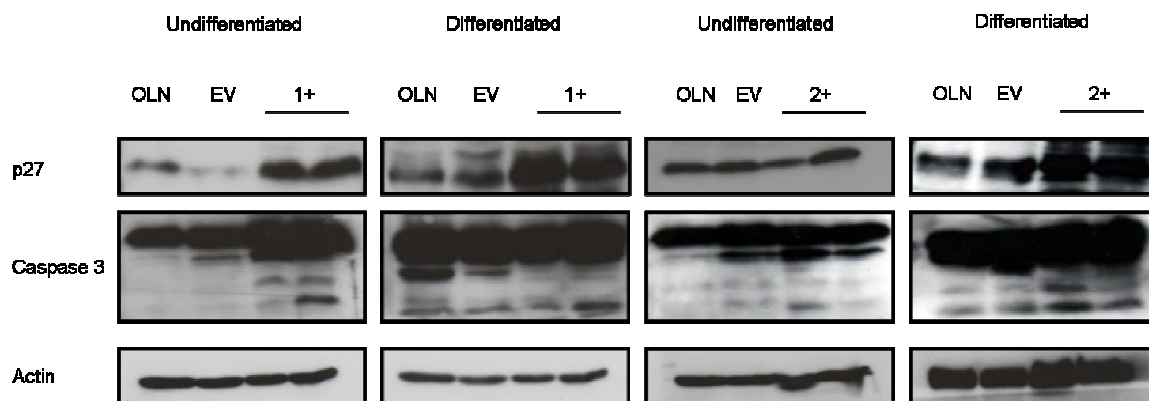
Figure 55: Proliferation and apoptotic protein marker expression in undifferentiated and differentiated over expressing IRS-1 and IRS-2 OLN-93 cells.
p27 (proliferation) and Caspase3 (apoptotic) expression levels are shown. Actin served as control. 400 µg of total proteins were used and separated via 10% and 15% SDS-PAGE gel.

Furthermore, Wnt signaling was analysed in undifferentiated and differentiated 1+ and 2+ cells.

Undifferentiated and differentiated 1+ cell displayed equal p-β-Cat and β-Cat levels, Wnt5a protein content was elevated in 1+ cells compared to OLN and EV cells. Actin protein content showed to be even (Fig. 56, left panel, first row; Fig. 56, left panel, second row).

Undifferentiated 2+ cells showed reduced phosphorylation of β-Cat and similar β-Cat and Wnt5a levels compared to OLN and EV cells. Actin protein amount was unchanged (Fig. 60, right panel, first row).

Differentiated 2+ cells showed equal phosphorylation of β-Cat, as well as β-Cat and Wnt5a levels compared to OLN and EV cells. Actin protein content was similar (Fig. 56, right panel, second row).
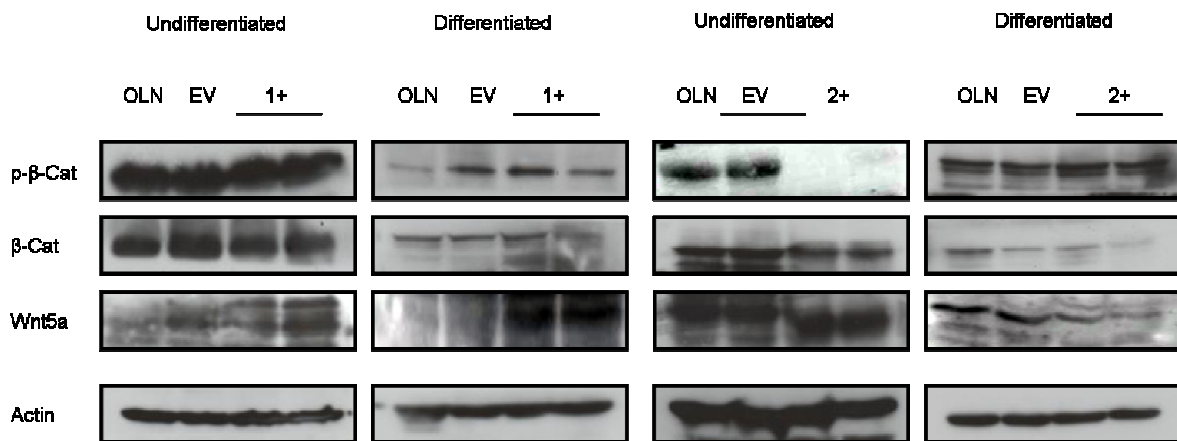
Figure 56: Wnt signaling pathway protein expression in undifferentiated and differentiated over expressing IRS-1 and IRS-2 OLN-93 cells.
Phosphorylation of β-Catenin (p-β-Cat, Ser33, Ser 37 and Thr41), β-Catenin and Wnt5a protein levels are shown. Actin served as control. 400µg of total protein were used and separated via 10% SDS-PAGE gel.

Myelin specific and Fyn kinase protein expression was also analysed refrerring to over expression of IRS-1 and IRS-2.

Undifferentiated 1+ cells had equal Fyn kinase, MBP and PLP protein levels compared to OLN and WT cells. CNP protein amount was elevated in 1+ cells. Actin protein content was similar in all samples (Fig. 57, left panel, first row).

Differentiated 1+ cells revealed increased CNP and PLP, whereas Fyn kinase and MBP were unchanged. Actin protein amount was unchanged (Fig. 57, left panel, second row).

Undifferentiated 2+ cells displayed similar protein levels of Fyn kinase, CNP, MBP and PLP. Actin protein content was equal (Fig. 57, right panel, first row).

Differentiated 2+ cells showed the same abundance for Fyn kinase, MBP and PLP, whereas CNP level was increased compared to OLN and EV cells. Actin protein expression was similar in all cell types (Fig. 57, right panel, second row).
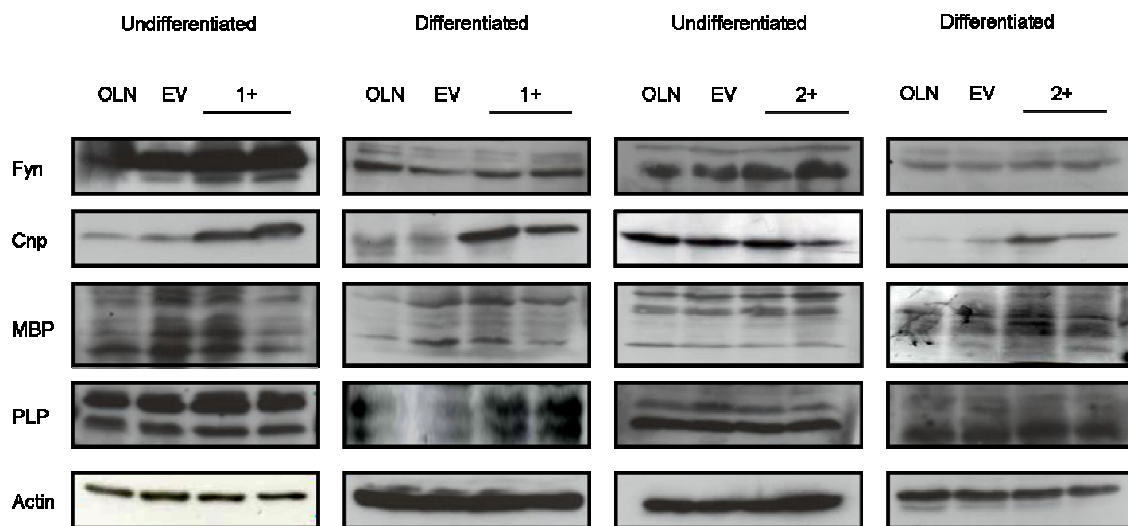
Figure 57: Myelin specific protein and Fyn kinase expression in undifferentiated and differentiated over expressing IRS-1 and IRS-2 OLN-93 cells.
Fyn kinase, CNP, MBP and PLP expression levels are shown. Actin served as control. 400µg of total protein were used and separated via 10% and 15% SDS-PAGE gel.

4.Discussion

4. Discussion

Multiple sclerosis (MS) is an inflammatory demyelinating disease that attacks the brain, spinal cord and optic nerves in the CNS, but skips the nerve roots and nerves of the peripheral nervous system (PNS). Axonal loss is an unstoppable result from MS and might be the pathological correlate to the irreversible neurological impairment of this disease [Ferguson, Matyszak, Esiri and Perry, 1997; Lovas et al., 2000; McGavern et al., 2000; Trapp et al., 1998]. Moreover oligodendrocytes progenitors are present in the lesion of MS they are unable to remyelinate those regions [Scolding 1998; Wolswijk; 1995; Wolswijk; 2000].

IGF-I an initiator of the InR/ IGF1R-signaling cascade is an fundamental player in myelination, as it acts as a survival factor for oligodendrocytes as well as their OPCs [Barres et al., 1992; Mason et al., 2000; McMorris et al., 1986; Ye and D'Ercole, 1999] and stimulates the synthesis of myelin [Roth et al., 1995]. Animal studies showed that over expression of IGF-I heightened myelin content [Carson et al., 1993; Ye et al., 1995] and reduction strongly decreases myelination and the number of OPCs [Beck et al., 1995]. Human studies showed that recombinant human IGF-I might not alter the course of MS on its own. But it has been proposed that it might be useful in combination with other therapies, due to its actions on oligodendrocytes and remyelination [Leist et al., 2002].

In previous studies homozygous IRS-2 deficient (IRS-2 ($^{-/-}$)) mice showed at P10 less myelin proteins (MBP, PLP and MOBP) in whole brain lysates but qualitatively unchanged myelination was observed. Therefore it was reasoned that IRS-2 is critical for appropriate initiation of myelination, but not for myelin maturation. Thus, IRS-1 only partly compensates for the loss of IRS-2 [Freude et al., 2008].

On the other hand mice lacking the InR revealed unchanged or altered myelination, indicating that myelination initiation signal is mainly transduced in the InR /IGF1R signalling cascade via the IGF1R [Freude et al., 2008].

The influence of increased IRS-2 signaling on myelination *in vivo* is still unknown. Thus mice with floxed-stopp-casette-IRS-2-sequence inserted into the Rosa26 locus (IR) were crossed with mice expressing the *CNP* driven Cre recombinase (CC) to guarantee an oligodendrocyte-specific over expression of IRS-2 (IRCC) (Fig. 10).

Homozygous CNP deficient (CC ($^{-/-}$)) mice are known to show normal myelin assembly. Furthermore, the ultrastructure and physical stability are not visibly changed in these mice. However, the axons developed abnormal swellings and were progressively lost leading to premature death of these mice mostly before one year of age. Therefore, those mice might present a usable MS model [Lappe-Siefke et al., 2003].

4.1. Oligodendrocyte specific over expression of IRS-2 in mice

For oligodendrocyte specific IRS-2 expression the CNP 1 promoter driven Cre recombinase (CC) expressing mice were used. Only heterozygous IRS-2 transgenic (IR) and Cre recombinase (CC) expressing mice have been used in the present experiments. As described previously homozygous CC mice showed obvious behavioural impairments at four month of age. For instance they developed ataxia and visible hind limb impairments [Nave et al., 2003].

In the present study mice over expressing IRS-2 in an oligodendrocyte specific manner, showed increased IRS-2 protein and eGFP protein expression in the white matter, as expected. Thus the IRS-2 over expression worked *in vivo*.

4.1.2. Body weight and brain body ratio of IRCC mice

Homozygous mice lacking the IGF1R in Olig1 expressing cells (IGF1R^{olig} ($^{-/-}$)) showed a significant decrease (up to 92% at 1 week of age) in brain weight compared to WT. Furthermore homozygous IGF1R knockout mice in PLP expressing cells (IGF1R^{PLP} ($^{-/-}$)) demonstrated later in live a reduction in brain weight as well. However, body growth of both mice displayed no abnormalities [Ye et al., 2007].

Previuos studies revealed that homozygous IRS-1 knockout mice (IRS-1 ($^{-/-}$)) exhibited an 18% reduction in brain weigth compared to WT. In those mice IRS-2 and IRS-4 compensate for the loss of IRS-1. As mice over expressing IGF-I and lacking IRS-1 displayed strongly increased myelination [Ye et al., 2002] IRS-1 was suggested to be not essential for IGF-I promoted oligodendrocyte development and myelination [D'Ercole et al., 2002]. Our own group investigated IRS-2 knockout mice and demonstrated that IRS-2 ($^{-/-}$) mice displayed smaller brain sizes compared to WT mice. This reduction correlated to the reduction of total cell number and not to impaired myelination [Schubert et al., 2003].

Interestingly CC ($^{-/-}$) showed a overall brain reduction after seven month of age [Nave et al., 2003]. Transgenic mice expressing IGF1R under the control of the MBP promoter displayed larger brain size compared to WT mice [Luzi et al., 2004].

Body weight and body brain ratio was measured from 5 till 140 days of age to analyse whether changes in body weight or brain size might be influenced in the mice investigated in the present study. Neither female nor male IRCC or CC mice showed any significant changes in their BMI and body brain ratio compared to WT or IR mice. Therefore it is concluded that IRS-2 over expression or CNP heterozygous knockout does not influence the development of the brain size as well as the BMI.

4.1.3. Behaviour of IRCC mice

Previous studies of our group using IRS-2 ($^{-/-}$) mice revealed no changes of general health assessment and during motor coordination testing no significant differences. Therefore IRS-2 deficiency does not have an impact on general health or motor function [Freude et al., 2008].

To investigate whether the oligodendrocyte specific over expression of IRS-2 (IRCC) or heterozygous CNP deficiency (CC) changes motor coordination Rotarod and Grip strength were tested at 12 weeks of age. Furthermore Trunk Curl test was performed at 40 weeks of age.

There were no significant differences detected during the Rotarod test comparing female and male IR and CC to WT and IRCC mice. Grip strength revealed slight differences in female mice, with decreased strength in CC ($^{-/-}$) (CC homo) and CC mice. Male mice displayed no differences in grip strength.

Thus IRS-2 over expression in oligodendrocytes has no strong effect onto motor function in mice earlier in life.

4.1.4. Morphological and structural brain analysis of IRCC mice

IGF1R ^{Olig} ($^{-/-}$) mice displayed a decreased volume of the corpus callosum and the anterior commissure with reduced cell density in 6 weeks old mice. Accordingly, 25 weeks old IGF1R ^{PLP} ($^{-/-}$) mice showed a significant reduction in the corpus callosum, cell density and total number of cells as well [Ye et al., 2007].

Our own studies in IRS-2 ($^{-/-}$) mice demonstrated no pathological abnormalities or dysplastic areas, whereas the corpus callosum and the anterior commissure were smaller compared to WT mice. However brains of those mice were also smaller, but did not vary in their cellular composition [Freude et al., 2008].

Nissl staining of 3,5 month old CC ($^{-/-}$) mice revealed that the density of oligodendroglial nuclei in the corpus callosum was unchanged [Nave et al., 2003]. In mice expressing IGF1R under the control of the MBP promoter an elevated density of myelinated axons, as well as larger brain size was observed [Luzi et al., 2004].

Investigation of both genders of the four genotypes of the present study at the age of 12, 8 and 5 weeks via Nissl staining and Klüver Barrera staining demonstrated no changes in morphology and structure of the brains.

IRS-2 over expression may therefore have no influence on the morphology of the brains up to 12 weeks of age.

4.1.5. Immunohistochemical analysis of Myelination in IRCC mice

Previous studies showed that IGF1R ^{Olig} ($^{-/-}$) mice display a reduced intensity of the immunostaining of the myelin proteins PLP and MBP in the brain at 2 weeks of age. Furthermore, IGF1R ^{PLP} ($^{-/-}$) mice showed decreased myelin specific proteins [Ye et al., 2007].

Our own group showed reduced staining of MBP in IRS-2 ($^{-/-}$) mice at day 10 of age [Freude et al., 2008].

CC ($^{-/-}$) mice revealed, up to 2.5 month of age, no differences in myelin proteins, as MBP [Nave et al., 2003].

Immunostaining of PLP and MBP in both genders of the four genotypes demonstrated no difference at 12, 8 and 5 weeks of age. Hence IRS-2 over expression in our CNP heterozygous background seems to have no significant influence onto the structure of myelin up to this time point. Further investigation of time points later in live would be intersentingly to reveal a possible influence of IRS-2 over expression in myelin maturation.

4.1.6. Quantity of myelin specific proteins in IRCC mice

As immunohistochemical analysis at day 10 aged IRS-2 ($^{-/-}$) mice revealed delayed MBP protein expression we investigated the changes of myelin composition at day 10 of age in these mice. Isolation of brain myelin at day 10 of age displayed no differences in the expression of the tested myelin specific proteins (MBP, PLP/DM20, MAG, MOBP, oligodendrocyte myelin glycoprotein). Therefore it was concluded that IRS-2 deficiency delays initiation of myelination quantitatively but does not change myelin protein composition at this time point of age [Freude et al., 2008].

Investigation of both genders and all four genotypes at described in the present study 12, 8, 5, 3 weeks and day 5 showed no obvious differences in the myelin composition. However IRS-2 over expression did reveal a reduced CNP protein expression at week 20 of age. There was an overall higher expression of the 18.5, 17 and 14kDa isoform of MBP in female mice of all four genotypes.

Taken together IRS-2 over expression results in an age dependent reduction of CNP protein expression. But IRS-2 does not seem to function on its own. An age dependent factor, which includes decreased CNP expression in myelin seems to be necessary.

4.1.7. Investigation of protein expression in IRCC mice

4.1.7.1. InR/ IGF1R signaling in IRCC mice

InR/ IGF1R signaling which might contribute to altered myelination was investigated in IRS-2 ($^{-/-}$) knockout mice by our group. Those studies revealed a significant increase of IGF1R, IRS-1, pAKT and pERK12 protein expression at postnatal day 10. In addition phosphorylation of GSK3β and ERK1/2 protein levels was elevated at day 14 of age. Later time points revealed no changes in InR/ IGF1R signaling. Furthermore, mice lacking the InR in the CNS showed no differences in myelin specific protein expression, as well as in downstream signaling of InR/ IGF1R during early postnatal development. Therefore initiation of myelination in the CNS is mediated via IGF1R/ IRS-2 regulated signals and seems to be independent of InR signaling.

Hence, upregulation of IGF1R signal transduction could be a mechanism to overcome the loss of IRS-2 to provide proper myelination [Freude et al., 2008].

Investigation of both genders of the four genotypes at the time points week 20, 12, 8, 5, 3 and additionally day 5 of age were therefore made in respect to InR/ IGF1R signaling.

Whole brain lysates of 20, 3 weeks and 5 days old mice revealed no significant differences in InR/ IGF1R signaling.

12 weeks old IRCC mice displayed a reduced IGF1R protein expression in both genders and elevated GSK3α phosphorylation at this time point. Comparing protein expression of 8 and 5 weeks old IRCC mice a similar decreased InR protein expression was found. Downstream of the InR/IGF1R CC and IRCC mice show the same elevated levels of phosphorylated AKT and reduction of ERK signals at this time point.

In contrast to IRS-2 ($^{-/-}$) mice, IRS-2 over expression results not in an early developmental phenotype, but shows transient changes in InR protein expression between week 5 and 8 of age. The decrease of InR expression is accompanied by with elevated levels of pAKT and pERK. This might be a compensatory mechanism similar to that observed in IRS-2 ($^{-/-}$) mice.

4.1.7.2. Inflammatory protein expression in IRCC mice

IGF1R ^{Olig} ($^{-/-}$) and IGF1R ^{PLP} ($^{-/-}$) mice displayed a significant increase of astrocytes in the corpus callosum, respectively in 2 week and 6 week old mice [Ye et al., 2007].

Furthermore the corpus callosum and the anterior commissure were smaller in IRS2 ($^{-/-}$) mice compared to WT mice, but the cell density was not different. Additionally, investigation of

astrocytes revealed no differences of GFAP staining in 8 weeks old mice. Therefore an inflammatory process in IRS2 ($^{-/-}$) was excluded [Freude et al., 2008].

It has been shown that the loss of CNP results in a progressive reduction of white matter tracts, which accounts for the loss of brain tissue in CNP ($^{-/-}$) mice aged 3.5 month and older. However neuronal cell death is not a feature in those mutant mice [Nave et al., 2003].

As CNP ($^{-/-}$) mice display axonal loss during aging an inflammatory process due to this axonal loss might play a role in the present mouse models. Therefore CC mice might show increased levels of MMP-9, prior to histological and morphological changes [Svejgaard et al., 2000].

TNFα is known to mediate serine phosphorylation of IRS proteins to attenuate insulin receptor signalling [Shier et al., 1989]. Therefore whole brain lysates of all four mutant mice were as well investigated for TNFα and MMP-9 expression.

IRCC mice showed at 3 weeks an elevated, at 5 weeks reduced, at 12 and at 20 weeks of age an increased TNFα protein expression. MMP-9 protein levels were higher at 3 weeks, at 5 weeks decreased, at 12 weeks increased and at 20 weeks again reduced.

Those transient protein expression patterns might be a developmental phenotype of IRS-2 over expression, compenstating for abnormal high IRS-2 levels and for decreased CNP levels. As CC mice showed only reduced protein expression of TNFα at 5, 8 and 12 weeks of age, whereas there was a reduction of MMP-9 at week 12.

These transient effect does not seem to correlate with the activity InR/ IGF1R signaling cascade as, there were no chanages of proteins or phosphorylation of the InR/ IGF1R signaling cascade visible at those time points.

4.1.7.3. Myelin specific protein expression in IRCC mice

IGF1R ^{Olig} ($^{-/-}$) as well as IGF1R ^{PLP} ($^{-/-}$) mice displayed at 6 weeks of age a significant reduction of MBP and CNP. Therefore a functional IGF1R is necessary for a proper myelination [Ye et al., 2007]. Our own group could has shown in IRS-2 ($^{-/-}$) mice that delayed inititation of myelination is due to the lack of IRS-2 [Freude et al., 2008]. CC ($^{-/-}$) mice displayed a slight elevation of MBP in whole brain lysate, but not in purified myelin. Whereas PLP showed no developmental change. Hence no significant signs of dysmyelination was found [Nave et al., 2003].

In the present study the reduction of Fyn kinase protein expression seems to be reduced by IRS-2 over expression in CC mice at least, as week 5 and 8 of age display. It is known for

Fyn deficient mice [Yamamoto et al., 1994] that decreaseed of MBP levels correlates with reduced Fyn kinase abundance. Therefore it was concluded, that Fyn kinase is involved in the myelination process [Chao et al., 1999; Werner et al., 2009] and induces MBP protein expression when activated [Werner et al., 2009].

IRS-2 is somehow influencing protein expression of CNP in CC mice, as IRCC mice do have lower levels of CNP compared to CC mice at least in isolated myelin in 20 weeks old mice. Therefore IRS-2 seems to be one of the factors that might negatively regulate CNP protein expression during later myelination processes or myelin maturation.

IRS-2 ($^{-/-}$) mice displayed reduced PLP in mice younger than 3 weeks of age and normal protein levels in older mice. This phenotype is exactly the opposite in IRCC mice, as week 5 old mice show increased, week 8 decreased and older than 8 weeks old unchanged levels. Hence it might be that IRS-2 over expression or Fyn kinase reduction is not promoting normal PLP and DM20 protein expression during myelination. However, it has been shown in cancer cells that the Ras/PI3K/Akt pathway is a mediator of Fyn kinase activation [Yadav and Denning, 2011]. As AKT phosphorylation is elevated in IRCC mice at 5 weeks of age, this increased AKT signals might lead to more phosphorylated Fyn reducing the amount of the active form.

Taken together the transient changes in protein expression of the Fyn kinase and the slight transient alteration in myelin specific proteins, as CNP and PLP/ DM20 in IRCC mice might point to an effect of IRS-2 during development, but it seems to be rapidly conter regulated. As the effects were minor, it seems that IRS-2 acts or is regulated by other co-factors.

4.1.7.4. Wnt-signaling in IRCC mice

Previous work of our group showed that IRS-2 ($^{-/-}$) mice up-regulate the IGF1R signaling pathway to overcome the lack of IRS-2. Between 10-14 days of age an increase of GSK3β protein expression was found [Freunde et al., 2008]. GSK3β is known to regulate β-catenin variety [Romanelli et al., 2007]. A lack of β-catenin expression results in reduced brain growth [Machon et al., 2003; Schuller and Rowitch, 2007]. Elevated levels of β-catenin might be regulated via IGF-I and its stimulation of the PI3K/Akt pathway. In addition suppression of GSK3β elevates IGF-I induced activation of β-catenin [D'Ercole et al., 2010].

In neurons it has been shown that GSK3 is regulated via Wnt3a. Although that the Wnt and insulin signalling cascades are largely independent (both can use non-GSK dependent pathways) some degree of crossover occurs, which is not dependent on Akt [Lovestone et al., 2011]. It is known that dysregulation of Wnt signaling contributes to failure of remyelination, both in mice and humans [Fancy et al., 2009; Rosenberg and Chan, 2009] as

Wnt/ β-catenin signaling influences expression of myelin genes and myelin sheath compaction [Massad et al., 2011].

Analysis of brain lysates of all four genotypes revealed no clear differences of Wnt5a, β-catenin and p- β-catenin protein expression.

As there was no correlation between IRS-2 over expression, AKT or serine phosphorylation of GSK3β, over expression of IRS-2 seems not to correlate with phosphorylation of GSK3 influencing the Wnt/ β-catenin signaling pathway at all time points investigated.

4.1.8. Inflammation in IRCC mice

As described in 4.1.7.2 an inflammatory process might play a role in the IRCC and CC mice. To further analyse this point imunohistochemical analysis were performed.

IRCC showed a stronger GFAP signal and a higher number of activated of astrocytes in the brain compared to WT. This effect was age dependent as 12 weeks old mice displayed less GFAP staining than 8 weeks old mice.

IRS-2 over expression in oligodendrocytes might alter the outer myelin membrane leading to the activation of astrcocytes. Future lines of research might be directed to further investigate the molecular mechanism leading to this transient astroctytosis.
Interestingly the activation of astrocytes in IRCC mice does not correlate with the activity of the InR/ IGF1R signaling cascade.

Furthermore the data abtained by Western Blot and via Immunohistochemistry did not show constant increased inflammation due to IRS-2 over expression in oligodendrocytes. Thus the transient effects observed might be results of IRS-2 over expression but the phenomenom gets rapidly compensated.

4.2. IRS-1 and IRS-2 over expressing OLN-93 cells

In the present study stably over expressing IRS-1 (1+) and IRS-2 (2+) OLN-93 cells were designed and analysed. ONL-93 cells were stably transfected with pCMV-Tag-2 B (EV) , pCMV-Tag-2 B IRS-1 (1+) and pCMV-Tag 2C IRS-2 (2+). Both IRS constructs were under the control of the pCMV promoter, which guaranties a strong over expression of the

particular genes. Both cell lines showed IRS-1 and respectively IRS-2 protein over expression, as expected.

4.2.1. Morphological analysis of undifferentiated and differentiated IRS-1 and IRS-2 over expressing OLN-93 cells

The spontaneously transformed cell line of primary rat brain glial cultures (OLN-93) was first described morphologically by Richter-Landsberg and Heinrich (1996). Undifferentiated cells show a bipolar cell body with long extensions, whereas differentiated cells display a globular appearance and long thin extensions and built up more connections between the different cell bodies.

Since IRS-1 is not essential in IGF-I promotion of oligodendrocyte development and myelination [D'Ercole ett al., 2002] we investigated those cells in respect of IRS-1 and IRS-2 over expression.

IRS-1 over expression of IRS-1 in OLN-93 cells did not change morphology. However in differentiated state those cells show more thin extensions. Therefore IRS-1 over expression might promote differentiation.

Our group has shown that IGF1R/ IRS-2 mediated signals are important for the correct timing of myelination in mice [Freude et al., 2008].

IRS-2 over expression in OLN-93 showed in the undifferentiated state reduced extensions, which was even more promoted when differentiated, suggesting that IRS-2 might inhibit differentiation at least *in vitro*.

4.2.2. Proliferation of stably over expressing IRS-1 and IRS-2 OLN93 cells

The proliferation assays did not give clear results, BrdU incorporation assays suggested, that IRS-1 over expression results in similar proliferation compared to WT.

However it might be that the starvation prior to the BrdU incubation causes differentiation of the OLN-93 cells and that the differentiation inhibits proliferation.

This could explain that even under condition of inhibition of the PI3K and the MAPK-kinase pathway the differences to just DMSO treated cells were minor.

Similar results were obtained for IRS-2 over expressing cells which had to be similary discussed as well.

4.2.3.1. Protein expression of the InR/ IGF1R signaling pathway in stably over expressing IRS-1 and IRS-2 OLN93 cells

The OLN-93 cell line shows morphological features as well as antigenic properties of 5- to 10 day old rat brain oligodendrocytes [Richter-Landsberg and Heinrich, 1996]. Therefore these cells have similar protein expression as isolated oligodendrocytes. Little is known about expression of proteins of the InR/ IGF1R signaling pathway in oligodendrocytes precursors and OLN-93 cells.

Over expression of IRS-1 in undifferentiated 1+ cells results in a equally elevated IRS-2 protein expression, which are both down regulated during differentiation. IGF1R protein amount was elevated due to IRS-1 over expression in undifferentiated as well as in differentiated status. Whereas the InR protein content is reduced in undifferentiated 1+ cells and of the same level as in WT when differentiated. Phosphorylation of AKT was increased in undifferentiated cells.

IRS-1 over expression in undifferentiated oligodendrocytes resulted in a reduction of IRS proteins during differentiation. IRS-1 was capable of stimulation IGF1R expression in undifferentiated as well as differentiated cells, whereas the InR protein amount and AKT phosphorylation were only influenced in the undifferentiated status via IRS-1.

IRS-2 over expression revealed the same characteristics in undifferentiated cells as undifferentiated 1+ cells. Hence when one IRS protein is over expressed the other is equally increased. But in contrast to 1+ cells, differentiated 2+ cells down regulated IRS-1 and IRS-2 concentrations to WT levels. Furthermore, undifferentiated 2+ cells revealed a higher IGF1R protein content, as 1+ cells. But this was lost during differentiation. Those elevated IGF1R levels seem to correlate with IRS-1 content. Interestingly, higher IRS-2 protein content leads at least in the differentiated status to a reduction of phosphorylated AKT.

Thus, IRS-1 over expression leads to complex changes within the InR/IGF1R signaling cascade. However, when differentiated signaling is nearly unaltered. IRS-2 over expression leads to elevated IGF1R and reduced phosphorylation levels of AKT, but those changes were lost during differentiation. Furthermore, elevated IGF1R level seem to be more correlated to IRS-1 than IRS-2.

There are several possibilities how IRS proteins many be downregulated during differentiation including e.g. degradation or silencing of the promoter. This interesting point needs further investigation

4.2.3.2. Downstream signaling of the InR/ IGF1R signaling pathway in stably over expressing IRS-1 and IRS-2 OLN93 cells

It is known, that deletion of PTEN results in over activation of AKT as well as downstream targets like mTOR. Transgenic mice with forced expression of activated AKT in oligodendrocytes develop significant hypermyelination [Flores et al., 2008] possibly through a mTOR dependent mechanism [Macklin et al., 2009]. Therefore a therapeutic benefit of PI3K/ mTOR pathway activation to increase myelination was suggested. Furthermore, PTEN is an essential player in regulation of myelin sheath thickness as well as axon and myelin integrity. In contrast no exclusive function of PTEN was found during remyelination in oliodendrocytes [Rowitch et al., 2010]. As the S6 kinase is a direct target of mTOR it might play an important role during this regulatory process [Fenton and Gout, 2011; Rowitch et al., 2010].

In 1+ and 2+ cells, differentiated as well as undifferentiated, no alteration in the protein expression of PTEN and S6 kinase was observed. This suggests that IRS-1 and IRS-2 over expression in OLN-93 cells does not result in constant downstream differences in the PI3K/ mTOR pathway. During differentiation a so far unkown regulatory mechanisms compensate for a possible over-activation of this pathway.

4.2.3.3. Proliferation and apoptotic protein marker expression in stably over expressing IRS-1 and IRS-2 OLN93 cells

IGF-I knockout mice displayed reduced numbers of oligodendrocytes and OPCs [Ye et al., 2002]. Furthermore IRS-2 ($^{-/-}$) mice showed a reduced brain size which emerges from a reduction of total cell number [Schubert et al., 2003].

1+ cells showed to have elevated p27 protein levels in the differentiated as well as in the undifferentiated status. Whereas 2+ cell displayed increased p27 protein expression only when differentiated.
Protein expression of Caspase3 and cleaved Caspase 3 was raised in undifferentiated 1+ cells and the same level as WT when differentiated. 2+ cells did not show any differences in undifferentiated as well as in the differentiated status in Caspase 3 levels.

In the differentiated status elevated p27 protein levels were expected, since for differentiation a cell cycle arrest is necessary. This was observed in 1+ and 2+ differentiated cells. 1+ cells had in the undifferentiated status higher p27 protein amount, which should result in a

reduced proliferation, which was not to be seen BrdU proliferation analysis, via BrdU proliferation assay. This might hint to the observation that IRS-1 induces differentiation. Interestingly cleaved Caspase 3 protein species are raised in 1+ cells, which should lead to increased apoptosis, but was not observed in 1+ cells. However, the ratio of full length Caspase 3 and cleaved Caspase 3 remained stable in 1+ cells.

This suggests that IRS-1 might trigger initial steps of differentiation in OLN-93 cells.

4.2.3.4. Wnt-signaling pathway in stably over expressing IRS-1 and IRS-2 OLN93 cells

Although the Wnt and insulin signaling cascades are largely independent (both can use the non-GSK dependent pathway) some degree of cross over occurs, which is not dependent on AKT [Lovestone et al., 2011]. Therefore changes were investigated due to over expression of IRS-1 and IRS-2 onto the Wnt signaling cascade.

1+ cells showed an increase of Wnt5a protein amount in differentiated and undifferentiated cells. 2+ cells demonstrated in the undifferentiated status reduced protein levels of phosphorylated β-Cat. However 1+ and 2+ cells did not display any changes in phosphorylated GSK3 protein expression. Therefore those changes seen in the Wnt signaling pathway do not seem to be primary events of the IRS proteins or the InR/ IGF1R signaling cascade.

4.2.3.5. Myelin specific proteins in stably over expressing IRS-1 and IRS-2 OLN93 cells

Cells did not show elevated myelin specific protein expression in the undifferentiated status. Both IRS proteins were able to increase the protein amount of CNP in differentiated OLN-93 cells. Interestingly IRS-1 was also capable to elevate PLP protein content slightly.

Therefore CNP protein expression seems to be regulated during differentiation via IRS-1 as well as IRS-2. Suggesting that both IRS proteins have the same function concerning CNP expression. However, IRS-1 seems to trigger differentiation in OLN-93 which might explain the induction of CNP in undifferentiated 1+ cells.

4.3 Correlation between *in vivo* and *in vitro* model

The experiments using OLN-93 cells suggest that IRS-1 triggers at least to a certain extend differentiation of these glial cells leading to increased numbers of cell processes in differentiated 1+ cells and increased p27 and CNP expression in the undifferentiated state. Furthermore, both IRS proteins are capable to induce CNP expression in differentiated cells, but not MBP or PLP suggesting a selective function of IRS-proteins to induce certain myelin-specific proteins. In contrast, the *in vivo* experiment using IRCC mice did not reveal any alterations of myelin protein composition, myelin protein expression or InR/ IGF1R signaling up to 12 weeks. Surprisingly, at 20 weeks of age the CNP abundance in myelin was reduced in IRCC mice but not in whole brain lysates suggesting, that the subcellular distribution of CNP is regulated via IRS-2 *in vivo*. However, the CNP distribution seems not to be regulated via IRS-2 exclusively but seems to be dependent on an age-dependent factor since decreased myelin CNP was observed only in animals over 12 weeks of age. Therefore, investigations to elucidate the role of IRS-2 in oligodendrocytes for myelin maturation and remyelination are interesting fields of future research. Moreover, neither IRS protein over expression in OLN-93 cells nor oligodendrocyte specific over expression of IRS-2 in mice did cause visible changes of the InR/ IGF1R signaling cascade suggesting that alterations of this signaling cascade gets rapidly compensated. The slight differences in InR/ IGF1R signaling observed in IRCC mice and the complex changes found in OLN-93 protein (e.g. IGF1R, InR) might just be a phenomenon to ensure and adjust proper downstream InR/ IGF1R signaling.

5. Summary

Myelin development and maturation are fundamental processes which enables rapid and coordinated movement. Several human diseases have been shown to affect myelin itself or myelin development. The most frequent disease involving myelin is multiple sclerosis (MS). Multiple sclerosis is an inflammatory demyelinating disease that attacks the brain, spinal cord and the optic nerves in the CNS. Axonal loss might be the pathological correlate for the irreversible neurological impairment of this disease. The Insulin receptor (InR)/ Insulin-like growth factor 1 (IGFI) receptor signaling cascade is an important player during myelination, as it acts as a survival factor for oligodendrocytes as well as their precursors (OPCs) and stimulates the synthesis of myelin. Animal studies showed that over expression of IGF-I increases myelin content and IGF-1 deletion strongly decreases myelination and the number of OPCs. The insulin receptor substrates (IRS) mediate insulin's and IGF-I's intracellular effects. The IRS protein family consist at least of 4 members, IRS-1 to 4. IRS-1 and 2 are expressed throughout the brain. Studies of our group showed that IRS-2 is critical for appropriate initiation of myelination, but not for myelin maturation. However, the influence of increased IRS-2 signaling on myelination is still unknown. Thus, stably IRS-1 or IRS-2 over expressing ONL-93 cells (oligodendrocyte-like cell line) were generated and analysed. Furthermore, mice with inserted floxed-stop-cassette IRS-2 into the Rosa26 locus (IR) were crossed with mice expressing the CNP driven Cre recombinase (CC) to induce an oligodendrocyte specific over expression of IRS-2 (IRCC). The different genotypes were analysed from day 5 up to 20 weeks of age. Interestingly, IRS-1 in OLN-93 cells triggers differentiation of these glial cells leading to increased numbers of cell processes in IRS-1 over expressing cells, increased p27 and CNP expression even in the undifferentiated state. Furthermore, both IRS proteins are capable to induce cnp expression in differentiated OLN-93 cells. In contrast, *in vivo* experiment using IRCC mice did not reveal any alterations of brain development, myelin protein composition, myelin protein expression, motor coordination or InR/IGF-1R signaling up to 12 weeks. Surprisingly, at 20 weeks of age the CNP abundance in isolated myelin was even reduced in IRCC mice but not in whole brain lysates, suggesting that the subcellular distribution of CNP is regulated via IRS-2 *in vivo*. Interestingly IRS-protein over expression in ONL93 cells or oligodendrocyte-specific IRS-2 over expression in mice did only cause minor changes of the InR/IGF-1R signaling cascade suggesting that alterations of this signaling cascade gets rapidly compensated. Thus, the present study revealed that i) IRS-1 and IRS-2 induces expression of CNP in OLN-93 cells, ii) IRS-1 triggers OLN-93 cell differentiation, iii) oligodendrocyte specific over expression of IRS-2 does not alter myelin development but influences CNP subcellular distribution after myelin development is completed.

6. Zusammenfassung

Myelin Entwicklung und Erhalt sind fundamentale Prozesse, welche schnelle und koordinierte Bewegungen ermöglichen. Verschiedene Krankheiten des Menschen sind bekannt dafür, dass sie Myelin oder dessen Entwicklung beeinträchtigen. Die häufigste Krankheit in Bezug auf Myelin ist dabei Multiple Sklerose (MS). MS ist eine entzündliche demyelinisierende Krankheit die, das Gehirn, das Rückenmarkt und den Sehnerv angreift. Verlust der Axone könnte das pathologische Korrelat für die unumkehrbare neurologische Beeinträchtigung bei dieser Erkrankung sein. Die Insulinrezeptor (InR)/ Insulin ähnliche Wachstumsfaktor I (IGFI) Rezeptor Signalkaskade ist ein wichtiger Faktor während der Myelinisierung. Da diese als Überlebensfaktor für Oligodendrozyten und deren Vorläuferzellen (OPCs) gilt und die Synthese von Myelin stimuliert. Tierstudien haben gezeigt, dass eine Überexpression von IGF-I zu einem erhöhten Myelin Anteil führt und eine Deletion zu einer drastischen Verringerung des Myelins und der Anzahl der OPCs. Die Insulin Rezeptor Substrate (IRS) leiten intrazellulär die von Insulin und IGF-I ausgelösten Effekte weiter. Die IRS Proteinfamilie besteht aus mindestens 4 Mitgliedern, IRS-1 bis 4. IRS-1 und 2 wereden im ganzen Gehirn exprimiert. Unsere Gruppe konnte zeigen, dass IRS-2 ein wichtiger Faktor für die richtige Einleitung der Myelinisierung ist. Dennoch ist der Einfluss von erhötem IRS-2 Signal auf die Myelinisierung immer noch unbekannt. Daher wurden stabil transfizierte OLN-93 (eine Oligodendrozyten Zelllinie) Zellen die IRS-1 und IRS-2 überexprimieren generiert und analysiert. Ebenso wurden Mäuse, welche eine in das Rosa26 Gen eingefügte Flox-Stop-Kasette mit IRS-2 (IR) tragen, mit Mäusen gekreuzt, welche die Cre Rekombinase unter der Kontrolle des CNP Promotors (CC) exprimieren. Dies sollte eine oligodendrozyten spezifische Überexpression von IRS-2 (IRCC) gewährleisten. Die verschiedenen Genotypen wurden im Alter von 5 Tagen bis 20 Wochen analysiert. Interessanter Weise löst IRS-1 in den OLN-93 Zellen die Differenzierung dieser Gliazellen aus und führt zu einer Vermehrung von Zellfortsätzen in IRS-1 überexprimierenden Zellen, sowie erhöhte p27 und CNP Proteinexpression im undifferenziertem Zustand. Ferner sind beide IRS Proteine fähig in differenzierten OLN-93 Zellen die CNP Expression zu indizieren. Im Gegensatz, zeigte das *in vivo* Experiment mit IRCC Mäusen keine erkennbaren Unterschiede in der Entwicklung des Gehirnes, in der Proteinzusammensetzung des Myelins, der Expression der Myelin Proteine, in der Motorkoordination oder in der InR/IGF1R Signalkaskade bis zum Alter von 12 Wochen.

Erstaunlicher Weise war die Menge an CNP in Woche 20 in isoliertem Myelin von IRCC Mäusen verringert, dies war aber nicht in Ganzhirnlysaten der Fall. Dies lässt schlussfolgern, dass *in vivo* die subzelluläre Verteilung von CNP durch IRS-2 reguliert werden könnte. Interessanter Weise führt eine Überexpression von IRS Proteinen in OLN-93 Zellen oder bei der Oligodendrozyten spezifischen IRS-2 Überexpression in Mäusen nur zu kleineren

Unterschieden in der InR/ IGF1R Signalksakade. Dies lässt darauf schliessen, das die Veränderungen in der Signalkaskade schnell kompensiert werden.

Zusammengefasst zeigte diese Studie, dass i) IRS-1 und IRS-2 die Expression von CNP in OLN-93 Zellen induzieren kann, ii) IRS-2 die Differenzierung in OLN-93 Zellen einleiten kann, iii) die Oligodendrozyten spezifische Überexprimierung von IRS-2 *in vivo* nicht die Entwicklung des Myelins beeinträchtigt, aber nachdem die Entwicklung des Myelins abgeschlossen ist, die subzelluläre Verteilung von CNP beinflusst.

7. References

Acebes, A. and M. Morales (2012). "At a PI3K crossroads: lessons from flies and rodents. " Rev Neurosci **23**(1): 29-37.

Agrawal, H. C., T. J. Sprinkle, et al. (1990). "2',3'-cyclic nucleotide-3'-phosphodiesterase in the central nervous system is fatty-acylated by thioester linkage." J Biol Chem **265**(20): 11849-53.

Alessi, D. R., M. Andjelkovic, et al. (1996). "Mechanism of activation of protein kinase B by insulin and IGF-1." EMBO J **15**(23): 6541-51.

Astrinidis, A. and E. P. Henske (2005). "Tuberous sclerosis complex: linking growth and energy signaling pathways with human disease." Oncogene **24**(50): 7475-81.

Azim, K. and A. M. Butt (2011). "GSK3beta negatively regulates oligodendrocyte differentiation and myelination in vivo." Glia **59**(4): 540-53.

Banik, N. L. and M. E. Smith (1977). "Protein determinants of myelination in different regions of developing rat central nervous system." Biochem J **162**(2): 247-55.

Baron-Van Evercooren, A., C. Olichon-Berthe, et al. (1991). "Expression of IGF-I and insulin receptor genes in the rat central nervous system: a developmental, regional, and cellular analysis." J Neurosci Res **28**(2): 244-53.

Barres, B. A., I. K. Hart, et al. (1992). "Cell death and control of cell survival in the oligodendrocyte lineage." Cell **70**(1): 31-46.

Barthel, A., D. Schmoll, et al. (2005). "FoxO proteins in insulin action and metabolism." Trends Endocrinol Metab **16**(4): 183-9.

Baumann, N. and D. Pham-Dinh (2001). "Biology of oligodendrocyte and myelin in the mammalian central nervous system." Physiol Rev **81**(2): 871-927.

Beck, K. D., L. Powell-Braxton, et al. (1995). "Igf1 gene disruption results in reduced brain size, CNS hypomyelination, and loss of hippocampal granule and striatal parvalbumin-containing neurons." Neuron **14**(4): 717-30.

Bernier, L., D. R. Colman, et al. (1988). "Chromosomal locations of genes encoding 2',3' cyclic nucleotide 3'-phosphodiesterase and glial fibrillary acidic protein in the mouse." J Neurosci Res **20**(4): 497-504.

Bifulco, M., C. Laezza, et al. (2002). "2',3'-Cyclic nucleotide 3'-phosphodiesterase: a membrane-bound, microtubule-associated protein and membrane anchor for tubulin." Proc Natl Acad Sci U S A **99**(4): 1807-12.

Biggs, W. H., 3rd, J. Meisenhelder, et al. (1999). "Protein kinase B/Akt-mediated phosphorylation promotes nuclear exclusion of the winged helix transcription factor FKHR1." Proc Natl Acad Sci U S A **96**(13): 7421-6.

Boison, D., H. Bussow, et al. (1995). "Adhesive properties of proteolipid protein are responsible for the compaction of CNS myelin sheaths." J Neurosci **15**(8): 5502-13.

Boura-Halfon, S. and Y. Zick (2009). "Phosphorylation of IRS proteins, insulin action, and insulin resistance." Am J Physiol Endocrinol Metab **296**(4): E581-91.

Brinkmann, B. G., A. Agarwal, et al. (2008). "Neuregulin-1/ErbB signaling serves distinct functions in myelination of the peripheral and central nervous system." Neuron **59**(4): 581-95.

Brosnan, C. F. and C. S. Raine (1996). "Mechanisms of immune injury in multiple sclerosis." Brain Pathol **6**(3): 243-57.

Broughton, S. and L. Partridge (2009). "Insulin/IGF-like signalling, the central nervous system and aging." Biochem J **418**(1): 1-12.

Brown, M. C., M. Besio Moreno, et al. (1993). "Vesicular transport of myelin proteolipid and cerebroside sulfates to the myelin membrane." J Neurosci Res **35**(4): 402-8.

Brunet, A., L. B. Sweeney, et al. (2004). "Stress-dependent regulation of FOXO transcription factors by the SIRT1 deacetylase." Science **303**(5666): 2011-5.

Bruno, R., L. Sabater, et al. (2002). "Multiple sclerosis candidate autoantigens except myelin oligodendrocyte glycoprotein are transcribed in human thymus." Eur J Immunol **32**(10): 2737-47.

Burns, J., A. Rosenzweig, et al. (1983). "Isolation of myelin basic protein-reactive T-cell lines from normal human blood." Cell Immunol **81**(2): 435-40.

Campagnoni, A. T. and W. B. Macklin (1988). "Cellular and molecular aspects of myelin protein gene expression." Mol Neurobiol **2**(1): 41-89.

Campagnoni, A. T., T. M. Pribyl, et al. (1993). "Structure and developmental regulation of Golli-mbp, a 105-kilobase gene that encompasses the myelin basic protein gene and is expressed in cells in the oligodendrocyte lineage in the brain." J Biol Chem **268**(7): 4930-8.

Capello, E., R. R. Voskuhl, et al. (1997). "Multiple sclerosis: re-expression of a developmental gene in chronic lesions correlates with remyelination." Ann Neurol **41**(6): 797-805.

Carson, M. J., R. R. Behringer, et al. (1993). "Insulin-like growth factor I increases brain growth and central nervous system myelination in transgenic mice." Neuron **10**(4): 729-40.

Chandler, S., R. Coates, et al. (1995). "Matrix metalloproteinases degrade myelin basic protein." Neurosci Lett **201**(3): 223-6.

Chandross, K. J., R. I. Cohen, et al. (1999). "Identification and characterization of early glial progenitors using a transgenic selection strategy." J Neurosci **19**(2): 759-74.

Chang, A., A. Nishiyama, et al. (2000). "NG2-positive oligodendrocyte progenitor cells in adult human brain and multiple sclerosis lesions." J Neurosci **20**(17): 6404-12.

Chang, A., W. W. Tourtellotte, et al. (2002). "Premyelinating oligodendrocytes in chronic lesions of multiple sclerosis." N Engl J Med **346**(3): 165-73.

Cheatham, B. and C. R. Kahn (1995). "Insulin action and the insulin signaling network." Endocr Rev **16**(2): 117-42.

Chesik, D., J. De Keyser, et al. (2010). "Insulin-like growth factor binding protein-1 activates integrin-mediated intracellular signaling and migration in oligodendrocytes." J Neurochem **113**(5): 1319-30.

Chou, C. K., T. J. Dull, et al. (1987). "Human insulin receptors mutated at the ATP-binding site lack protein tyrosine kinase activity and fail to mediate postreceptor effects of insulin." J Biol Chem **262**(4): 1842-7.

Chou, Y. K., M. Vainiene, et al. (1989). "Response of human T lymphocyte lines to myelin basic protein: association of dominant epitopes with HLA class II restriction molecules." J Neurosci Res **23**(2): 207-16.

Cichy, S. B., S. Uddin, et al. (1998). "Protein kinase B/Akt mediates effects of insulin on hepatic insulin-like growth factor-binding protein-1 gene expression through a conserved insulin response sequence." J Biol Chem **273**(11): 6482-7.

Clark, K. L., E. D. Halay, et al. (1993). "Co-crystal structure of the HNF-3/fork head DNA-recognition motif resembles histone H5." Nature **364**(6436): 412-20.

Cochran, F. B., Jr., R. K. Yu, et al. (1982). "Myelin gangliosides in vertebrates." J Neurochem **39**(3): 773-9.

Colognato, H., S. Ramachandrappa, et al. (2004). "Integrins direct Src family kinases to regulate distinct phases of oligodendrocyte development." J Cell Biol **167**(2): 365-75.

Cossins, J. A., J. M. Clements, et al. (1997). "Enhanced expression of MMP-7 and MMP-9 in demyelinating multiple sclerosis lesions." Acta Neuropathol **94**(6): 590-8.

Daitoku, H., M. Hatta, et al. (2004). "Silent information regulator 2 potentiates Foxo1-mediated transcription through its deacetylase activity." Proc Natl Acad Sci U S A **101**(27): 10042-7.

Davies, S., M. C. Richardson, et al. (2004). "Progesterone inhibits insulin-like growth factor binding protein-1 (IGFBP-1) production by explants of the Fallopian tube." Mol Hum Reprod **10**(12): 935-9.

De Angelis, D. A. and P. E. Braun (1994). "Isoprenylation of brain 2',3'-cyclic nucleotide 3'-phosphodiesterase modulates cell morphology." J Neurosci Res **39**(4): 386-97.

Deber, C. M. and S. J. Reynolds (1991). "Central nervous system myelin: structure, function, and pathology." Clin Biochem **24**(2): 113-34.

Dijkers, P. F., R. H. Medema, et al. (2000). "Expression of the pro-apoptotic Bcl-2 family member Bim is regulated by the forkhead transcription factor FKHR-L1." Curr Biol **10**(19): 1201-4.

Dijkers, P. F., R. H. Medema, et al. (2000). "Forkhead transcription factor FKHR-L1 modulates cytokine-dependent transcriptional regulation of p27(KIP1)." Mol Cell Biol **20**(24): 9138-48.

Duan, C. and Q. Xu (2005). "Roles of insulin-like growth factor (IGF) binding proteins in regulating IGF actions." Gen Comp Endocrinol **142**(1-2): 44-52.

Edgar, J. M., M. McLaughlin, et al. (2009). "Early ultrastructural defects of axons and axon-glia junctions in mice lacking expression of Cnp1." Glia **57**(16): 1815-24.

Edgar, J. M., M. McLaughlin, et al. (2004). "Oligodendroglial modulation of fast axonal transport in a mouse model of hereditary spastic paraplegia." J Cell Biol **166**(1): 121-31.

Engleka, M. J., F. Folli, et al. (1996). "Insulin-receptor substrate-1 is required for normal myelination." Journal of Neurochemistry **66**: S20-S20.

Esposito, C., M. Scrima, et al. (2008). "Structures and micelle locations of the nonlipidated and lipidated C-terminal membrane anchor of 2',3'-cyclic nucleotide-3'-phosphodiesterase." Biochemistry **47**(1): 308-19.

Fancy, S. P., S. E. Baranzini, et al. (2009). "Dysregulation of the Wnt pathway inhibits timely myelination and remyelination in the mammalian CNS." Genes Dev **23**(13): 1571-85.

Fantin, V. R., B. E. Lavan, et al. (1999). "Cloning, tissue expression, and chromosomal location of the mouse insulin receptor substrate 4 gene." Endocrinology **140**(3): 1329-37.

Farrer, R. G. and J. A. Benjamins (1992). "Entry of newly synthesized gangliosides into myelin." J Neurochem **58**(4): 1477-84.

Fazakerley, J. K. and M. J. Buchmeier (1993). "Pathogenesis of virus-induced demyelination." Adv Virus Res **42**: 249-324.

Feigenson, K., M. Reid, et al. (2009). "Wnt signaling is sufficient to perturb oligodendrocyte maturation." Mol Cell Neurosci **42**(3): 255-65.

Ferguson, B., M. K. Matyszak, et al. (1997). "Axonal damage in acute multiple sclerosis lesions." Brain **120 (Pt 3)**: 393-9.

Firth, S. M. and R. C. Baxter (2002). "Cellular actions of the insulin-like growth factor binding proteins." Endocr Rev **23**(6): 824-54.

Folli, F., L. Bonfanti, et al. (1994). "Insulin receptor substrate-1 (IRS-1) distribution in the rat central nervous system." J Neurosci **14**(11 Pt 1): 6412-22.

Frasca, F., G. Pandini, et al. (1999). "Insulin receptor isoform A, a newly recognized, high-affinity insulin-like growth factor II receptor in fetal and cancer cells." Mol Cell Biol **19**(5): 3278-88.

Frederick, T. J., J. Min, et al. (2007). "Synergistic induction of cyclin D1 in oligodendrocyte progenitor cells by IGF-I and FGF-2 requires differential stimulation of multiple signaling pathways." Glia **55**(10): 1011-22.

Freude, S., U. Leeser, et al. (2008). "IRS-2 branch of IGF-1 receptor signaling is essential for appropriate timing of myelination." J Neurochem **107**(4): 907-17.

Freude, S. and M. D. Schubert (2010). Insulin receptor substrate signaling in the central nervous system. Hauppauge, N.Y., Nova Science.

Fruman, D. A., L. E. Rameh, et al. (1999). "Phosphoinositide binding domains: embracing 3-phosphate." Cell **97**(7): 817-20.

Furuyama, T., T. Nakazawa, et al. (2000). "Identification of the differential distribution patterns of mRNAs and consensus binding sequences for mouse DAF-16 homologues." Biochem J **349**(Pt 2): 629-34.

Gao, C., C. Holscher, et al. (2012). "GSK3: a key target for the development of novel treatments for type 2 diabetes mellitus and Alzheimer disease." Rev Neurosci **23**(1): 1-11.

Garcia-Segura, L. M., A. Sanz, et al. (2006). "Cross-talk between IGF-I and estradiol in the brain: focus on neuroprotection." Neuroendocrinology **84**(4): 275-9.

Genain, C. P., K. Abel, et al. (1996). "Late complications of immune deviation therapy in a nonhuman primate." Science **274**(5295): 2054-7.

Genain, C. P., B. Cannella, et al. (1999). "Identification of autoantibodies associated with myelin damage in multiple sclerosis." Nat Med **5**(2): 170-5.

Gilley, J., P. J. Coffer, et al. (2003). "FOXO transcription factors directly activate bim gene expression and promote apoptosis in sympathetic neurons." J Cell Biol **162**(4): 613-22.

Giulian, D. and S. Moore (1980). "Identification of 2':3'-cyclic nucleotide 3'-phosphodiesterase in the vertebrate retina." J Biol Chem 255(13): 5993-5.

Gleeson, L. M., C. Chakraborty, et al. (2001). "Insulin-like growth factor-binding protein 1 stimulates human trophoblast migration by signaling through alpha 5 beta 1 integrin via mitogen-activated protein Kinase pathway." J Clin Endocrinol Metab 86(6): 2484-93.

Goldstein, B. J. and C. R. Kahn (1989). "Analysis of mRNA heterogeneity by ribonuclease H mapping: application to the insulin receptor." Biochem Biophys Res Commun 159(2): 664-9.

Goujet-Zalc, C., C. Babinet, et al. (1993). "The proximal region of the MBP gene promoter is sufficient to induce oligodendroglial-specific expression in transgenic mice." Eur J Neurosci 5(6): 624-32.

Goverman, J., A. Woods, et al. (1993). "Transgenic mice that express a myelin basic protein-specific T cell receptor develop spontaneous autoimmunity." Cell 72(4): 551-60.

Gow, A., V. L. Friedrich, Jr., et al. (1992). "Myelin basic protein gene contains separate enhancers for oligodendrocyte and Schwann cell expression." J Cell Biol 119(3): 605-16.

Griffiths, I., M. Klugmann, et al. (1998). "Axonal swellings and degeneration in mice lacking the major proteolipid of myelin." Science 280(5369): 1610-3.

Grima, B., D. Zelenika, et al. (1992). "A novel transcript overlapping the myelin basic protein gene." J Neurochem 59(6): 2318-23.

Grimes, C. A. and R. S. Jope (2001). "The multifaceted roles of glycogen synthase kinase 3beta in cellular signaling." Prog Neurobiol 65(4): 391-426.

Griot, C., T. Burge, et al. (1989). "Antibody-induced generation of reactive oxygen radicals by brain macrophages in canine distemper encephalitis: a mechanism for bystander demyelination." Acta Neuropathol 78(4): 396-403.

Gual, P., T. Gremeaux, et al. (2003). "MAP kinases and mTOR mediate insulin-induced phosphorylation of insulin receptor substrate-1 on serine residues 307, 612 and 632." Diabetologia 46(11): 1532-42.

Gual, P., Y. Le Marchand-Brustel, et al. (2005). "Positive and negative regulation of insulin signaling through IRS-1 phosphorylation." Biochimie 87(1): 99-109.

Gveric, D., M. L. Cuzner, et al. (1999). "Insulin-like growth factors and binding proteins in multiple sclerosis plaques." Neuropathol Appl Neurobiol 25(3): 215-25.

Gyllensten, L. and T. Malmfors (1963). "Myelinization of the optic nerve and its dependence on visual function--a quantitative investigation in mice." J Embryol Exp Morphol 11: 255-66.

Hafler, D. A. (2004). "Multiple sclerosis." J Clin Invest 113(6): 788-94.

Hara, K., K. Yonezawa, et al. (1994). "1-Phosphatidylinositol 3-kinase activity is required for insulin-stimulated glucose transport but not for RAS activation in CHO cells." Proc Natl Acad Sci U S A 91(16): 7415-9.

Hay, N. and N. Sonenberg (2004). "Upstream and downstream of mTOR." Genes Dev 18(16): 1926-45.

He, X., M. Semenov, et al. (2004). "LDL receptor-related proteins 5 and 6 in Wnt/beta-catenin signaling: arrows point the way." Development 131(8): 1663-77.

Henriksen, E. J. and B. B. Dokken (2006). "Role of glycogen synthase kinase-3 in insulin resistance and type 2 diabetes." Curr Drug Targets 7(11): 1435-41.

Herschkovitz, A., Y. F. Liu, et al. (2007). "Common inhibitory serine sites phosphorylated by IRS-1 kinases, triggered by insulin and inducers of insulin resistance." J Biol Chem 282(25): 18018-27.

Hildebrand, C., S. Remahl, et al. (1993). "Myelinated nerve fibres in the CNS." Prog Neurobiol 40(3): 319-84.

Hoekman, M. F., F. M. Jacobs, et al. (2006). "Spatial and temporal expression of FoxO transcription factors in the developing and adult murine brain." Gene Expr Patterns 6(2): 134-40.

Holgado-Madruga, M., D. R. Emlet, et al. (1996). "A Grb2-associated docking protein in EGF- and insulin-receptor signalling." Nature 379(6565): 560-4.

Hoshina, N., T. Tezuka, et al. (2007). "Focal adhesion kinase regulates laminin-induced oligodendroglial process outgrowth." Genes Cells **12**(11): 1245-54.

Hotamisligil, G. S., P. Peraldi, et al. (1996). "IRS-1-mediated inhibition of insulin receptor tyrosine kinase activity in TNF-alpha- and obesity-induced insulin resistance." Science **271**(5249): 665-8.

Hresko, R. C., H. Murata, et al. (2003). "Phosphoinositide-dependent kinase-2 is a distinct protein kinase enriched in a novel cytoskeletal fraction associated with adipocyte plasma membranes." J Biol Chem **278**(24): 21615-22.

Huang, H. and D. J. Tindall (2007). "Dynamic FoxO transcription factors." J Cell Sci **120**(Pt 15): 2479-87.

Huseby, E. S., D. Liggitt, et al. (2001). "A pathogenic role for myelin-specific CD8(+) T cells in a model for multiple sclerosis." J Exp Med **194**(5): 669-76.

Huttner, W. B. and J. Zimmerberg (2001). "Implications of lipid microdomains for membrane curvature, budding and fission." Curr Opin Cell Biol **13**(4): 478-84.

Ibanez, C., S. A. Shields, et al. (2004). "Systemic progesterone administration results in a partial reversal of the age-associated decline in CNS remyelination following toxin-induced demyelination in male rats." Neuropathol Appl Neurobiol **30**(1): 80-9.

Ichikawa, S. and Y. Hirabayashi (1998). "Glucosylceramide synthase and glycosphingolipid synthesis." Trends Cell Biol **8**(5): 198-202.

Jackman, N., A. Ishii, et al. (2009). "Oligodendrocyte development and myelin biogenesis: parsing out the roles of glycosphingolipids." Physiology (Bethesda) **24**: 290-7.

Jacobs, F. M., L. P. van der Heide, et al. (2003). "FoxO6, a novel member of the FoxO class of transcription factors with distinct shuttling dynamics." J Biol Chem **278**(38): 35959-67.

Jacobs, S., F. C. Kull, Jr., et al. (1983). "Somatomedin-C stimulates the phosphorylation of the beta-subunit of its own receptor." J Biol Chem **258**(16): 9581-4.

Jacque, C., J. M. Bourre, et al. (1971). "[Fatty acid composition of total lipids and cerebrosides of the brain in normal and Quaking mice as a function of age]." Biochimie **53**(10): 1121-4.

Jahn, O., S. Tenzer, et al. (2009). "Myelin proteomics: molecular anatomy of an insulating sheath." Mol Neurobiol **40**(1): 55-72.

Jones, J. I. and D. R. Clemmons (1995). "Insulin-like growth factors and their binding proteins: biological actions." Endocr Rev **16**(1): 3-34.

Juurlink, B. H. J. (1997). Cell biology and pathology of myelin : evolving biological concepts and therapeutic approaches. New York ; London, Plenum Press.

Kahn, C. R., K. L. Baird, et al. (1978). "Direct demonstration that receptor crosslinking or aggregation is important in insulin action." Proc Natl Acad Sci U S A **75**(9): 4209-13.

Kanety, H., R. Feinstein, et al. (1995). "Tumor necrosis factor alpha-induced phosphorylation of insulin receptor substrate-1 (IRS-1). Possible mechanism for suppression of insulin-stimulated tyrosine phosphorylation of IRS-1." J Biol Chem **270**(40): 23780-4.

Kassmann, C. M., C. Lappe-Siefke, et al. (2007). "Axonal loss and neuroinflammation caused by peroxisome-deficient oligodendrocytes." Nat Genet **39**(8): 969-76.

Kasuga, M., Y. Zick, et al. (1982). "Insulin stimulation of phosphorylation of the beta subunit of the insulin receptor. Formation of both phosphoserine and phosphotyrosine." J Biol Chem **257**(17): 9891-4.

Kieseier, B. C., T. Seifert, et al. (1999). "Matrix metalloproteinases in inflammatory demyelination: targets for treatment." Neurology **53**(1): 20-5.

Kimelman, D. and W. Xu (2006). "beta-catenin destruction complex: insights and questions from a structural perspective." Oncogene **25**(57): 7482-91.

Kira, J., T. Kanai, et al. (1996). "Western versus Asian types of multiple sclerosis: immunogenetically and clinically distinct disorders." Ann Neurol **40**(4): 569-74.

Kitamura, Y. I., T. Kitamura, et al. (2005). "FoxO1 protects against pancreatic beta cell failure through NeuroD and MafA induction." Cell Metab **2**(3): 153-63.

Klein, C., E. M. Kramer, et al. (2002). "Process outgrowth of oligodendrocytes is promoted by interaction of fyn kinase with the cytoskeletal protein tau." J Neurosci **22**(3): 698-707.

Klein, L., M. Klugmann, et al. (2000). "Shaping of the autoreactive T-cell repertoire by a splice variant of self protein expressed in thymic epithelial cells." Nat Med **6**(1): 56-61.

Klugmann, M., M. H. Schwab, et al. (1997). "Assembly of CNS myelin in the absence of proteolipid protein." Neuron **18**(1): 59-70.

Kolch, W. (2000). "Meaningful relationships: the regulation of the Ras/Raf/MEK/ERK pathway by protein interactions." Biochem J **351 Pt 2**: 289-305.

Kolter, T., R. L. Proia, et al. (2002). "Combinatorial ganglioside biosynthesis." J Biol Chem **277**(29): 25859-62.

Kops, G. J., T. B. Dansen, et al. (2002). "Forkhead transcription factor FOXO3a protects quiescent cells from oxidative stress." Nature **419**(6904): 316-21.

Kotani, M., I. Kawashima, et al. (1994). "Immunohistochemical localization of minor gangliosides in the rat central nervous system." Glycobiology **4**(6): 855-65.

Kuhl, N. M., J. De Keyser, et al. (2002). "Insulin-like growth factor binding proteins-1 and -2 differentially inhibit rat oligodendrocyte precursor cell survival and differentiation in vitro." J Neurosci Res **69**(2): 207-16.

Kuhl, N. M., D. Hoekstra, et al. (2003). "Insulin-like growth factor-binding protein 6 inhibits survival and differentiation of rat oligodendrocyte precursor cells." Glia **44**(2): 91-101.

Kurihara, T., K. Monoh, et al. (1990). "Alternative splicing of mouse brain 2',3'-cyclic-nucleotide 3'-phosphodiesterase mRNA." Biochem Biophys Res Commun **170**(3): 1074-81.

Lagarde, W. H., R. Benjamin, et al. (2007). "A non-transformed oligodendrocyte precursor cell line, OL-1, facilitates studies of insulin-like growth factor-I signaling during oligodendrocyte development." Int J Dev Neurosci **25**(2): 95-105.

Lannert, H., K. Gorgas, et al. (1998). "Functional organization of the Golgi apparatus in glycosphingolipid biosynthesis. Lactosylceramide and subsequent glycosphingolipids are formed in the lumen of the late Golgi." J Biol Chem **273**(5): 2939-46.

Lappe-Siefke, C., S. Goebbels, et al. (2003). "Disruption of Cnp1 uncouples oligodendroglial functions in axonal support and myelination." Nat Genet **33**(3): 366-74.

Lavan, B. E., V. R. Fantin, et al. (1997). "A novel 160-kDa phosphotyrosine protein in insulin-treated embryonic kidney cells is a new member of the insulin receptor substrate family." J Biol Chem **272**(34): 21403-7.

Lavan, B. E., W. S. Lane, et al. (1997). "The 60-kDa phosphotyrosine protein in insulin-treated adipocytes is a new member of the insulin receptor substrate family." J Biol Chem **272**(17): 11439-43.

Lawlor, M. A. and D. R. Alessi (2001). "PKB/Akt: a key mediator of cell proliferation, survival and insulin responses?" J Cell Sci **114**(Pt 16): 2903-10.

Lee, J., M. Gravel, et al. (2005). "Process outgrowth in oligodendrocytes is mediated by CNP, a novel microtubule assembly myelin protein." J Cell Biol **170**(4): 661-73.

Lee, J. and M. S. Kim (2007). "The role of GSK3 in glucose homeostasis and the development of insulin resistance." Diabetes Res Clin Pract **77 Suppl 1**: S49-57.

LeRoith, D., H. Werner, et al. (1995). "Molecular and cellular aspects of the insulin-like growth factor I receptor." Endocr Rev **16**(2): 143-63.

Li, W., S. G. Kennedy, et al. (2003). "daf-28 encodes a C. elegans insulin superfamily member that is regulated by environmental cues and acts in the DAF-2 signaling pathway." Genes Dev **17**(7): 844-58.

Linington, C., M. Bradl, et al. (1988). "Augmentation of demyelination in rat acute allergic encephalomyelitis by circulating mouse monoclonal antibodies directed against a myelin/oligodendrocyte glycoprotein." Am J Pathol **130**(3): 443-54.

Liu, S. J., A. H. Zhang, et al. (2003). "Overactivation of glycogen synthase kinase-3 by inhibition of phosphoinositol-3 kinase and protein kinase C leads to hyperphosphorylation of tau and impairment of spatial memory." J Neurochem **87**(6): 1333-44.

Louvi, A., D. Accili, et al. (1997). "Growth-promoting interaction of IGF-II with the insulin receptor during mouse embryonic development." Dev Biol **189**(1): 33-48.

Lovas, G., N. Szilagyi, et al. (2000). "Axonal changes in chronic demyelinated cervical spinal cord plaques." Brain **123 (Pt 2)**: 308-17.

Lucchinetti, C., W. Bruck, et al. (1999). "A quantitative analysis of oligodendrocytes in multiple sclerosis lesions. A study of 113 cases." Brain **122 (Pt 12)**: 2279-95.

Ludwin, S. K. (1997). "The pathobiology of the oligodendrocyte." J Neuropathol Exp Neurol **56**(2): 111-24.

Luo, M., P. Langlais, et al. (2007). "Phosphorylation of human insulin receptor substrate-1 at Serine 629 plays a positive role in insulin signaling." Endocrinology **148**(10): 4895-905.

Luo, M., S. Reyna, et al. (2005). "Identification of insulin receptor substrate 1 serine/threonine phosphorylation sites using mass spectrometry analysis: regulatory role of serine 1223." Endocrinology **146**(10): 4410-6.

Luzi, P., M. Zaka, et al. (2004). "Generation of transgenic mice expressing insulin-like growth factor-1 under the control of the myelin basic protein promoter: increased myelination and potential for studies on the effects of increased IGF-1 on experimentally and genetically induced demyelination." Neurochem Res **29**(5): 881-9.

MacDonald, B. T., K. Tamai, et al. (2009). "Wnt/beta-catenin signaling: components, mechanisms, and diseases." Dev Cell **17**(1): 9-26.

Maeda, A. and R. A. Sobel (1996). "Matrix metalloproteinases in the normal human central nervous system, microglial nodules, and multiple sclerosis lesions." J Neuropathol Exp Neurol **55**(3): 300-9.

Maehama, T. and J. E. Dixon (1998). "The tumor suppressor, PTEN/MMAC1, dephosphorylates the lipid second messenger, phosphatidylinositol 3,4,5-trisphosphate." J Biol Chem **273**(22): 13375-8.

Maghzi, A. H., H. Ghazavi, et al. (2010). "Increasing female preponderance of multiple sclerosis in Isfahan, Iran: a population-based study." Mult Scler **16**(3): 359-61.

Maier, O., D. Hoekstra, et al. (2008). "Polarity development in oligodendrocytes: sorting and trafficking of myelin components." J Mol Neurosci **35**(1): 35-53.

Manning, B. D. and L. C. Cantley (2007). "AKT/PKB signaling: navigating downstream." Cell **129**(7): 1261-74.

Martenson, R. E. (1992). Myelin : biology and chemistry. Boca Raton, CRC Press.

Martin, R., D. Jaraquemada, et al. (1990). "Fine specificity and HLA restriction of myelin basic protein-specific cytotoxic T cell lines from multiple sclerosis patients and healthy individuals." J Immunol **145**(2): 540-8.

Martin, R., H. F. McFarland, et al. (1992). "Immunological aspects of demyelinating diseases." Annu Rev Immunol **10**: 153-87.

Mason, J. L., P. Ye, et al. (2000). "Insulin-like growth factor-1 inhibits mature oligodendrocyte apoptosis during primary demyelination." J Neurosci **20**(15): 5703-8.

Matute, C. (1998). "Characteristics of acute and chronic kainate excitotoxic damage to the optic nerve." Proc Natl Acad Sci U S A **95**(17): 10229-34.

McClain, D. A. (1991). "Different ligand affinities of the two human insulin receptor splice variants are reflected in parallel changes in sensitivity for insulin action." Mol Endocrinol **5**(5): 734-9.

McCormick, F. (1993). "Signal transduction. How receptors turn Ras on." Nature **363**(6424): 15-6.

McFarlin, D. E. and H. F. McFarland (1982). "Multiple sclerosis (first of two parts)." N Engl J Med **307**(19): 1183-8.

McFarlin, D. E. and H. F. McFarland (1982). "Multiple sclerosis (second of two parts)." N Engl J Med **307**(20): 1246-51.

McGavern, D. B., P. D. Murray, et al. (2000). "Axonal loss results in spinal cord atrophy, electrophysiological abnormalities and neurological deficits following demyelination in a chronic inflammatory model of multiple sclerosis." Brain **123 Pt 3**: 519-31.

McMorris, F. A., T. M. Smith, et al. (1986). "Insulin-like growth factor I/somatomedin C: a potent inducer of oligodendrocyte development." Proc Natl Acad Sci U S A **83**(3): 822-6.

Medema, R. H., G. J. Kops, et al. (2000). "AFX-like Forkhead transcription factors mediate cell-cycle regulation by Ras and PKB through p27kip1." Nature **404**(6779): 782-7.

Megyesi, K., C. R. Kahn, et al. (1974). "Insulin and non-suppressible insulin-like activity (NSILA-s): evidence for separate plasma membrane receptor sites." Biochem Biophys Res Commun **57**(1): 307-15.

Miyamoto, Y., J. Yamauchi, et al. (2007). "Cdk5 regulates differentiation of oligodendrocyte precursor cells through the direct phosphorylation of paxillin." J Cell Sci **120**(Pt 24): 4355-66.

Mohan, S., Y. Nakao, et al. (1995). "Studies on the mechanisms by which insulin-like growth factor (IGF) binding protein-4 (IGFBP-4) and IGFBP-5 modulate IGF actions in bone cells." J Biol Chem **270**(35): 20424-31.

Mohan, S., G. R. Thompson, et al. (2002). "ADAM-9 is an insulin-like growth factor binding protein-5 protease produced and secreted by human osteoblasts." Biochemistry **41**(51): 15394-403.

Moll, L., J. Zemva, M. Schubert (2011). " Role of central insulin-like growth factor-1 receptor signalling in ageing and endocrine regulation". Endocrinology and Metabolism ISBN 978-953-307-340-8

Moller, D. E., A. Yokota, et al. (1989). "Tissue-specific expression of two alternatively spliced insulin receptor mRNAs in man." Mol Endocrinol **3**(8): 1263-9.

Morell, P., S. Greenfield, et al. (1972). "Changes in the protein composition of mouse brain myelin during development." J Neurochem **19**(11): 2545-54.

Morello, D., A. Dautigny, et al. (1986). "Myelin proteolipid protein (PLP and DM-20) transcripts are deleted in jimpy mutant mice." EMBO J **5**(13): 3489-93.

Morrione, A., B. Valentinis, et al. (1997). "Insulin-like growth factor II stimulates cell proliferation through the insulin receptor." Proc Natl Acad Sci U S A **94**(8): 3777-82.

Mosthaf, L., K. Grako, et al. (1990). "Functionally distinct insulin receptors generated by tissue-specific alternative splicing." EMBO J **9**(8): 2409-13.

Nakahara, J., K. Tan-Takeuchi, et al. (2003). "Signaling via immunoglobulin Fc receptors induces oligodendrocyte precursor cell differentiation." Dev Cell **4**(6): 841-52.

Nave, K. A., C. Lai, et al. (1987). "Splice site selection in the proteolipid protein (PLP) gene transcript and primary structure of the DM-20 protein of central nervous system myelin." Proc Natl Acad Sci U S A **84**(16): 5665-9.

Niino, M., S. Kikuchi, et al. (2002). "No association of vitamin D-binding protein gene polymorphisms in Japanese patients with MS." J Neuroimmunol **127**(1-2): 177-9.

Nojima, H., C. Tokunaga, et al. (2003). "The mammalian target of rapamycin (mTOR) partner, raptor, binds the mTOR substrates p70 S6 kinase and 4E-BP1 through their TOR signaling (TOS) motif." J Biol Chem **278**(18): 15461-4.

Norton, W. T. and S. E. Poduslo (1973). "Myelination in rat brain: changes in myelin composition during brain maturation." J Neurochem **21**(4): 759-73.

Numan, S. and D. S. Russell (1999). "Discrete expression of insulin receptor substrate-4 mRNA in adult rat brain." Brain Res Mol Brain Res **72**(1): 97-102.

O'Kusky, J. and P. Ye (2012). "Neurodevelopmental effects of insulin-like growth factor signaling." Front Neuroendocrinol.

Okada, T., Y. Kawano, et al. (1994). "Essential role of phosphatidylinositol 3-kinase in insulin-induced glucose transport and antilipolysis in rat adipocytes. Studies with a selective inhibitor wortmannin." J Biol Chem **269**(5): 3568-73.

Olsson, T., W. W. Zhi, et al. (1990). "Autoreactive T lymphocytes in multiple sclerosis determined by antigen-induced secretion of interferon-gamma." J Clin Invest **86**(3): 981-5.

Omlin, F. X. (1997). "Optic disc and optic nerve of the blind cape mole-rat (Georychus capensis): a proposed model for naturally occurring reactive gliosis." Brain Res Bull **44**(5): 627-32.

Oshiro, N., K. Yoshino, et al. (2004). "Dissociation of raptor from mTOR is a mechanism of rapamycin-induced inhibition of mTOR function." Genes Cells **9**(4): 359-66.

Osterhout, D. J., A. Wolven, et al. (1999). "Morphological differentiation of oligodendrocytes requires activation of Fyn tyrosine kinase." J Cell Biol **145**(6): 1209-18.

Ota, K., M. Matsui, et al. (1990). "T-cell recognition of an immunodominant myelin basic protein epitope in multiple sclerosis." Nature **346**(6280): 183-7.

Ozawa, K., G. Suchanek, et al. (1994). "Patterns of oligodendroglia pathology in multiple sclerosis." Brain **117 (Pt 6)**: 1311-22.

Pandini, G., F. Frasca, et al. (2002). "Insulin/insulin-like growth factor I hybrid receptors have different biological characteristics depending on the insulin receptor isoform involved." J Biol Chem **277**(42): 39684-95.

Partridge, L. and J. C. Bruning (2008). "Forkhead transcription factors and ageing." Oncogene **27**(16): 2351-63.

Pete, G., C. R. Fuller, et al. (1999). "Postnatal growth responses to insulin-like growth factor I in insulin receptor substrate-1-deficient mice." Endocrinology **140**(12): 5478-87.

Pette, M., K. Fujita, et al. (1990). "Myelin basic protein-specific T lymphocyte lines from MS patients and healthy individuals." Neurology **40**(11): 1770-6.

Pettinelli, C. B. and D. E. McFarlin (1981). "Adoptive transfer of experimental allergic encephalomyelitis in SJL/J mice after in vitro activation of lymph node cells by myelin basic protein: requirement for Lyt 1+ 2- T lymphocytes." J Immunol **127**(4): 1420-3.

Pieringer, J., G. S. Rao, et al. (1977). "The association of the sulphogalactosylglycerolipid of rat brain with myelination." Biochem J **166**(3): 421-8.

Pitt, D., P. Werner, et al. (2000). "Glutamate excitotoxicity in a model of multiple sclerosis." Nat Med **6**(1): 67-70.

Poliak, S. and E. Peles (2003). "The local differentiation of myelinated axons at nodes of Ranvier." Nat Rev Neurosci **4**(12): 968-80.

Pollak, M. (2012). "The insulin and insulin-like growth factor receptor family in neoplasia: an update." Nat Rev Cancer **12**(3): 159-69.

Popken, G. J., M. Dechert-Zeger, et al. (2005). "Brain development." Adv Exp Med Biol **567**: 187-220.

Popot, J. L., D. Pham Dinh, et al. (1991). "Major Myelin proteolipid: the 4-alpha-helix topology." J Membr Biol **120**(3): 233-46.

Pribyl, T. M., C. W. Campagnoni, et al. (1993). "The human myelin basic protein gene is included within a 179-kilobase transcription unit: expression in the immune and central nervous systems." Proc Natl Acad Sci U S A **90**(22): 10695-9.

Privat, A., C. Jacque, et al. (1979). "Absence of the major dense line in myelin of the mutant mouse "shiverer"." Neurosci Lett **12**(1): 107-12.

Qin, X., D. D. Strong, et al. (1998). "Structure-function analysis of the human insulin-like growth factor binding protein-4." J Biol Chem **273**(36): 23509-16.

Quon, M. J., A. J. Butte, et al. (1994). "Insulin receptor substrate 1 mediates the stimulatory effect of insulin on GLUT4 translocation in transfected rat adipose cells." J Biol Chem **269**(45): 27920-4.

Raff, M. C., R. Mirsky, et al. (1978). "Galactocerebroside is a specific cell-surface antigenic marker for oligodendrocytes in culture." Nature **274**(5673): 813-6.

Rajaram, S., D. J. Baylink, et al. (1997). "Insulin-like growth factor-binding proteins in serum and other biological fluids: regulation and functions." Endocr Rev **18**(6): 801-31.

Rajasekharan, S., K. A. Baker, et al. (2009). "Netrin 1 and Dcc regulate oligodendrocyte process branching and membrane extension via Fyn and RhoA." Development **136**(3): 415-26.

Ramagopalan, S. V., N. J. Maugeri, et al. (2009). "Expression of the multiple sclerosis-associated MHC class II Allele HLA-DRB1*1501 is regulated by vitamin D." PLoS Genet **5**(2): e1000369.

Rechler, M. M. and D. R. Clemmons (1998). "Regulatory Actions of Insulin-like Growth Factor-binding Proteins." Trends Endocrinol Metab **9**(5): 176-83.

Reynolds, R. and G. P. Wilkin (1991). "Oligodendroglial progenitor cells but not oligodendroglia divide during normal development of the rat cerebellum." J Neurocytol **20**(3): 216-24.

Richert, J. R., D. E. McFarlin, et al. (1983). "Expansion of antigen-specific T cells from cerebrospinal fluid of patients with multiple sclerosis." J Neuroimmunol **5**(3): 317-24.

Roach, A., K. Boylan, et al. (1983). "Characterization of cloned cDNA representing rat myelin basic protein: absence of expression in brain of shiverer mutant mice." Cell **34**(3): 799-806.

Rosenbluth, J., W. Stoffel, et al. (1996). "Myelin structure in proteolipid protein (PLP)-null mouse spinal cord." J Comp Neurol **371**(2): 336-44.

Roth, G. A., V. Spada, et al. (1995). "Insulin-like growth factor I increases myelination and inhibits demyelination in cultured organotypic nerve tissue." Brain Res Dev Brain Res **88**(1): 102-8.

Rubin, J. B., M. A. Shia, et al. (1983). "Stimulation of tyrosine-specific phosphorylation in vitro by insulin-like growth factor I." Nature **305**(5933): 438-40.

Ruggero, D. and N. Sonenberg (2005). "The Akt of translational control." Oncogene **24**(50): 7426-34.

Saini, H. S., K. M. Gorse, et al. (2004). "Neurotrophin-3 and a CREB-mediated signaling pathway regulate Bcl-2 expression in oligodendrocyte progenitor cells." J Neurochem **89**(4): 951-61.

Sawka-Verhelle, D., V. Baron, et al. (1997). "Tyr624 and Tyr628 in insulin receptor substrate-2 mediate its association with the insulin receptor." J Biol Chem **272**(26): 16414-20.

Sawka-Verhelle, D., S. Tartare-Deckert, et al. (1996). "Insulin receptor substrate-2 binds to the insulin receptor through its phosphotyrosine-binding domain and through a newly identified domain comprising amino acids 591-786." J Biol Chem **271**(11): 5980-3.

Scherer, S. S., P. E. Braun, et al. (1994). "Differential regulation of the 2',3'-cyclic nucleotide 3'-phosphodiesterase gene during oligodendrocyte development." Neuron **12**(6): 1363-75.

Schmidt-Schultz, T. and H. H. Althaus (1994). "Monogalactosyl diglyceride, a marker for myelination, activates oligodendroglial protein kinase C." J Neurochem **62**(4): 1578-85.

Schubert, M., D. P. Brazil, et al. (2003). "Insulin receptor substrate-2 deficiency impairs brain growth and promotes tau phosphorylation." J Neurosci **23**(18): 7084-92.

Sciacchitano, S. and S. I. Taylor (1997). "Cloning, tissue expression, and chromosomal localization of the mouse IRS-3 gene." Endocrinology **138**(11): 4931-40.

Scolding, N., R. Franklin, et al. (1998). "Oligodendrocyte progenitors are present in the normal adult human CNS and in the lesions of multiple sclerosis." Brain **121 (Pt 12)**: 2221-8.

Seamons, A., A. Perchellet, et al. (2003). "Immune tolerance to myelin proteins." Immunol Res **28**(3): 201-21.

Seino, S. and G. I. Bell (1989). "Alternative splicing of human insulin receptor messenger RNA." Biochem Biophys Res Commun **159**(1): 312-6.

Seino, S., M. Seino, et al. (1990). "Human insulin-receptor gene." Diabetes **39**(2): 129-33.

Sellebjerg, F., J. Jensen, et al. (2000). "HLA DRB1*1501 and intrathecal inflammation in multiple sclerosis." Tissue Antigens **55**(4): 312-8.

Sharfi, H. and H. Eldar-Finkelman (2008). "Sequential phosphorylation of insulin receptor substrate-2 by glycogen synthase kinase-3 and c-Jun NH2-terminal kinase plays a role in hepatic insulin signaling." Am J Physiol Endocrinol Metab **294**(2): E307-15.

Shier, P. and V. M. Watt (1989). "Primary structure of a putative receptor for a ligand of the insulin family." J Biol Chem **264**(25): 14605-8.

Siegel, G. J. (1994). Basic neurochemistry : molecular, cellular, and medical aspects. New York, Raven Press.

Siegel, G. J. (2006). Basic neurochemistry : molecular, cellular, and medical aspects. Amsterdam ; Boston ; London, Elsevier.

Soldan, M. M. and I. Pirko (2012). "Biogenesis and significance of central nervous system myelin." Semin Neurol **32**(1): 9-14.

Solinas, G., W. Naugler, et al. (2006). "Saturated fatty acids inhibit induction of insulin gene transcription by JNK-mediated phosphorylation of insulin-receptor substrates." Proc Natl Acad Sci U S A **103**(44): 16454-9.

Song, G., G. Ouyang, et al. (2005). "The activation of Akt/PKB signaling pathway and cell survival." J Cell Mol Med **9**(1): 59-71.

Songyang, Z., K. L. Carraway, 3rd, et al. (1995). "Catalytic specificity of protein-tyrosine kinases is critical for selective signalling." Nature **373**(6514): 536-9.

Sospedra, M. and R. Martin (2005). "Immunology of multiple sclerosis." <u>Annu Rev Immunol</u> **23**: 683-747.

Sperber, B. R., E. A. Boyle-Walsh, et al. (2001). "A unique role for Fyn in CNS myelination." <u>J Neurosci</u> **21**(6): 2039-47.

Sperber, B. R. and F. A. McMorris (2001). "Fyn tyrosine kinase regulates oligodendroglial cell development but is not required for morphological differentiation of oligodendrocytes." <u>J Neurosci Res</u> **63**(4): 303-12.

Sprinkle, T. J. (1989). "2',3'-cyclic nucleotide 3'-phosphodiesterase, an oligodendrocyte-Schwann cell and myelin-associated enzyme of the nervous system." <u>Crit Rev Neurobiol</u> **4**(3): 235-301.

Sprinkle, T. J., F. A. McMorris, et al. (1985). "Differential expression of 2':3'-cyclic nucleotide 3'-phosphodiesterase in cultured central, peripheral, and extraneural cells." <u>Neurochem Res</u> **10**(7): 919-31.

Steinman, L. (2000). "Multiple approaches to multiple sclerosis." <u>Nat Med</u> **6**(1): 15-6.

Stokoe, D., L. R. Stephens, et al. (1997). "Dual role of phosphatidylinositol-3,4,5-trisphosphate in the activation of protein kinase B." <u>Science</u> **277**(5325): 567-70.

Sun, D., J. N. Whitaker, et al. (2001). "Myelin antigen-specific CD8+ T cells are encephalitogenic and produce severe disease in C57BL/6 mice." <u>J Immunol</u> **166**(12): 7579-87.

Sun, X. J., P. Rothenberg, et al. (1991). "Structure of the insulin receptor substrate IRS-1 defines a unique signal transduction protein." <u>Nature</u> **352**(6330): 73-7.

Sun, X. J., L. M. Wang, et al. (1995). "Role of IRS-2 in insulin and cytokine signalling." <u>Nature</u> **377**(6545): 173-7.

Sweatt, J. D. (2001). "The neuronal MAP kinase cascade: a biochemical signal integration system subserving synaptic plasticity and memory." <u>J Neurochem</u> **76**(1): 1-10.

Taguchi, A., L. M. Wartschow, et al. (2007). "Brain IRS2 signaling coordinates life span and nutrient homeostasis." <u>Science</u> **317**(5836): 369-372.

Taniguchi, S., H. Liu, et al. (2003). "p250GAP, a neural RhoGAP protein, is associated with and phosphorylated by Fyn." <u>Biochem Biophys Res Commun</u> **306**(1): 151-5.

Tector, A. J., R. P. Gabriel, et al. (1976). "Reduction of blood usage in open heart surgery." <u>Chest</u> **70**(4): 454-7.

Theret, N., P. Boulenguer, et al. (1988). "Acylgalactosylceramides in developing dysmyelinating mutant mice." <u>J Neurochem</u> **50**(3): 883-8.

Trapp, B. D., L. Bernier, et al. (1988). "Cellular and subcellular distribution of 2',3'-cyclic nucleotide 3'-phosphodiesterase and its mRNA in the rat central nervous system." <u>J Neurochem</u> **51**(3): 859-68.

Trapp, B. D., J. Peterson, et al. (1998). "Axonal transection in the lesions of multiple sclerosis." <u>N Engl J Med</u> **338**(5): 278-85.

Tzakos, A. G., A. Troganis, et al. (2005). "Structure and function of the myelin proteins: current status and perspectives in relation to multiple sclerosis." <u>Curr Med Chem</u> **12**(13): 1569-87.

Ullrich, A., A. Gray, et al. (1986). "Insulin-like growth factor I receptor primary structure: comparison with insulin receptor suggests structural determinants that define functional specificity." <u>EMBO J</u> **5**(10): 2503-12.

Umemori, H., Y. Kadowaki, et al. (1999). "Stimulation of myelin basic protein gene transcription by Fyn tyrosine kinase for myelination." <u>J Neurosci</u> **19**(4): 1393-7.

Umemori, H., S. Sato, et al. (1994). "Initial events of myelination involve Fyn tyrosine kinase signalling." <u>Nature</u> **367**(6463): 572-6.

van Meeteren, M. E., M. A. Koetsier, et al. (2005). "Markers for OLN-93 oligodendroglia differentiation." <u>Brain Res Dev Brain Res</u> **156**(1): 78-86.

van Noort, J. M., A. C. van Sechel, et al. (1995). "The small heat-shock protein alpha B-crystallin as candidate autoantigen in multiple sclerosis." <u>Nature</u> **375**(6534): 798-801.

Van Obberghen, E., M. Ksauga, et al. (1981). "Biosynthetic labeling of insulin receptor: studies of subunits in cultured human IM-9 lymphocytes." <u>Proc Natl Acad Sci U S A</u> **78**(2): 1052-6.

Van Wauwe, J. and B. Haefner (2003). "Glycogen synthase kinase-3 as drug target: from wallflower to center of attention." Drug News Perspect **16**(9): 557-65.

Vanhaesebroeck, B., K. Ali, et al. (2005). "Signalling by PI3K isoforms: insights from gene-targeted mice." Trends Biochem Sci **30**(4): 194-204.

Vanhaesebroeck, B., S. J. Leevers, et al. (2001). "Synthesis and function of 3-phosphorylated inositol lipids." Annu Rev Biochem **70**: 535-602.

Vogel, U. S. and R. J. Thompson (1988). "Molecular structure, localization, and possible functions of the myelin-associated enzyme 2',3'-cyclic nucleotide 3'-phosphodiesterase." J Neurochem **50**(6): 1667-77.

Wang, P. S., J. Wang, et al. (2009). "Protein-tyrosine phosphatase alpha acts as an upstream regulator of Fyn signaling to promote oligodendrocyte differentiation and myelination." J Biol Chem **284**(48): 33692-702.

Weigert, C., A. M. Hennige, et al. (2005). "The phosphorylation of Ser318 of insulin receptor substrate 1 is not per se inhibitory in skeletal muscle cells but is necessary to trigger the attenuation of the insulin-stimulated signal." J Biol Chem **280**(45): 37393-9.

Weigert, C., M. Kron, et al. (2008). "Interplay and effects of temporal changes in the phosphorylation state of serine-302, -307, and -318 of insulin receptor substrate-1 on insulin action in skeletal muscle cells." Mol Endocrinol **22**(12): 2729-40.

Weimbs, T. and W. Stoffel (1992). "Proteolipid protein (PLP) of CNS myelin: positions of free, disulfide-bonded, and fatty acid thioester-linked cysteine residues and implications for the membrane topology of PLP." Biochemistry **31**(49): 12289-96.

Wekerle, H. (1993). "Experimental autoimmune encephalomyelitis as a model of immune-mediated CNS disease." Curr Opin Neurobiol **3**(5): 779-84.

Wekerle, H. (1998). "The viral triggering of autoimmune disease." Nat Med **4**(7): 770-1.

Welsh, G. I. and C. G. Proud (1993). "Glycogen synthase kinase-3 is rapidly inactivated in response to insulin and phosphorylates eukaryotic initiation factor eIF-2B." Biochem J **294 (Pt 3)**: 625-9.

White, M. F. (1997). "The insulin signalling system and the IRS proteins." Diabetologia **40 Suppl 2**: S2-17.

White, M. F. (1998). "The IRS-signaling system: a network of docking proteins that mediate insulin and cytokine action." Recent Prog Horm Res **53**: 119-38.

White, M. F. (2002). "IRS proteins and the common path to diabetes." Am J Physiol Endocrinol Metab **283**(3): E413-22.

White, M. F., R. Maron, et al. (1985). "Insulin rapidly stimulates tyrosine phosphorylation of a Mr-185,000 protein in intact cells." Nature **318**(6042): 183-6.

White, M. F. and L. Yenush (1998). "The IRS-signaling system: a network of docking proteins that mediate insulin and cytokine action." Curr Top Microbiol Immunol **228**: 179-208.

Wilczak, N., D. Chesik, et al. (2008). "IGF binding protein alterations on periplaque oligodendrocytes in multiple sclerosis: implications for remyelination." Neurochem Int **52**(8): 1431-5.

Wolf, R. M., J. J. Wilkes, et al. (2001). "Tyrosine phosphorylation of p190 RhoGAP by Fyn regulates oligodendrocyte differentiation." J Neurobiol **49**(1): 62-78.

Wolswijk, G. (1995). "Strongly GD3+ cells in the developing and adult rat cerebellum belong to the microglial lineage rather than to the oligodendrocyte lineage." Glia **13**(1): 13-26.

Wolswijk, G. (2000). "Oligodendrocyte survival, loss and birth in lesions of chronic-stage multiple sclerosis." Brain **123 (Pt 1)**: 105-15.

Wolswijk, G. (2002). "Oligodendrocyte precursor cells in the demyelinated multiple sclerosis spinal cord." Brain **125**(Pt 2): 338-49.

Wood, D. D. and M. A. Moscarello (1989). "The isolation, characterization, and lipid-aggregating properties of a citrulline containing myelin basic protein." J Biol Chem **264**(9): 5121-7.

Wu, H., Y. Yan, et al. (2007). "Regulation of class IA PI3Ks." Biochem Soc Trans **35**(Pt 2): 242-4.

Wujek, J. R., C. Bjartmar, et al. (2002). "Axon loss in the spinal cord determines permanent neurological disability in an animal model of multiple sclerosis." J Neuropathol Exp Neurol **61**(1): 23-32.

Yamaguchi, Y., J. S. Flier, et al. (1991). "Functional properties of two naturally occurring isoforms of the human insulin receptor in Chinese hamster ovary cells." Endocrinology **129**(4): 2058-66.

Yang, E., J. Zha, et al. (1995). "Bad, a heterodimeric partner for Bcl-XL and Bcl-2, displaces Bax and promotes cell death." Cell **80**(2): 285-91.

Ye, P., J. Carson, et al. (1995). "In vivo actions of insulin-like growth factor-I (IGF-I) on brain myelination: studies of IGF-I and IGF binding protein-1 (IGFBP-1) transgenic mice." J Neurosci **15**(11): 7344-56.

Ye, P. and A. J. D'Ercole (1999). "Insulin-like growth factor I protects oligodendrocytes from tumor necrosis factor-alpha-induced injury." Endocrinology **140**(7): 3063-72.

Ye, P., L. Li, et al. (2002). "Deficient expression of insulin receptor substrate-1 (IRS-1) fails to block insulin-like growth factor-I (IGF-I) stimulation of brain growth and myelination." Brain Res Dev Brain Res **136**(2): 111-21.

Yenush, L. and M. F. White (1997). "The IRS-signalling system during insulin and cytokine action." Bioessays **19**(6): 491-500.

Yi, X., M. Schubert, et al. (2005). "Insulin receptor substrate 2 is essential for maturation and survival of photoreceptor cells." J Neurosci **25**(5): 1240-8.

Yin, X., T. O. Crawford, et al. (1998). "Myelin-associated glycoprotein is a myelin signal that modulates the caliber of myelinated axons." J Neurosci **18**(6): 1953-62.

Yong, V. W., C. A. Krekoski, et al. (1998). "Matrix metalloproteinases and diseases of the CNS." Trends Neurosci **21**(2): 75-80.

Yong, V. W., C. Power, et al. (2001). "Metalloproteinases in biology and pathology of the nervous system." Nat Rev Neurosci **2**(7): 502-11.

Yu, W. P., E. J. Collarini, et al. (1994). "Embryonic expression of myelin genes: evidence for a focal source of oligodendrocyte precursors in the ventricular zone of the neural tube." Neuron **12**(6): 1353-62.

Yuan, S., Y. Shi, et al. (2012). "Wnt Signaling in the Pathogenesis of Multiple Sclerosis-Associated Chronic Pain." J Neuroimmune Pharmacol.

Zalc, B., M. Monge, et al. (1981). "Immunohistochemical localization of galactosyl and sulfogalactosyl ceramide in the brain of the 30-day-old mouse." Brain Res **211**(2): 341-54.

Zamvil, S. S. and L. Steinman (1990). "The T lymphocyte in experimental allergic encephalomyelitis." Annu Rev Immunol **8**: 579-621.

Zha, J., H. Harada, et al. (1997). "BH3 domain of BAD is required for heterodimerization with BCL-XL and pro-apoptotic activity." J Biol Chem **272**(39): 24101-4.

Zhang, J., B. M. Moats-Staats, et al. (2007). "Expression of insulin-like growth factor system genes during the early postnatal neurogenesis in the mouse hippocampus." J Neurosci Res **85**(8): 1618-27.

Zhuang, S. and R. G. Schnellmann (2006). "A death-promoting role for extracellular signal-regulated kinase." J Pharmacol Exp Ther **319**(3): 991-7.

8. Supplementary

8.1. Acknowledgement

First I would like to thank PD Dr. Schubert for providing me with this interesting project. I appreciate the support and advice for me and my work as well as the possibility to learn and work in his lab.

I would like to thank Prof. Dr. Jens Brüning, Prof. Dr. Wilhelm Krone, Prof. Dr. Peter Kloppenburg and Dr Marion Rozowski to form my thesis committee.

Furthermore, I would like to thank the work group of Prof Dr. Stoffel, the work group Prof Dr. Neiss and Dr. Michael Udelhoven for their help and advice. Additionally, I would like to thank my present and former colleagues as well for their help, advice and the nice atmosphere in the lab. Especially I would like to thank Dr. Lorna Moll, Nicole Blank, Karin Krystofiak, Petra Hofman und Heike Krämer.

Just as my friends and my family for their help and support. Especially I would like to thank my my mum which made all this possible and was always a great support.

8.2. Erklärung

Ich versichere, dass ich die von mir vorgelegte Dissertation selbständig angefertigt, die benutzten Quellen und Hilfsmittel vollständig angegeben und die Stellen der Arbeit − einschließlich Tabellen, Karten und Abbildungen −, die anderen Werken im Wortlaut oder dem Sinn nach entnommen sind, in jedem Einzelfall als Entlehnung kenntlich gemacht habe; dass diese Dissertation noch keiner anderen Fakultät oder Universität zur Prüfung vorgelegen hat; dass sie noch nicht veröffentlicht worden ist sowie, dass ich eine solche Veröffentlichung vor Abschluss des Promotionsverfahrens nicht vornehmen werde. Die Bestimmungen der Promotionsordnung sind mir bekannt. Die von mir vorgelegte Dissertation ist von Prof. Dr. Jens C. Brüning betreut worden.

Köln, den 19.11.12   Jessica Drake